Title
NUMERICAL COMPUTATION OF FLOW PAST OBSTACLES

Author
Sih, Ping Huei.

Publication Date
1966

UCRL-16653

University of California

Ernest O. Lawrence Radiation Laboratory

NUMERICAL COMPUTATION OF FLOW PAST OBSTACLES

DISCLAIMER

Special thesis

UCRL-16653

UNIVERSITY OF CALIFORNIA

Lawrence Radiation Laboratory
Berkeley, California

AEC Contract No. W-7405-eng-48

NUMERICAL COMPUTATION OF FLOW PAST OBSTACLES

Ping Huei Sih

(Masters Thesis)

January 1966

NUMERICAL COMPUTATION OF FLOW PAST OBSTACLES

Ping Huei Sih

Master's Thesis

Inorganic Materials Research Division,
Lawrence Radiation Laboratory, and
Department of Chemical Engineering
University of California, Berkeley

January 1966

Committee in Charge:

John S. Newman

E. A. Grens II

S. A. Berger

NUMERICAL COMPUTATION OF FLOW PAST OBSTACLES

Ping Huei Sih

Lawrence Radiation Laboratory, Inorganic Materials Research Division
Department of Chemical Engineering
University of California, Berkeley, California

January 1966

ABSTRACT

The unsteady state flow past a cylinderical obstacle in a two dimensional channel is investigated by the methods of numerical approximation. The numerical methods employed are designed by Peaceman and Rachford and by Fromm. More appropriate boundary conditions are used as compared to Fromm's work. The finite difference equations for any arbitrarily shaped obstacle are developed such that fine detail near the surface of the obstacle can be studied.

Two tests at Re = 5 and 300 are made. The results at Re = 5 indicate that the equations and methods used are appropriate. However, at Re = 300 the methods break down, which indicates that some different approach should be used at high Reynolds numbers.

TABLE OF CONTENTS

I. INTRODUCTION

The problem of determining the steady and unsteady state flow past fixed, cylindrical obstacles in a uniform stream of viscous incompressible fluid has been studied by many people in the field of fluid mechanics. The differential equation describing such a physical problem is the Navier-Stokes equation. Due to its non-linear nature it has so far not been solved except for the limiting cases of very small or large Reynolds numbers. For small Reynolds numbers approximate equations may be developed, since the inertial terms are small. For example, steady state solutions for flow past spheres and circular cylinders have been obtained by Proudman and Pearson[8] and Kaplun.[5] For large Reynolds numbers, the viscous terms are important only in the region close to the obstacle, and beyond this region the flow, in general, is assumed to be potential flow. Thus the boundary layer approach can be used to simplify the Navier-Stokes equation. However, such an approach does not yield any information about wakes where eddies are present.

Another possibility is to solve the equation by methods of numerical approximation, such as the computation of steady flow past a circular cylinder by Thom,[10,11] Appelt,[2] Southwell and Squire,[9] and Allen and Southwell.[1] The recent work of Fromm[3] further suggests that numerical methods can be used successfully to describe the unsteady flow at high Reynolds numbers for an arbitrary geometrical shape of the obstacle. However, Fromm did not investigate in detail the flow near the surface of the obstacle. The objective of this work is to develop a numerical method such that the flow pattern near any arbitrarily shaped obstacles can be computed.

For convenience in comparing results with the literature values the obstacle chosen is a circular cylinder. By symmetry, the flow pattern of half of the system is the mirror image of the other, if the shedding of the vortices can be avoided. Although, it is known that vortex shedding does occur at high Reynolds numbers, in some experiments, such as the experiment by Grove,[4] for the purpose of studying steady wakes splitter plates have been placed into the fluid to prevent shedding. Computationally, such shedding can be avoided by requiring a plane of symmetry, which can be achieved by computing only half of the system.

The Navier-Stokes equation is re-expressed in terms of the vorticity and stream function. The fluid continuity is satisfied by the definition of the stream function. Two numerical methods, one by Peaceman and Rachford[7] and the other by Fromm,[3] are used to compute the vorticity at any time step. The stream function is evaluated from the vorticity. The vorticity on the surface of the obstacle is computed from the stream function and is, then, used as the boundary condition for calculating the vorticity at a new time step. Two Reynolds numbers, 5 and 300, are used to test the methods. At Reynolds number 5, both methods worked quite well, but at Reynolds number 300 neither method is adequate.

In the first part of this report the system and its boundary conditions are given from the physical point of view (Chapter II). Then, the numerical methods and the working equations are listed, and their application is mentioned (Chapter III). The derivation of these equations is shown in Appendix I. The numerical results, including plotted figures of stream function and vorticity, are given in Chapter V.

II. MATHEMATICAL PROBLEM STATEMENT

The flow channel on which the numerical computation is based, is shown in Fig. 1. The channel walls are parallel and in the x-direction. They may be frictional or frictionless, although they are frictionless in the examples used in this work.

A. Differential Equations

In the usual Cartesian coordinates (x^*, y^*) and time t^*, the differential equations that describe the two dimensional flow of an incompressible Newtonian fulid are the equation of continuity and the Navier-Stokes equations, and they can be written as follows:

Equation of Continuity

$$\frac{\partial u^*}{\partial x^*} + \frac{\partial v^*}{\partial y^*} = 0 \qquad (2\text{-}1)$$

Navier-Stokes Equations:

$$\rho\left(\frac{\partial u^*}{\partial t^*} + u^* \frac{\partial u^*}{\partial x^*} + v^* \frac{\partial u^*}{\partial y^*}\right) = -\frac{\partial p^*}{\partial x^*} + \rho g_x^* + \mu\left(\frac{\partial^2 u^*}{\partial x^{*2}} + \frac{\partial^2 u^*}{\partial y^{*2}}\right) \qquad (2\text{-}2)$$

$$\rho\left(\frac{\partial v^*}{\partial t^*} + u^* \frac{\partial v^*}{\partial x^*} + v^* \frac{\partial v^*}{\partial y^*}\right) = -\frac{\partial p^*}{\partial y^*} + \rho g_y^* + \mu\left(\frac{\partial^2 u^*}{\partial x^{*2}} + \frac{\partial^2 u^*}{\partial y^{*2}}\right) \qquad (2\text{-}3)$$

u^*, v^* are the velocity components in x^*, y^* directions, respectively. p^* is the pressure, g^* is the gravitational accelaration, and ρ and μ are the density and viscosity of the fluid.

After differentiationg Eqs. (2-2) and (2-3) with respect to y^* and x^*, respectively, the pressure and gravitational force can be eliminated by subtraction of the two resultant equations. Further, let us define the vorticity as

$$\omega^* = -\left(\frac{\partial u^*}{\partial y^*} - \frac{\partial v^*}{\partial x^*}\right) \tag{2-4}$$

We obtain the vorticity transport equation

$$\frac{\partial \omega^*}{\partial t^*} + u^* \frac{\partial \omega^*}{\partial x^*} + v^* \frac{\partial \omega^*}{\partial y^*} = \nu \left(\frac{\partial^2 \omega^*}{\partial x^{*2}} + \frac{\partial^2 \omega^*}{\partial y^{*2}}\right) \tag{2-5}$$

where $\nu = \frac{\mu}{\rho}$, the kinematic viscosity of the fluid.

Since a circular cylinder is used as the obstacle in the numerical examples, we shall use its radius R* as the characteristic length. Also, let us denote the uniform upstream velocity by u_∞^* and a reference pressure by P_o^*; then we may form a set of dimensionless variables as follows:

$$x = \frac{x^*}{R^*}, \quad y = \frac{y^*}{R^*}, \quad t = \frac{t^* u_\infty^*}{R^*}$$

$$u = \frac{u^*}{u_\infty^*}, \quad v = \frac{v^*}{u_\infty^*}, \quad P = \frac{P^* - P_o^*}{1/2 \rho u_\infty^{*2}}, \quad \omega = \frac{\omega^* R^*}{u_\infty^*}$$

When these dimensionless variables are introduced into Eqs.(2-1), (2-4) and (2-5), we obtain

$$\frac{\partial u}{\partial x} + \frac{\partial v}{\partial y} = 0 \tag{2-6}$$

$$\omega = -\left(\frac{\partial u}{\partial y} - \frac{\partial v}{\partial x}\right) \tag{2-7}$$

$$\frac{\partial \omega}{\partial t} + u \frac{\partial \omega}{\partial x} + v \frac{\partial \omega}{\partial y} = \delta \left(\frac{\partial^2 \omega}{\partial x^2} + \frac{\partial^2 \omega}{\partial y^2}\right) \tag{2-8}$$

where δ is 2.0/Re with Re, the Reynolds number, defined by

$$\frac{2R^* u_\infty^* \rho}{\mu}$$

Generally, Eq. (2-6) can be satisfied by defining a stream function ψ such that

$$u = \frac{\partial \psi}{\partial y} \qquad \text{and} \quad v = - \frac{\partial \psi}{\partial x} \tag{2-9}$$

Eq. (2-7) can then be written as

$$\frac{\partial^2 \psi}{\partial x^2} + \frac{\partial^2 \psi}{\partial y^2} = - \omega \tag{2-10}$$

which is a form of Possion's equation. Equations (2-10) and (2-8), supplemented by Eq. (2-9), are coupled to yield the vorticity and stream function of the flow field.

B. Boundary Conditions

As shown in Fig. 1, the boundaries prescribed in the two-dimensional channel may be classified into four types; namely, the inlet, the outlet, the frictionless walls, and the solid obstacles (this includes the frictional walls). Since we are solving both Eqs. (2-8) and (2-10), the vorticity and the stream function should be specified at the boundaries.

1. Inlet

We assume the incoming flow is not rotational, i.e., $\omega = 0$. Physically, we may desire a uniform flow in the x-direction which may be achieved by setting u = constant. This can be accomplished here by letting

$$\psi = y$$

so that

$$\frac{\partial \psi}{\partial y} = u = 1 \tag{2-11}$$

Therefore, the inlet boundary conditions may be summarized as

$$\left.\begin{aligned} \omega &= 0 \\ \psi &= y \end{aligned}\right\} \tag{2-12}$$

This means that the x velocity is uniform. It also means that $\partial^2\psi/\partial x^2 = 0$, but not that $v = 0$.

2. Outlet

Since the differential equations are elliptic, an end boundary condition is necessary at the channel exit. One wants to select this boundary condition so that the resulting solution will approximate that for an infinitely long channel.

If we assume that the channel is sufficiently long with flow confined between two parallel frictional or frictionless walls, then at the outlet the flow is mainly in the x-direction, and we could expect the vorticity gradient to be small. Consequently, the vorticity is mainly transported by convection, not by diffusion. Hence, $\frac{\partial^2 \omega}{\partial x^2}$, which contributes to the diffusion of vorticity in the x-direction, may be considered negligible.

By a similar reason we could expect $\frac{\partial v}{\partial x} = 0$, which implies that

$$\frac{\partial^2 \psi}{\partial x^2} = 0$$

So, we chose the outlet boundary conditions to be

$$\left.\begin{aligned} \frac{\partial^2 \omega}{\partial x^2} &= 0 \\ \frac{\partial^2 \psi}{\partial x^2} &= 0 \end{aligned}\right\} \qquad (2\text{-}13)$$

For a thorough investigation, it would be necessary to verify that a displacement of the mathematical end of the channel further downstream causes no significant change in the computed flow pattern. However, on second thought, it seems that better boundary conditions at the outlet would be

$$\frac{\partial \omega}{\partial x} = \frac{\partial \psi}{\partial x} = 0$$

Since $\frac{\partial^2 \omega}{\partial x^2} = 0$ implies a constant vorticity gradient, thus for an infinitely long channel, the vorticity at infinite tends to be $\pm \infty$. But no real difficulties arose in this work from those in Eq. (2-13), because the magnitude of the vorticity at the outlet (Re = 5) is insignificant.

3. Frictionless Walls

In order to approximate flow problems in infinite media we may wish to make part or all of the channel walls frictionless so that the undisturbed channel flow is uniform instead of parabolic.

By frictionless walls we mean that the shear stress, τ, at the wall is zero. According to Newton's law of viscosity,

$$\tau = - \mu \frac{\partial u}{\partial y} \Big)_{y \text{ at the wall}}$$

Since $\mu \neq 0$, the wall must be moving in such a way that $\frac{\partial u}{\partial y} = 0$. Also, the fluid will not penetrate through the wall, $v = 0$; then from Eq. (2-7) we conclude that $\omega = 0$ at these walls. Thus the boundary conditions become

$$- \frac{\partial \psi}{\partial x} = v = 0 \qquad (2\text{-}14)$$

In addition, $\frac{\partial \psi}{\partial x} = 0$ implies that ψ is a constant for any particular value of y, so for each wall ψ is a constant.

4. Solid Boundaries

We assume no slipping at the solid boundaries, i.e.,

$$\frac{\partial \psi}{\partial t} = 0 \quad \frac{\partial \psi}{\partial n} = 0 \qquad (2\text{-}15)$$

where t is the tangent to the boundary and n is the normal to the boundary. Equation (2-15) also implies that

$$\frac{\partial \psi}{\partial x} = \frac{\partial \psi}{\partial y} = 0 \qquad (2\text{-}16)$$

at the boundary. Thus, a solid boundary must be a streamline of some constant value, which in this work is set at zero, and is used as the reference streamline.

It is not possible to specify a boundary condition for the vorticity in the same way as the other boundaries, because at the solid boundaries it is an unknown which must be computed. However, by means of Eq. (2-10), an up-to-date vorticity at this boundary can be provided for Eq. (2-8). It is a rather involved scheme; detailed discussion is given in Chapter III, Section (D-3).

5. Summary of Boundary Conditions

a. Inlet

$$\left.\begin{aligned} \omega &= 0 \\ \psi &= y \end{aligned}\right\} \qquad (2\text{-}12)$$

b. Outlet

$$\left.\begin{aligned} \frac{\partial^2 \omega}{\partial x^2} &= 0 \\ \frac{\partial^2 \psi}{\partial x^2} &= 0 \end{aligned}\right\} \qquad (2\text{-}13)$$

C. Frictionless walls

$$\left.\begin{aligned} \omega &= 0 \\ \psi &= \text{constant} \end{aligned}\right\} \qquad (2\text{-}14)$$

d. Solid boundary

$$\left.\begin{aligned} &\frac{\partial \psi}{\partial x} = \frac{\partial \psi}{\partial y} = 0 \\ &\psi = \text{constant} = 0 \\ &\omega \quad \text{is to be computed.} \end{aligned}\right\} \qquad (2\text{-}16)$$

C. Initial Conditions

Since this is a time-dependent problem, an initial condition at time zero must be provided to initiate computation. The condition chosen here is the potential flow of the system which would apply if the walls and obstacles are all frictionless. Then at time zero the frictional, solid boundaries are introduced and the corresponding vorticity is calculated. These initial conditions may be viewed as impulsive motion, in which a cylindrical obstacle in a pool of still water is suddenly given a velocity $-u_\infty^*$.

III. SOLUTION METHODS BY FINITE DIFFERENCE EQUATIONS

In numerical computation one must work with numbers; hence Eqs. (2-8), (2-9), and (2-10) are represented in terms of a set of values of ω and ψ taken at discrete intervals of x and y. Generally, the derivatives in the differential equations are represented by finite difference formulas. The derivation is given in Appendix I.

In the following sections the finite difference equations for Eqs. (2-8), (2-9), and (2-10) are listed and their usage is discussed. But before doing that let us refer to Fig. 2, where some mesh points inside the channel are shown. There is a central point E with four adjacent points 1,2,3, and 4, each, respectively, at P_1h, P_2h, P_3h, and P_4h distances away. The mesh size, h, is some abritrarily chosen unit distance between two adjacent points. For mesh points interior to the boundaries P_i's are all equal to one, but for the points near the boundaries this is not necessarily true. For convenience in discussion we shall adopt the convention that the variables (e.g., ψ and ω) at point E are to be computed.

Also, in order to make the finite difference equations more meaningful, the overall calculation shceme will be discussed in the next section.

A. Overall Calculation Scheme

In the following sections the methods employed in calculating the stream function, velocity, and vorticity are discussed separately. The overall scheme which incorporates all these methods is shown, diagramatically, in Fig. 6. First, an initial solution is calculated. This may begin with some simple, arbitrary stream function field which is corrected by the iterative procedure (details discussed in Sec. (B-3)) to obtain the

potential solution of the particular geometry of the system. This potential solution is then used as the initial stream function solution. At this moment the vorticity is zero everywhere. However, at the solid boundary the no-slip condition must be satisfied. This, theoretically, causes infinite vorticity at the solid surface. Obviously, it is not possible to express infinity numerically. However, when the numerical result is calculated from Eq. (2-10) by the finite difference equations discussed in Sec. (D-3), the surface vorticity is finite because the mesh size h is not zero. Consequently, these initial values of surface vorticity have no physical significance. The velocity field is computed from the equations discussed in Sec. C.

After the vorticity at the solid surface, the initial stream function and the velocity are obtained, we advance to a new time, $t = \Delta t$. For this new time, we seek the corresponding ψ and ω. First, ω is calculated by the Peaceman and Rachford[7] or the Fromm[3] method as mentioned in Sec. (D-1) and Sec. (D-2). Note that the solid surface vorticity being used as a boundary condition cannot be brought to the same time t at this point. However, the stream function field can be brought to the new time by using the new vorticity values. This is possible, because the stream function at the solid surface is a constant and the surface vorticity is not involved in the equations used.

With the new stream function, the corresponding new velocity field can be obtained. The one thing left is the solid surface vorticity. This can now be calculated from the new stream function by means of Eq. (2-10), whose various difference equations are given in Sec. (D-3). Thus, the stream function, vorticity, and velocity fields are all brought to the new time $t = \Delta t$. Once again a new time advancement may be made; but in

place of the initial solution, we have the solution at $t = \Delta t$. This scheme is repeated until steady state is reached; that is, no more change in ψ or ω is observed for further time increments.

Actually we have complicated this basic computation scheme by trying to predict the surface vorticity at the end of the time step and introducing a successive approximation procedure for refining this prediction.

B. Stream Function

The stream function is computed by means of Eq. (2-10) with the vorticity field known. In Appendix I, Sec. A, we adopted the convention that Eq. (2-10) has the following finite difference representation:

$$\psi^{(r+1)}(E) = \psi^{(r)}(E) + \frac{\Omega}{C_E}\left[L_{xx}(E) + L_{yy}(E) + h^2\omega(E)\right] \qquad (3\text{-}1)$$

where Ω is the overrelaxation factor which is discussed in Part 3 of this section. $\psi(i)$, ($i = E, 1, 2, 3,$ and 4), is the stream function at mesh point i. Superscript r denotes the corresponding iteration number to which the stream function belongs. $L_{xx}(E)$ and $L_{yy}(E)$ are the finite difference representation of the second order partial derivatives at point E, $\psi_{xx}(E)$ and $\psi_{yy}(E)$, after being multiplied by h^2. These finite difference formulas depend on the geometry of the meshes. This is discussed in the next two parts. C_E is the sum of the coefficients in front of $\psi(E)$ from the difference formula $L_{xx}(E)$ and $L_{yy}(E)$. $\omega(E)$ is the vorticity at mesh point E.

1. Finite Difference Equations in Bulk Flow

For the stream functions away from curved boundaries where only square mesh points are involved;

$$L_{xx}(E) = h^2\psi_{xx}(E) = \psi(3) + \psi(1) - 2\psi(E) + O(h^4)$$

$$L_{yy}(E) = h^2\psi_{yy}(E) = \psi(4) + \psi(2) - 2\psi(E) + O(h^4) \qquad (3\text{-}2)$$

and

$$C_E = 2 + 2 = 4$$

where $O(h^4)$ indicates that the accuracy of the formula is to the order of h^4. Note, the accuracy for $\psi_{xx}(E)$ and $\psi_{yy}(E)$ is $O(h^2)$. By substituting Eq. (3-2) into Eq- (3-1) we obtain

$$\psi^{(r+1)}(E) = \psi^{(r)}(E) + \frac{\Omega}{4}\left(\psi^{(r)}(3) + \psi^{(r+1)}(1) + \psi^{(r)}(4) + \psi^{(r+1)}(2) - 4\psi^{(r)}(E) + h^2\omega(E)\right) \qquad (3\text{-}3)$$

2. Finite Difference Equation Near the Curved Boundary

For the stream function near the curved boundary, $\psi_{xx}(E)$ and $\psi_{yy}(E)$ involve a more complicated representation to maintain the accuracty to $O(h^2)$.

Figure 3 shows a general case of curved boundary. Point B is the boundary point which may or may not coincide with the square mesh points. Points E, 3 and I are the regular mesh points in the channel. The direction of the grid-line (straight line) may be either x or y. The distance between point E and B is scaled by P. This may be P_1, P_2, P_3, or P_4 depending on the direction. Also, as mentioned before, the stream function at the solid boundary is set to zero. With this configuration, in Appendix I we arrive at the following expression for $\psi_{xx}(E)$ and $\psi_{yy}(E)$:

$$\psi_{xx}(E) \text{ or } \psi_{yy}(E) = \frac{1}{h^2}\left(2\,\frac{2-P}{1+P}\,\psi(3) + \frac{P-1}{P+2}\,\psi(I) - \frac{3-P}{P}\,\psi(E)\right) + O(h^2) \qquad (3\text{-}4)$$

Equation (3-4) is substituted into Eq- (3-1) in place of Eq. (3-2) at the curved boundaries. And C_E becomes

$$\frac{3-P}{P} + 2 \quad \text{or} \quad \frac{3-P}{P} + \frac{3-P'}{P'}$$

where prime indicated a different adjacent mesh point. Also note that at $P = 1$, C_E reduces to 4.

3. "Successive-Overrelaxation" Iteration Procedure

The computation procedure used for the stream function calculation is the "extrapolated Liehmann" or "successive-overrelaxation" method. The detailed description can be found in the Digital Computation for Chemical Engineers by Lapidus.[6]

Equation (3-3) as first derived in Appendix I is in the form

$$\psi_{(E)}^{(r+1)} = \psi_{(E)}^{(r)} + \frac{1}{4}\left(\psi_{(3)}^{(r)} + \psi_{(1)}^{(r)} + \psi_{(4)}^{(r)} + \psi_{(2)}^{(r)} - 4.0\times\psi_{(E)}^{(r)} + h^2\,\omega(E)\right)$$

The ψs on the right side are all at the rth iteration, and the overrelaxation factor Ω is absent.

During a computation, for example, starting from the lower lefthand corner of the channel moving in y-direction first, the stream functions $\psi(1)$ and $\psi(2)$ will have values of the (r+1)th iteration while $\psi(E)$, $\psi(3)$, and $\psi(4)$ only have values at the rth iteration. It is advantageous, for faster convergence and less storage, to use $\psi_{(1)}^{(r+1)}$, $\psi_{(2)}^{(r+1)}$ in place of $\psi_{(1)}^{(r)}$ and $\psi_{(2)}^{(r)}$. In addition, an overrelaxation factor, Ω, is introduced to magnify the correction term $\left\{\frac{1}{4}\left(\psi_{(3)}^{(r)} + \psi_{(1)}^{(r+1)} + \ldots + h^2\omega(E)\right)\right\}$ which brings a faster convergence. The value of Ω used is

$$\Omega = 1 + 0.8\left[\frac{2}{1 + 3\sqrt{M}} - 1\right] = 1.682 \qquad (3\text{-}5)$$

where M is the number of mesh points. For the Dirichlet Problem of Laplaces equation on rectangular domain the upper bound on Ω is very close to 2, but in this work the boundary conditions are different and the equation also is different. It is not clear what value of Ω is the best, although it is expected to be near two.

4. Convergence Criterion

The solution is assumed to be attained if the stream function variation of each mesh point between iterations is less than some error limit, i.e.,

$$|\psi(E)^{(r+1)} - \psi(E)^{(r)}| < \text{SERR (Stream function error limit)}$$

SERR used is 0.0001 or smaller.

The stream function calculated seems to be sufficiently accurate and does not contribute noticeable errors to the vorticity field.

C. Velocity Calculation

By definition of the stream function

$$u = \frac{\partial \psi}{\partial y}, \quad v = -\frac{\partial \psi}{\partial x} \tag{2-9}$$

From Appendix I, for the interior mesh points

$$\left.\begin{aligned} u(E) &= \frac{\psi(4) - \psi(2)}{2h} + O(h^2) \\ v(E) &= \frac{\psi(1) - \psi(3)}{2h} + O(h^2) \end{aligned}\right\} \tag{3-6}$$

However, at the boundaries Eq. (3-6) cannot be applied directly, because it involves mesh points external to the defined boundaries.

1. Inlet and Outlet

From the boundary conditions, Eqs. (2-12) and (2-13), we have

$$\frac{\partial^2 \psi}{\partial x^2} = 0$$

If point E of Fig. 2 is at the boundary and P values are all unity, then the above differential equation can be approximated by

$$\frac{\psi(1) + \psi(3) - 2\psi(E)}{h^2} + O(h^2) = 0$$

To the accuracy $O(h^2)$ we have

$$\psi(1) + \psi(3) - 2\psi(E) = 0 \qquad (3\text{-}7)$$

Suppose point E is at the outlet, then $\psi(3)$ is outside of the boundary and v(E) of Eq. (3-6) cannot be used. But by means of Eq. (3-7) $\psi(3)$ can be replaced by $2\psi(E) - \psi(1)$. Thus at the outlet

$$v(E) = \frac{\psi(1) - \psi(E)}{h} \qquad (3\text{-}8)$$

A similar expression would apply at the inlet.

2. Frictionless Walls

The frictionless walls of the channel are parallel to the x-axis; therefore, there is no flow in the y-direction, and v = 0. Besides, the boundary conditions for frictional walls discussed in Chapter 2, Sec. (B-3) imply $\frac{\partial^2 \psi}{\partial x^2} = \frac{\partial^2 \psi}{\partial y^2} = 0$. Thus, after a modification similar to the inlet and outlet, the velocity u(E) can be computed from Eq. (3-6).

3. Solid Boundary

Since we assume no slipping, u = v = 0, no computation is needed.

4. Points Adjacent to the Curved Boundaries

Since near the curved boundaries P values are not necessarily unity, Eq. (3-6) is not applicable. Again, based on the configuration in Fig. 3, it is shown in Appendix I, Sec. (B-2) that u(E) or v(E)

$$= \pm \frac{\psi(4) - (1-P)^2 \psi(E) P^2}{2h} + O(h^2) \qquad (3-9)$$

The plus sign is for u(E) and the minus sign is for v(E).

D. Vorticity

The finite difference form of Eq. (2-8) takes various forms depending on the computation scheme used. In this work two forms are used, namely, the Peaceman-Rachford alternating direction implicit form and Fromm's central time difference form.

1. Peaceman and Rachford Alternating-Direction Implicit Iteration Procedure

This procedure is first used by Peaceman and Rachford to solve the unsteady state heat conduction equation:

$$\frac{\partial T}{\partial t} = \frac{\partial^2 T}{\partial x^2} + \frac{\partial^2 T}{\partial y^2} \qquad (3-10)$$

First, Eq. (3-10) is converted into the finite difference equation

$$\frac{T_{i,j}^{n+\frac{1}{2}} - T_{i,j}^{n}}{\Delta t} = \frac{T_{i+1,j} + T_{i-1,j} - 2T_{i,j}}{h^2} + \frac{T_{i,j+1} + T_{i,j-1} - 2T_{i,j}}{h^2} \qquad (3-11)$$

The subscript i,j are the indices of the mesh points in x and y directions, respectively, while the superscript n is the index on the time steps. Note, on the righthand side no time step on the temperature is indicated.

According to Peaceman and Rachford Eq. (3-11) can be rearranged so that at the first increment of time $\frac{\partial^2 T}{\partial y^2}$ is represented by the values at the time step n while $\frac{\partial^2 T}{\partial x^2}$ is at the time step $n+\frac{1}{2}$. Hence, Eq. (3-11) becomes

$$\frac{T_{i,j}^{n+\frac{1}{2}} - T_{i,j}^{n}}{\Delta t} = \frac{T_{i+1,j}^{n+\frac{1}{2}} + T_{i-1,j}^{n+\frac{1}{2}} - 2T_{i,j}^{n+\frac{1}{2}}}{h^2} + \frac{T_{i,j+1}^{n} + T_{i,j-1}^{n} - 2T_{i,j}^{n}}{h^2}$$

and after further rearrangement it yields

$$T_{i+1j}^{n+\frac{1}{2}} - (2 + \frac{1}{\beta'}) T_{ij}^{n+\frac{1}{2}} + T_{i-1,j}^{n+\frac{1}{2}}$$

$$= - T_{i,j+1}^{n} + (2 - \frac{1}{\beta'}) T_{ij}^{n} - T_{i,j-1}^{n} \qquad (3\text{-}12)$$

where $\beta' = \frac{\Delta t}{h^2}$

The values on the righthand side are known. With boundary values given, Eq. (3-12) forms a set of linear equations for all the mesh points.

$$\begin{cases} B_o T_o + C_o T_1 = D_o, \\ A_r T_{r-1} + B_r T_r + C_r T_{r+1} = D_r \\ A_{N-1} T_{N-2} + B_{N-1} T_{N-1} = D_{N-1} \end{cases} \qquad (3\text{-}13)$$

D_i is the righthand side of Eq. (3-12). Its value is calculated from the known temperatures at time step n. N is the total number of mesh points. The solution of these equations may be obtained in the following manner:

$$\begin{cases} W_o = B_o \\ W_r = B_r - A_r b_{r-1} \qquad (1 \le r \le N - 1) \end{cases} \qquad (3\text{-}14)$$

$$b_r = \frac{C_r}{W_r} \qquad (0 \le r \le N - 2) \qquad (3\text{-}15)$$

and

$$\begin{cases} G_o = \frac{D_o}{W_o} \\ G_r = \frac{D_r - A_r G_{r-1}}{W_r} \qquad (1 \le r \le N - 1) \end{cases} \qquad (3\text{-}16)$$

The solution is

$$T_{N-1} = G_{N-1}$$

$$T_r = G_r + b_r T_{r+1} \qquad (0 \leq r \leq N-2) \qquad (3\text{-}17)$$

Thus, W, b, and G are computed in order of increasing r, and T is computed in order of decreasing r.

During the second time increment a change in "direction" is made; that is, $\frac{\partial^2 T}{\partial y^2}$ is represented by the values at the time step $n+\frac{1}{2}$. Hence Eq. (3-11) becomes

$$T^{n+1}_{i,j+1} - (2 + \frac{1}{\beta'})\, T^{n+1}_{i,j} + T^{n+1}_{i,j-1}$$

$$= T^{n+\frac{1}{2}}_{i+1,j} + (2 - \frac{1}{\beta'})\, T^{n+\frac{1}{2}}_{i,j} - T^{n+\frac{1}{2}}_{i-1,j} \qquad (3\text{-}18)$$

Equation (3-12) is called the x-direction implicit formula and Eq. (3-18) is called the y-direction implicit formula. The advantage of this method is that when x and y "direction" formulas are used alternately (Δt has to be the same in both directions) it guarantees absolute stability over all time steps. However, when it is applied to Eq. (2-8) with the convective terms present, this is not necessarily true.

The corresponding equations for Eq. (2-8) are derived in Appendix I, Sec. C., and they are of the form:

In x-direction:

$$(1 + \alpha u^n(E))\, \omega^{n+\frac{1}{2}}(1) - (2 + \frac{1}{\beta})\omega^{n+\frac{1}{2}}(E) + (1 - \alpha u^n(E))\, \omega^{n+\frac{1}{2}}(3)$$

$$= -\,(1 + \alpha v^n(E))\, \omega^n(2) + (2 - \frac{1}{\beta})\omega^n(E) + (1 - \alpha v^n(E))\, \omega^n(4) \qquad (3\text{-}19)$$

In y-direction

$$(1+\alpha v^n(E))\omega^{n+\frac{1}{2}}(4) - (2+\frac{1}{\beta})\omega^{n+1}(E) + (1-\alpha v^n(E))\omega^{n+1}(2)$$

$$= -(1+\alpha u^n(E))\omega^{n+\frac{1}{2}}(1) + (2-\frac{1}{\beta})\omega^{n+\frac{1}{2}}(E) - (1-\alpha u^n(E))\omega^{n+\frac{1}{2}}(3) \qquad (3\text{-}20)$$

where $\beta = \frac{\delta\Delta t}{h^2}$ and $\alpha = \frac{h}{2\delta}$

Note that the velocity is being held at time step n. Equations (3-19) and (3-20) apply to the interior points and are used to calculate the vorticity at the new time steps $n+\frac{1}{2}$ and n+1.

The boundary conditions for these equations are discussed in the boundary condition sections. At the inlet and the frictionless walls ω is set to zero, and at the solid boundary ω of the preceding time step is used. As indicated in Chapter II, Sec. (B-4), this vorticity is an unknown. The method used for computing this vorticity is given in Sec. (D-3).

At the outlet $\frac{\partial^2\omega}{\partial x^2} = 0$, which implies that

$$\omega(1) + \omega(3) - 2\omega(E) = 0 \qquad (3\text{-}21)$$

If point E in Fig. 2 is on the outlet boundary then point 3 is undefined in Eqs. (3-19) and (3-20). But from Eq. (3-21), $\omega(3)$ can be eliminated which yields for x-direction

$$2\alpha u^{n+\frac{1}{2}}(E)\,\omega(1) - (2\alpha u^{n+\frac{1}{2}}(E) + \frac{1}{\beta})\,\omega^{n+\frac{1}{2}}(E)$$

$$= -(1-\alpha v^n(E))\,\omega^n(2) + (2-\frac{1}{\beta})\,\omega^n(E) - (1+\alpha v^n(E))\omega^n(4) \qquad (3\text{-}22)$$

and y-direction

$$(1+\alpha v^n(E))\,\omega^{n+1}(2) - (2+\frac{1}{\beta})\,^{n+1}(E) + (1-\alpha v^n(E))\omega^{n+1}$$

$$= -(2\alpha u^n(E) - \frac{1}{\beta})\,\omega^{n+\frac{1}{2}}(E) - 2\alpha u^n(E)\;\omega^{n+\frac{1}{2}}(1) \qquad (3\text{-}23)$$

The detailed derivation is also given in Appendix I, Sec. C.

2. Fromm's Central Time Difference Form

Let us write Eq. (2-8) in the form

$$\frac{\partial \omega}{\partial t} = \delta \left(\frac{\partial^2 \omega}{\partial x^2} + \frac{\partial^2 \omega}{\partial y^2} \right) - v_x \frac{\partial \omega}{\partial x} - v_y \frac{\partial \omega}{\partial y} \tag{3-24}$$

Instead of replacing $\frac{\partial \omega}{\partial t}$ by $\frac{\omega^{n+\frac{1}{2}}(E) - \omega^{n}(E)}{\Delta t}$ as in Peaceman and Rachford's method the central time difference formula $\frac{\omega^{n+1}(E) - \omega^{n-1}(E)}{2\Delta t}$ is used. Equation (3-24), hence, can be written as

$$\frac{\omega^{n+1}(E) - \omega^{n-1}(E)}{2\Delta t} = \delta \left(\frac{\omega^n(1) + \omega^n(3) + \omega^n(2) + \omega^n(4) - 4\omega^n(E)}{h^2} \right)$$

$$- u^n(E) \left(\frac{\omega^n(3) - \omega^n(1)}{2h} \right) - v^n(E) \left(\frac{\omega^n(4) - \omega^n(2)}{2h} \right) \tag{3-25}$$

However, Eq. (3-25) is unstable, and Fromm selected

$$-2\omega^{n+1}(E) - 2\omega^{n-1}(E)$$

to replace

$$-4\omega^n(E)$$

in order to achieve stability. Then we have

$$\omega^{n+1}(E)\left(1+\frac{4\delta\Delta t}{h^2}\right) = \omega^{n-1}(E) + \frac{2\delta\Delta t}{h^2}\left(\omega^n(3) + \omega^n(1) + \omega^n(4) + \omega^n(2) - 2\omega^{n-1}(E)\right)$$

$$- \frac{\Delta t}{h}\left(u^n(E)\left(\omega^n(3) - \omega^n(1)\right) + v^n(E)\left(\omega^n(4) - \omega^n(2)\right)\right) \tag{3-26}$$

Equation (3-26) corresponds to Eq. (3-19) and (3-20). It applies to the interior points to bring $\omega(E)$ to the new time step n+1. At the outlet we have Eq. (3-21)

$$\omega(1) + \omega(3) - 2\omega(E) = 0$$

Replacing $\omega(E)$ by $\omega^{n+1}(E) + \omega^{n-1}(E)$ then we have

$$\omega^n(3) + \omega^n(1) - \omega^{n+1}(E) - \omega^{n-1}(E) = 0 \qquad (3\text{-}27)$$

By substituting Eq. (3-27) into Eq. (3-26) we obtain the equation for the outlet boundary

$$\omega^{n+1}(E)\left(1 + \frac{2\delta\Delta t}{h^2} + \frac{\Delta t}{h}\, u^n(E)\right)$$

$$= \frac{2\delta\Delta t}{h^2}\left(\omega^n(4) + \omega^n(2) - \omega^{n-1}(E)\right) - \frac{\Delta t}{h}\left[u^n(E)\left(\omega^{n-1}(E) - 2\omega^n(1)\right)\right.$$

$$\left. + v^n(E)\left(\omega^n(4) - \omega^n(2)\right)\right] \qquad (3\text{-}28)$$

3. Vorticity at the Solid, Curved Boundary

The vorticity at the solid boundary is an unknown in this problem, and it varies from time to time, but it is a necessary boundary condition before either Peaceman and Rachford's or Fromm's method can be used. Let us look at Eq. (2-10) more closely

$$\frac{\partial^2\psi}{\partial x^2} + \frac{\partial^2\psi}{\partial y^2} = -\omega \qquad (2\text{-}10)$$

We see that the vorticity is related to the second order partial derivatives of the stream function. So if these partial derivatives at the solid boundary can be estimated, then, by Eq. (2-10) we can compute the vorticity there.

For convenience let us take the initial start as an example. As mentioned in Chapter II, Sec. C, initially a potential flow solution is provided which means that the stream function throughout the system is known. In addition let us assume the boundary coincides with the square meshes as those shown in Fig. 4a. Then the finite difference equation for Eq. (2-10) is

$$\frac{\psi(1) + \psi(2) + \psi(3) + \psi(4) - 4\psi(E)}{h^2} = -\omega(E) + O(h^2) \qquad (3\text{-}29)$$

If point E is at the solid boundary, as mentioned in the boundary condition section, $\psi(E) = 0$. So,

$$-\omega(E) = \frac{\psi(1) + \psi(2) + \psi(3) + \psi(4)}{h^2} \qquad (3\text{-}30)$$

However, if point E is at the solid boundary, then at least one of its adjacent points is within the solid obstacle where the stream function is not defined. To eliminate these undefined points the no-slip condition can be used; that is,

$$\frac{\partial\psi}{\partial x} = \frac{\partial\psi}{\partial y} = 0 \qquad \text{at the solid boundary.}$$

Their finite difference equations are

$$\left.\begin{aligned} \frac{\psi(3) - \psi(1)}{2h} &= 0 + O(h^2) \Longrightarrow \psi(3) = \psi(1) \\ \frac{\psi(4) - \psi(2)}{2h} &= 0 + O(h^2) \Longrightarrow \psi(4) = \psi(2) \end{aligned}\right\} \qquad (3\text{-}31)$$

Thus, supplemented by Eq. (3-31) we can compute the vorticity at the solid boundary by means of Eq. (3-30).

When a curved boundary is encountered, such as shown in Fig. 4b, the situation becomes more complicated. First, the so-called "pseudo-boundary" points, denoted by PB, are introduced. Although these points may be interior to the solid, if mathematically we can estimate their vorticity, they can be used just as the previous boundary points. Then the vorticity calculation equations for interior points need not be changed for the curved boundary. This simplifies the computation

considerably. As shown in Fig. 4b, some of the PB points are adjacent to two boundary points (type 1) while some are adjacent to only one boundary point (type 2). The finite difference equations accurate to $O(h^2)$ for both types are derived in Appendix I, Sec. (C-3). For PB points adjacent to two boundary points we have

$$\psi_{xx}(PB) \quad \text{or} \quad \psi_{yy}(PB)$$

$$= \frac{4\psi(E)\ (2-P)}{P^2h^2} - \frac{2\psi(3)\ (3-2P)}{h^2(1+P)^2} + O(h^2) \tag{3-32}$$

where the mesh points are arranged in the manner as shown in Fig. 3. For PB points adjacent to one boundary point only we have the configuration shown in Fig. 5., where x', y' axes are tangent and normal to the solid boundary at the point B. Since ψ is constant at the solid boundary, its derivatives with respect to x' equal zero; i.e., $\psi_{x'x'}(B) = 0$. Thus, at point PB, as shown in Appendix I, Sec. (C-3),

$$\psi_{x'x'}(PB) + O(h^2) = 0$$

and

$$\omega(PB) = \psi_{y'y'}(PB) + O(h^2) \tag{3-33}$$

where

$$\psi_{y'y'}(PB) = \frac{4\psi(E)}{P^2h^2}\left[\frac{1}{\cos^2\alpha} + (1-P)\left(1 + \frac{\sin\alpha}{\cos\alpha}\right)\right]$$

$$- \frac{2\psi(4)}{(1+P)^2h^2}\left[\frac{1}{\cos^2\alpha} + 2 - 2P\right]$$

$$- \frac{4(1-P)\cos\alpha\sin\alpha}{h^2(P\cos\alpha + \sin\alpha)^2}\ \psi\ (1) + O(h^2) \tag{3-33'}$$

The vorticity at the actual boundary points themselves using x', y' coordinates is given by

$$-\omega(B) = \psi_{y'y'}(B)$$

$$= \frac{2(1+P)\psi(E)}{Ph\cos\alpha} + \frac{2\psi(4)P}{(1+P)h\cos\alpha} \qquad (3\text{-}34)$$

These values have physical significance, although they are not used in the numerical calculations as boundary conditions while the pseudo-boundary points are.

IV. STABILITY ANALYSIS

It is known that a typical Fourier component solution, $\omega_{ij}^{n} = \omega_o e^{ik_1 j} e^{ik_2 j} r^n$, satisfies the differential equation

$$\frac{\partial \omega}{\partial t} = \delta \left(\frac{\partial^2 \omega}{\partial x^2} + \frac{\partial^2 \omega}{\partial y^2} \right) \tag{4-1}$$

where ω_o is some reference level of the vorticity component. The i's before the k's are the imaginary number $\sqrt{-1}$. k_1 and k_2 are wave numbers of the component variations in the x and y directions, respectively. r is a growth factor of the variation, and the condition for boundedness of the solution is

$$|r| \leq 1 \tag{4-2}$$

For small Re, the convective terms are less important and Eq. (2-8) can be approximated by Eq. (4-1). If Peaceman and Rachford's method is used, the finite-difference form of Eq. (4-1) in the x-direction is

$$\frac{\omega_{ij}^{n+1} - \omega_{ij}^{n-1}}{\Delta t} = \delta \left(\frac{\omega_{i+1j}^{n+1} + \omega_{i-1j}^{n+1} - 2\omega_{ij}^{n+1}}{h^2} + \frac{\omega_{ij+1}^{n} + \omega_{ij-1}^{n} - 2\omega_{ij}^{n}}{h^2} \right) \tag{4-3}$$

After substituting the Fourier solution into Eq. (4-3), we obtain

$$r = \frac{(1-2\beta) + 2\beta \cos k_2}{(1+2\beta) - 2\beta \cos k_1} \tag{4-4}$$

where

$$\beta = \frac{\delta \Delta t}{h^2} \tag{4-5}$$

When the x and y directions are combined together then

$$r^2 = \frac{(1-2\beta)+2\beta \cos k_2}{(1+2\beta)-2\beta \cos k_1} \times \frac{(1-2\beta)+2\beta \cos k_1}{(1+2\beta)-2\beta \cos k_2} \tag{4-6}$$

which has an absolute value less than unity for all values of β and k's. However, β must be the same for the two time steps.

If Fromm's method is used, Eq. (4-1) has the form

$$\frac{\omega_{ij}^{n+1} - \omega_{ij}^{n-1}}{2\Delta t} = \frac{\delta}{h^2}\left(\omega_{i+1j}^{n} + \omega_{i-1j}^{n} + \omega_{ij+1}^{n} + \omega_{ij-1}^{n} - 2\omega_{ij}^{n+1} - 2\omega_{ij}^{n-1}\right) \tag{4-7}$$

Substitution of the Fourier solution into the above equation leads to

$$r^2 - \frac{4\beta}{4\beta+1}(\cos k_2 + \cos k_1)r + \frac{4\beta-1}{4\beta+1} = 0 \tag{4-8}$$

Let $$\gamma = 2\beta(\cos k_1 + \cos k_2) \tag{4-9}$$

then

$$r = \frac{1}{4\beta+1}\left(\gamma \pm \sqrt{\gamma^2 - 16\beta + 1}\right) \tag{4-10}$$

From Eq. (4-9) we note

$$-4\beta \leq \gamma \leq 4\beta$$

For r real, $\gamma^2 + 1 - 16\beta^2 > 0$.

The left hand side is at its maximum when $\gamma = \pm 4\beta$

$$r_{max} = \frac{4\beta+1}{4\beta+1} = 1 \tag{4-11}$$

For r imaginary, $\gamma^2 + 1 - 16\beta^2 < 0$. The lefthand side is at is minimum when $\gamma = 0$.

$$\bar{rr} = \frac{4\beta-1}{4\beta+1} < 1 \tag{4-12}$$

Therefore, at small Re Fromm's method is also stable for all time steps. For large Re the convective terms become more important. In the asymptotic case Re $\rightarrow \infty$, Eq. (2-8) becomes

$$\frac{\partial \omega}{\partial t} = - u \frac{\partial \omega}{\partial x} - v \frac{\partial \omega}{\partial y} \tag{4-13}$$

In finite difference form it becomes

$$\frac{\omega_{ij}^{n+1} - \omega_{ij}^{n}}{\Delta t} = -u_{ij} \frac{\omega_{i+1,j} - \omega_{i-1,j}}{2h} - v_{ij} \frac{\omega_{ij+1} - \omega_{ij-1}}{2h} \tag{4-14}$$

If we assume that the Fourier solution is still valid, then for Peaceman and Rachford's method we obtain for the x-direction

$$r = \frac{1-\alpha' v_{ij}(i \sin k_2)}{1+\alpha' u_{ij}(i \sin k_1)} \tag{4-15}$$

where

$$\alpha' = \frac{\Delta t}{h} \tag{4-16}$$

For two time steps

$$|r^2| = \left| \frac{1-\alpha' v_{ij}(i \sin k_2)}{1+\alpha' u_{ij}(i \sin k_1)} \cdot \frac{1-\alpha' u_{ij}(i \sin k_1)}{1+\alpha' v_{ij}(i \sin k_2)} \right| \leq 1 \tag{4-17}$$

which shows a neutral stability. However, these results are rather unrealistic, because at large Re the convection of vorticity is so high that the finite difference formula no longer adequately represents the differential equations. This can be visualized by inspecting the x-direction difference equation,

$$(1+\alpha u_{ij}^{n})\omega_{i-1j}^{n+1} - \left(2+\frac{1}{\beta}\right)\omega_{ij}^{n+1} + (1-\alpha' u_{ij})\omega_{i+1j}^{n+1}$$

$$= -(1-\alpha v_{ij}^{n})\omega_{ij+1}^{n} + \left(2-\frac{1}{\beta}\right)\omega_{ij}^{n} - (1+\alpha v_{ij}^{n})\omega_{ij-1}^{n}$$

with $$\alpha = \frac{h}{2\delta}$$

$$\beta = \frac{\delta \Delta t}{h^2}$$

When the above set of difference equations is solved for all the mesh points, it is necessary to have the coefficients $1+\alpha u_{ij}$ and $1-\alpha u_{ij}$ remain positive. Otherwise one will observe an oscillating vorticity field (the sign on the vorticity changes on every other mesh point) and eventually the stream functions will diverge. Since $\alpha = \frac{h}{2\delta}$, as Re increases, α also increases. u and v are generally on the order of unity, hence, for

$$1-\alpha u_{ij} > 0$$

$$u \cdot \frac{h}{2\delta} < 1 \qquad (4\text{-}18)$$

Therefore, as Re $\rightarrow \infty$, h must $\rightarrow 0$, which implies that an infinite number of mesh points is needed. Such a requirement makes the Peaceman-Rachford method impractical.

However, Fromm applied his method to cases with Re as high as 6000. His stability analysis for the high Re is summarized below, although in practice the size of the time step still has to be found by experimenting. The finite difference equation for Eq. (4-13) is

$$\frac{\omega_{ij}^{n+1} - \omega_{ij}^{n-1}}{2\Delta t} = -\frac{1}{h}\left[u_{ij}^{n}\left(\omega_{i+1j}^{n} - \omega_{i-1j}^{n}\right) + v_{ij}^{n}\left(\omega_{ij+1}^{n} - \omega_{ij-1}^{n}\right)\right] \qquad (4\text{-}19)$$

By substituting the Fourier solution into Eq. (4-19), we obtain

$$r - \frac{1}{r} = -2i \frac{\Delta t}{h} (u \sin k_1 + v \sin k_2) \tag{4-20}$$

Let $$\zeta = \frac{\Delta t}{h} (u \sin k_1 + v \sin k_2) \tag{4-21}$$

then Eq. (4-20) becomes

$$r^2 + 2\zeta\, ir - 1 = 0 \tag{4-22}$$

For stability,

$$\zeta \leq 1 \tag{4-23}$$

or

$$\frac{|u| + |v|}{h} \cdot \Delta t < 1 \tag{4-24}$$

However, after trying Fromm's method at Re = 300, we notice that the accuracy of his equation (not discussed in his report) is also limited by the creiterion shown by Eq. (4-18). This can be shown by rearranging Eq. (3-26) in the following manner:

$$\begin{aligned} &\overset{n+1}{\omega}(E)\left(1+\frac{4\delta\Delta t}{h^2}\right) \\ &= \overset{n+1}{\omega}(E) + \left(\frac{2}{\beta} - \frac{\Delta t}{h} u^n(E)\right)\omega^n(3) + \left(\frac{2}{\beta} + \frac{\Delta t}{h} u^n(E)\right)\omega^n(1) \\ &+ \left(\frac{2}{\beta} - \frac{\Delta t}{h} v^n(E)\right)\omega^n(4) + \left(\frac{2}{\beta} + \frac{\Delta t}{h} v^n(E)\right)\omega^n(2) \\ &- \frac{4}{\beta}\overset{n-1}{\omega}(E) \end{aligned} \tag{4-25}$$

The coefficients in front of the vorticities at the time step n should not change sign if the equation truly represents the differential equation.

Thus

$$\frac{2}{\beta} > \frac{\Delta t}{h} u$$

or

$$1 - \frac{h}{2\delta} u > 0$$

which is Eq. (4-18).

V. RESULTS

The obstacle used in the numerical computation is a circular cylinder. If the cylinder is placed at the center of the two walls, by symmetry, half of the flow pattern will be the mirror image of the other and the front and rear stagnation streamlines are equivalent to a frictionless wall, i.e., $\omega = 0$. Although, at high Re it is known that the vortex behind the object is unstable, theoretically, this can be prevented by computing only half of the channel. Thus, if desired, steady wakes may be studied.

The boundary conditions used are discussed in Chapter II, Sec. B. The channel walls are frictionless, and the only object that is frictional is the circular cylinder. The radius of the cylinder used is 6 mesh points, and the center is placed at the 20th mesh point from the inlet.

Two Reynolds numbers, 5 and 300 are used to test the numerical methods. For the low Reynolds number both Peaceman and Rachford's and Fromm's methods are appliable, and the numerical results are presented below. Unfortunately, neither of the two methods can be used at high Reynolds number. The difficulty is discussed in Chapter VI.

A. Effect of the Impulsive Start at Time Zero

As shown in Fig. 7, at time zero the vorticity at the cylinder is not smooth when plotted with respect to position. This is due to the impulsive motion at zero time which induces an infinite velocity gradient at the surface. Such a gradient is not possible to express numerically. Arbitrarily, a surface vorticity is computed from the potential flow stream functions. Since there are only about 15 mesh points to represent the curved surfaces, some roughness should be expected. However, as shown in the same figure at time 0.0368, diffusion of vorticity has smoothed out the roughness.

B. Stream Function

The stream function at different times is shown in Figs. 8 to 18. ψ_{max} is 4.0 at the upper wall and ψ_{min} is 0.0 at the low wall. $\Delta\psi$ between each streamline is 1/6. There are no negative stream functions near the rear stagnation region, and no vortex is observed. The movement of the stream streamlines can clearly be seen from time to time.

C. Vorticity

Although at such small Re no separation takes place, it is interesting to observe how the vorticity is transported at different time intervals. At small times, vorticity, as expected, is high at the surface, and it is not transported by convection but by diffusion. As shown in Figs.19 to 25, the vorticity is mostly diffusing in the radial direction. In Fig. 25, the vorticity is not quite symmetric, which indicates that the elapsed time is long enough to allow some convective transport of vorticity. Eventually, as steady state is approached, the diffusional and convective transport reach a balance. The vorticity contour at various times are shown in Figs. 19 to 29.

The surface vorticity at time t = 4.0287 (steady state) is shown in Fig. 30. Comparison is made with the values computed by Allen and Southwell[1] at Re = 10.0 and Thom,[10,11] at Re = 10 and 20. There seems no consistancy in the values. In this work the cylinder is in a channel instead of in an infinite medium, thus higher velocity and vorticity values near the top of the cylinder are expected. Also, by comparing Apelt's[2] result at Re = 40.0, Allen and Southwell's results seem to be too high.

VI. DISCUSSION

A. Comparison with Fromm's Method

This work, in many ways, is inspired by the report made by Fromm in Los Alamos. In his report various interesting computational results about unsteady flow past obstacles are shown. Since his main interest is to show that the shedding of the vortices and vortex streets behind the obstacles can be obtained from numerical computations, the fine detail near the obstacles is not studied. The obstacle used in his report is a small rectangular cylinder, but in this work we are interested in obstacles of any arbitrary shape. In addition, it seems that some appropriate changes may be made to his work.

1. Inlet and Outlet Boundary Conditions

The periodic boundary conditions at the inlet and outlet, as used by Fromm, is eliminated.

The consequence of the periodic boundary conditions is that as time progresses the disturbance leaving the outlet is introduced back into the system through the inlet. Also, the instabilities leaving the inlet are re-introduced at the outlet. To replace this periodic boundary condition we introduced $\frac{\partial^2 \psi}{\partial x^2} = \frac{\partial^2 \omega}{\partial x^2} = 0$ at the outlet and $\omega = 0$ and $u =$ constant at the inlet. As shown in the boundary condition section, we are assuming that the channel is sufficiently long. To test the adequacy of the boundary conditions, the channel should be extended further downstream to see if any significant change in the solution occurs. However, due to lack of time this had not been tested.

2. Boundary Conditions at the Channel Walls

In Fromm's work the channel walls are supposed to be miving such that "no extraneous vorticity will creep into the system". In other words, the walls must be moving with the same speed as the fluid in contact with them. To avoid vorticity diffusion through the walls he introduced a pseudo-velocity, which equals the velocity of the wall, exterior to the channel. Such a complicated scheme seems unnecessary, since the same criterion can be attained by setting $\omega = 0$ at the channel walls.

The velocity of the moving walls used by Fromm is constant. As the velocity at the inlet and outlet are not restricted, the periodic boundary conditions and the constant speed walls cause the flow to be slowed down as if there were a series of identical objects upstream. This is undesirable as it becomes impossible to study a single obstacle at some fixed Reynolds number. Thus, by fixing the velocity at the inlet and letting the channel walls be frictionless the total flow rate can be specified.

3. Velocity Evaluation

The velocity components are evaluated at the mesh points in this work, while Fromm evaluated them in between the mesh points, which seems to be cumbersome as the other variables are evaluated at the mesh points.

4. Curved Boundary Introduction

One of the objectives of this work is to investigate the effects of flow past a circular cylinder, not the vortex street far downstream but the vorticity and velocity field near the cylinder. In this case a curved solid boundary is involved. Several lengthy finite difference equations are developed to maintain the computational accuracy to the

order of h^2. The particular dimensionless radius used in the example is 6 mesh units, which gives less than twenty mesh points on the solid surface, yet a smooth vorticity distribution at the surface is obtained. This indicates that the technique used is quite satisfactory. Although the particular geometry used is a circular cylinder, the equations are applicable to any geometry.

5. Methods of Vorticity Computation

In addition to Fromm's central time difference method the Peaceman and Rachford method is also used. From the stability analysis, both methods are supposed to be stable when convection of vorticity is absent. However, at Re = 5, the computational results indicate that the Peaceman and Rachford method is more stable, and larger time steps can be taken. In addition, the time step becomes larger as time progresses. Thus, the computation time required is less. On the contrary, when equivalent time steps are taken, Fromm's method tends to make the stream function diverge. Therefore, at least for low Reynolds numbers, Peaceman and Rachford's method seems to be more efficient.

B. Comparison of Results with Literature Values

A comparison of the surface vorticity with some steady state solution is shown in Fig. 30. The result obtained in this work does seem to be in agreement with the work done by Thom, Apelt, and Southwell and Squire, although the effect of the confinement of the channel causes a higher surface vorticity at the top of the cylinder. The numerical values are given in Table I. The results by Allen and Southwell and Thom at Re = 10 are obtained from the figures shown in their publications; thus it is not the exact result of their work. However, the result by Allen and Southwell

seems to disagree with the other works. Also, the results by Thom at Re = 10 and 20 are too close in magnitude. By comparison it seems that the result for Re = 20 should be higher in order to be consistent with other works.

Table I. The Steady State Surface Vorticity at Re = 5

θ	ω_o	θ	ω_o
0	0	99.59	-2.4964
9.59	-0.8210	109.47	-2.0441
19.47	-1.5523	120.00	-1.3994
30.00	-2.3066	131.81	-0.9000
41.81	-2.9715	138.19	-0.6041
48.19	-3.2105	150.00	-0.3837
60.00	-3.2434	160.53	-0.1259
70.53	-3.3670	170.41	-0.0443
80.41	-3.2074	180.00	0
90.00	-2.9029		

C. High Reynolds Number

As mentioned previously, Fromm was able to show flow patterns downstream at Reynolds numbers as high as 6000. However, his method is not applicable to the problem in this study. It is shown in the stability analysis that at high Re the finite difference representation of the differential equations is no longer accurate unless very fine meshes are used. At Re = 300, the Peaceman-Rachford method breaks down as vorticity at the surface is swept downstream and convergence on the stream function calculation fails. For Fromm's method the stream function is able to converge to a solution when a small time increment is used, but such a

solution does not have any physical meaning when oscillation in the vorticity field occurs. The reason for such a difference in breakdown is not obvious, since both methods have the same stability criterion. Although this may be due to the different computation scheme used.

Also, physically, from boundary layer theory at steady state the boundary layer thickness is in the order of $(Re)^{-1/2}$, which is much less than unity at Re = 300. Therefore, in the front of the cylinder the diffusion of vorticity cannot be accounted for with the mesh size used.

The criterion for a true solution, in addition to the stability with respect to time, is

$$1 - u \frac{h}{2\delta} > 0,$$

which is in agreement with Apelt.[2] With D = 12.0 and u = 1.0, h is approximately 0.013 at Re = 300. Certainly a solution can be obtained by using such small meshes, but the time required on computation makes such attempts formidable. Thus, we conclude that the straightforward application of finite difference methods is not feasible for solving the Navier-Stokes equation when quantitative results near the obstacle surface are desired. Consequently, the results shown by Fromm can only be used for qualitative purposes.

At the same time, the results of this work suggest that if a more general method for high Re is desired, some other approach to the problem has to be made. For example, if the steady state solution is desired, maybe the Lagrangian form of the vorticity transport equation:

$$\frac{D\omega}{Dt} = \delta \nabla^2 \omega$$

is more appropriate. Since for the limiting case, viscosity equal to zero, the vorticity on each fluid element, as it is transported by convection, is an invariant, the diffusion of vorticity may be superimposed on to the flow field. However, how to estimate the diffusion term as the fluid element moves to a new position is not obvious. The numerical method might then resemble the method of characteristics.

VII. CONCLUSIONS

1. The Peaceman-Rachford implicit alternating-direction iteration procedure is applicable to approximate the Navier-Stokes equation at low Reynolds number, and it is superior to the central time difference method of Fromm in rate of convergence and ease in time increment control.
2. General difference equations have been developed to approximate a curved boundary in square meshes to the order of h^2. The result is satisfactory.
3. At low Re, the transient behavior of an impulsively started cylinder can be studied by the numerical scheme used in this work.
4. At high Re, the straightforward application of finite difference method is not feasible to solve the Navier-Stokes equation for the case where fine detail near the surface of the obstacle is desired. It seems that some different approach to the problem should be used.

ACKNOWLEDGEMENTS

This work was supposed under the auspices of the United States Atomic Energy Commission.

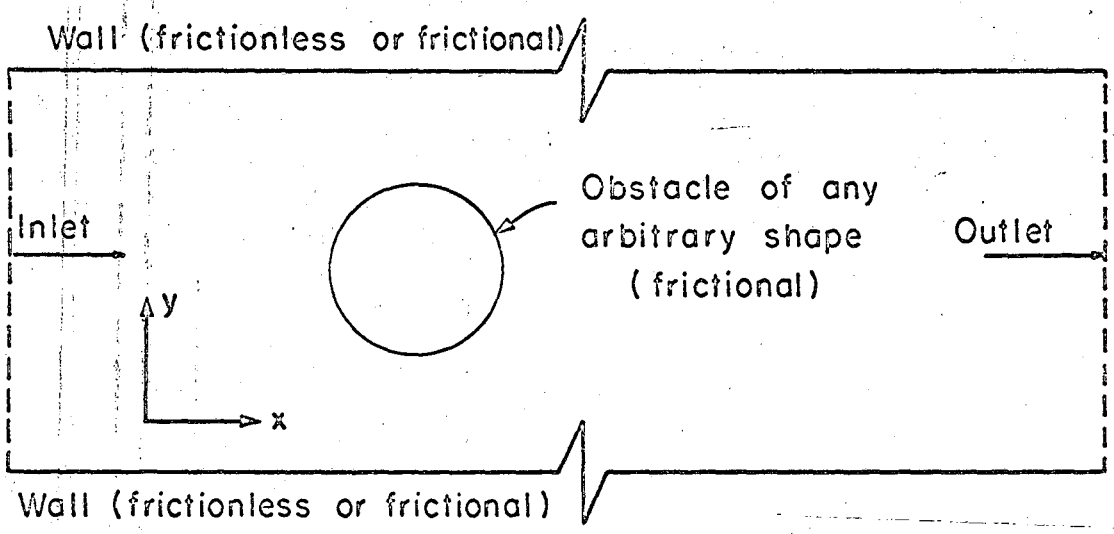

MU.37219

Fig. 1

Flow Channel

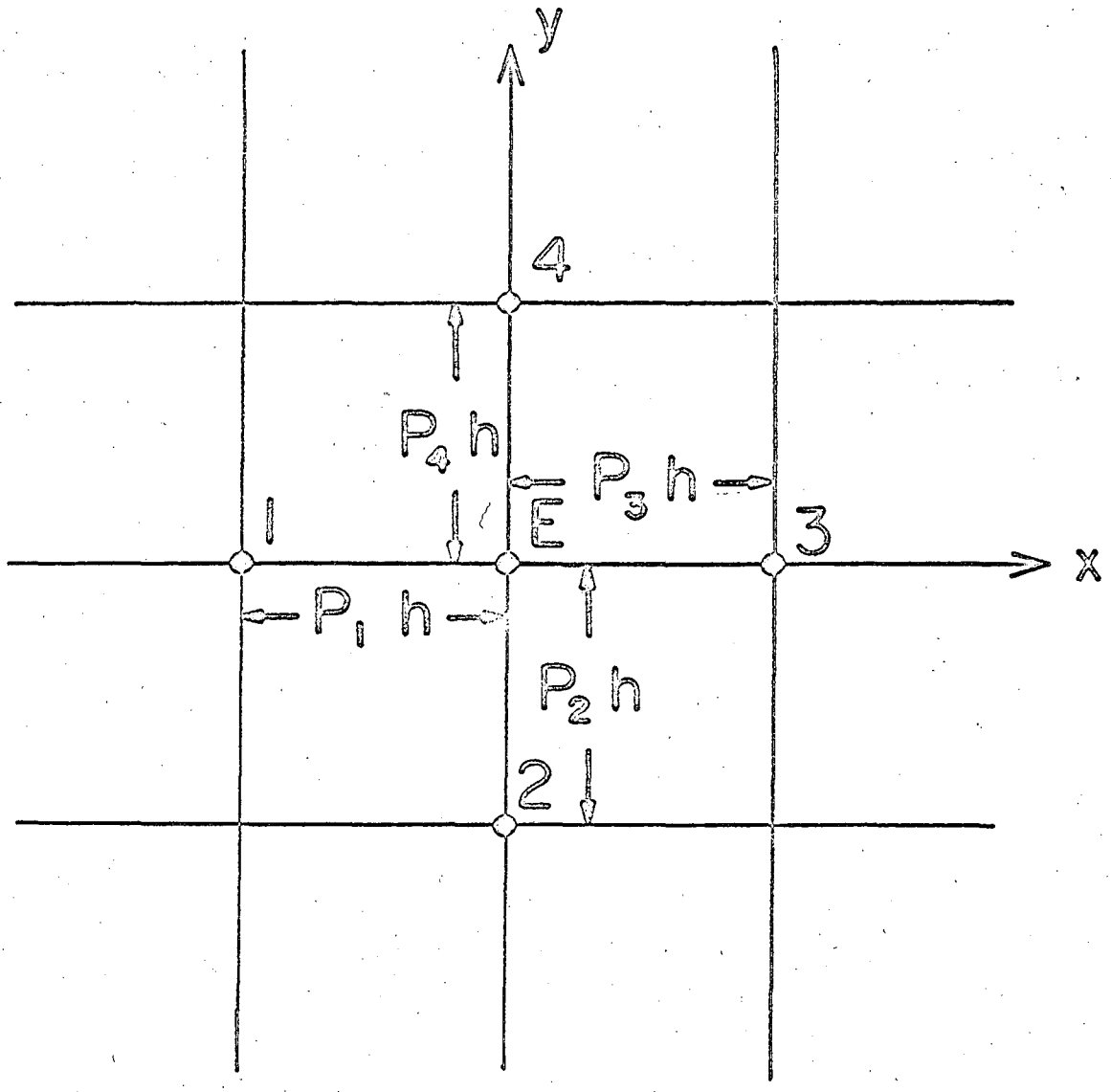

MU-37220

Fig. 2

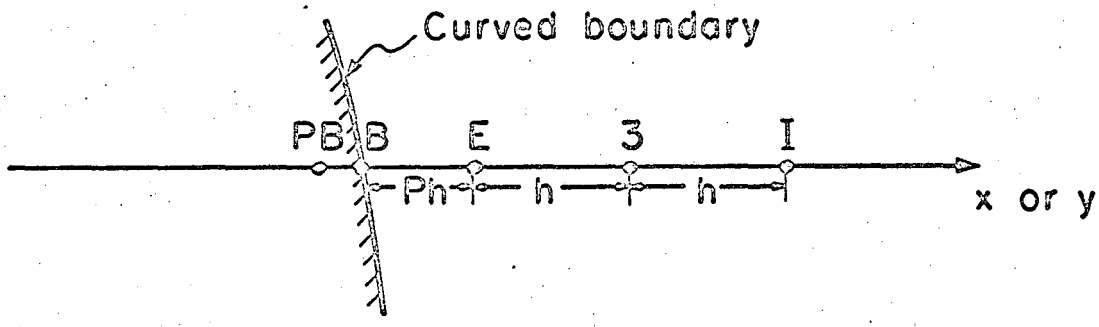

MU-37222

Fig. 3

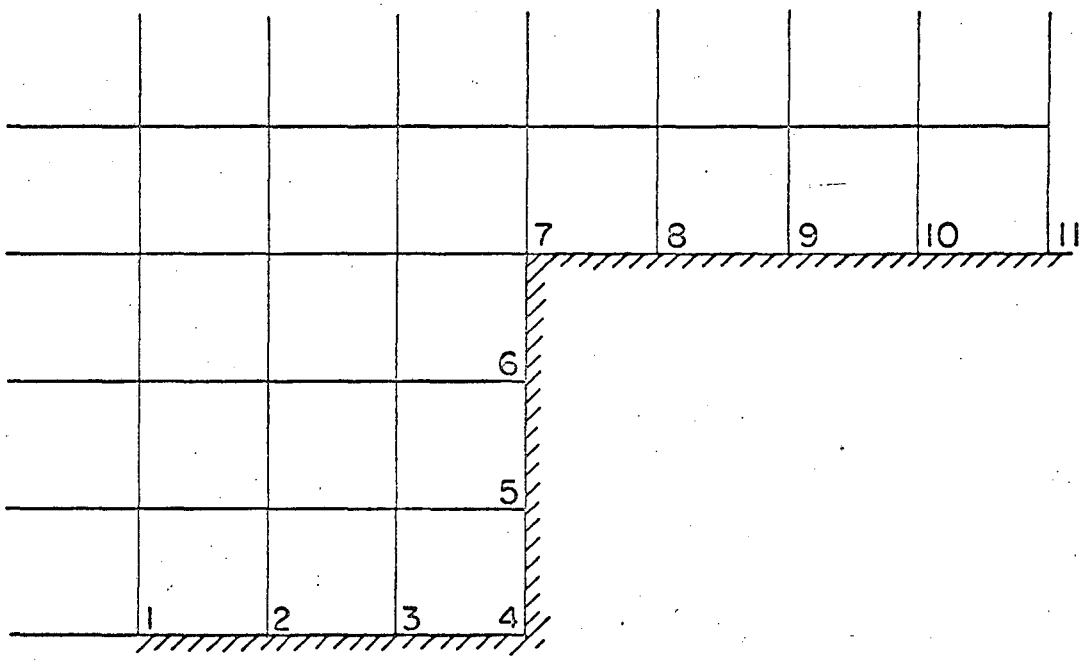

MU-37225

Fig. 4a

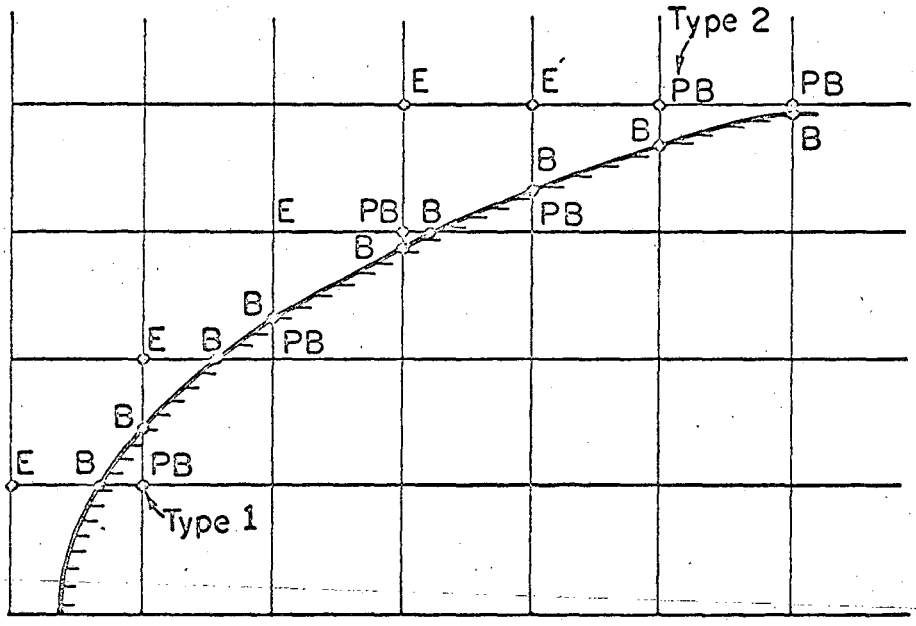

MU-37223

Fig. 4b

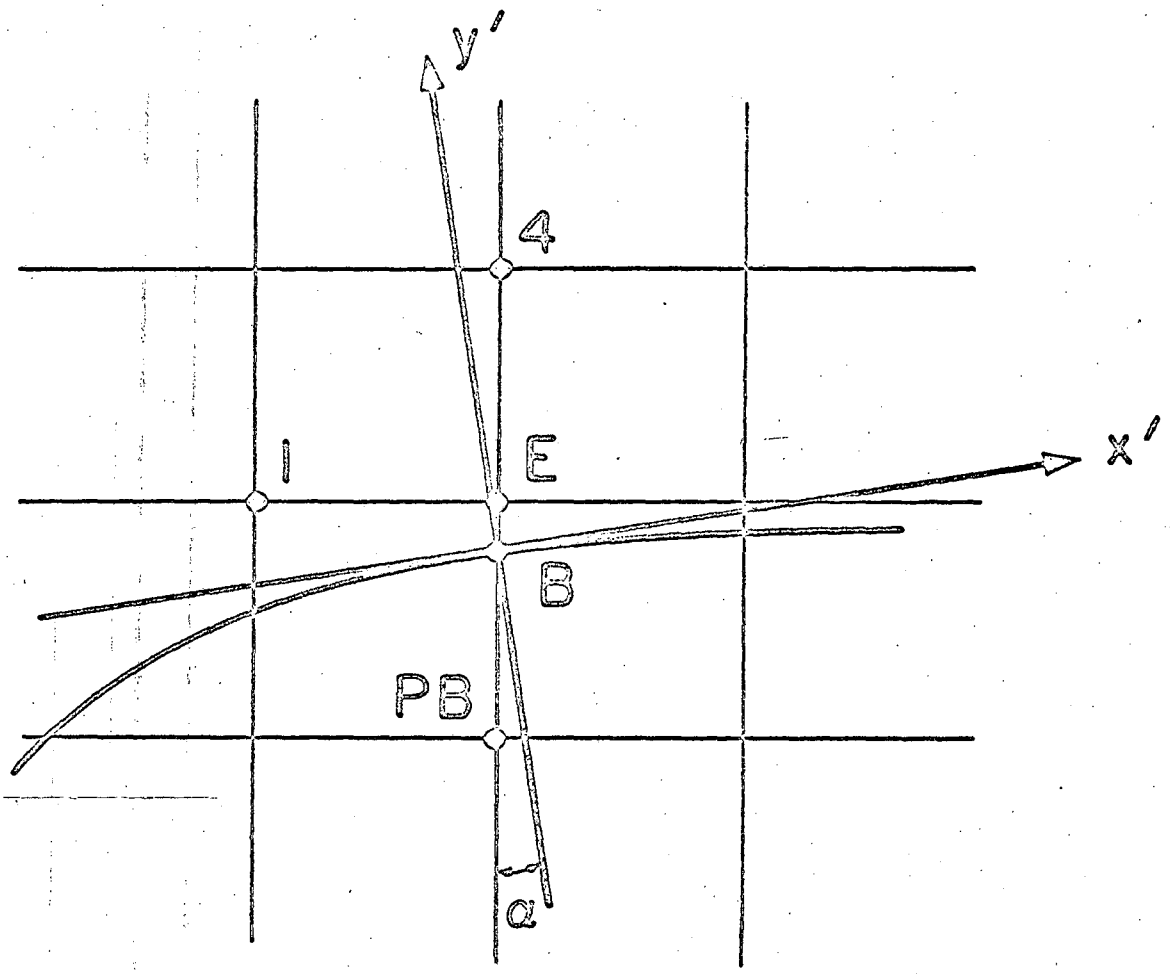

MU-37221

Fig. 5

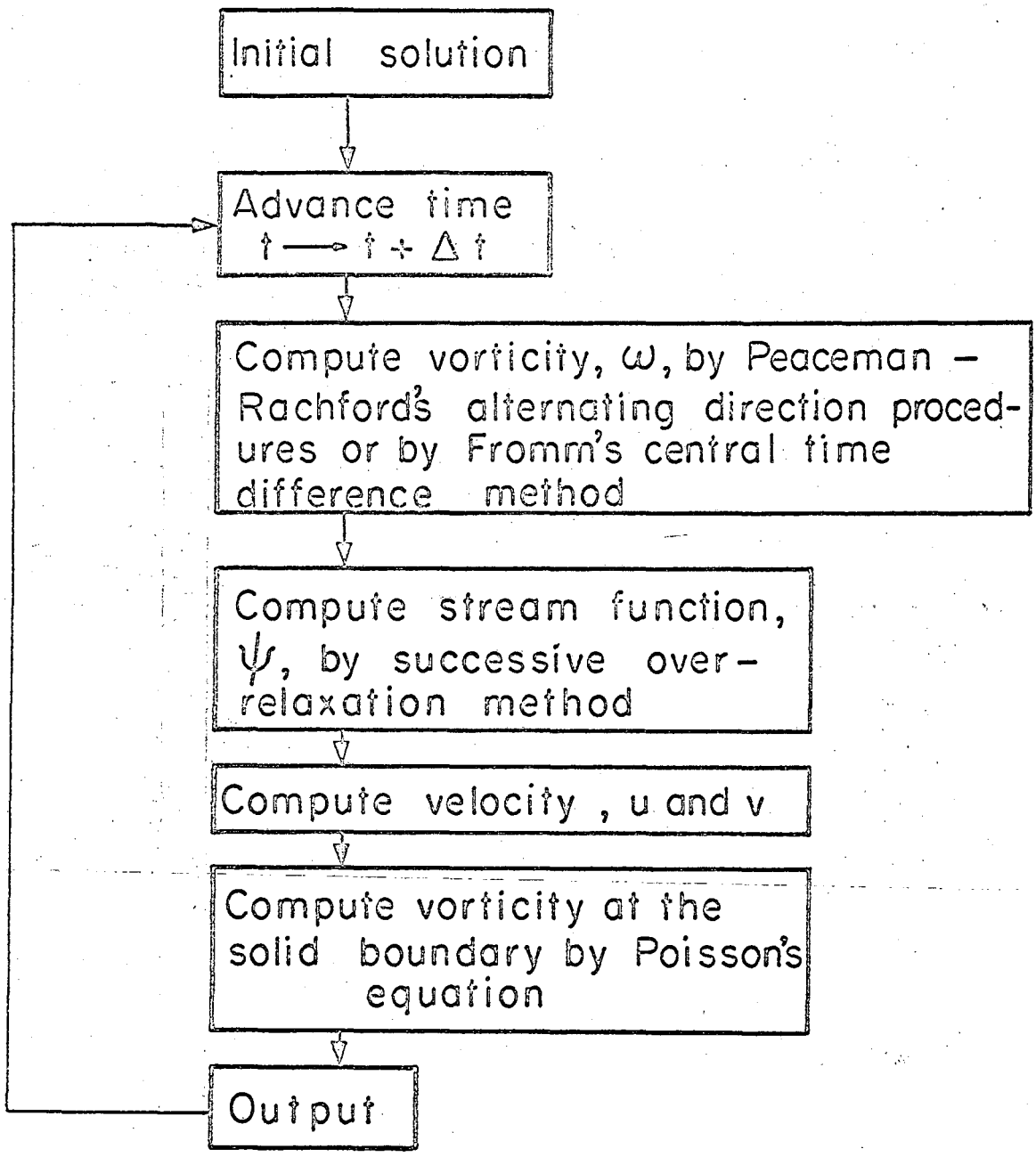

MU-37224

Fig. 6

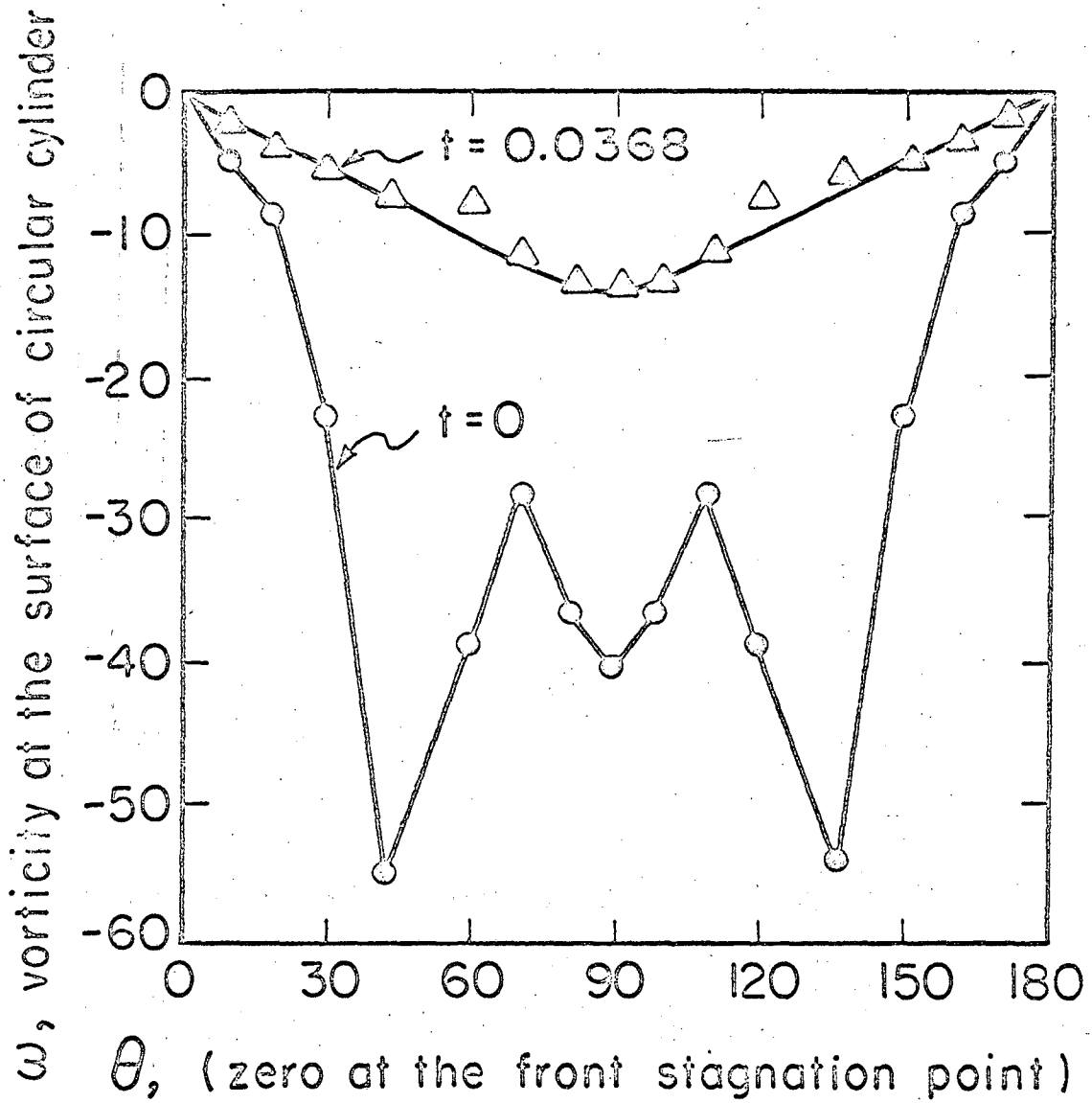

MU-37218

Fig. 7

Damping of the Surface Vorticity

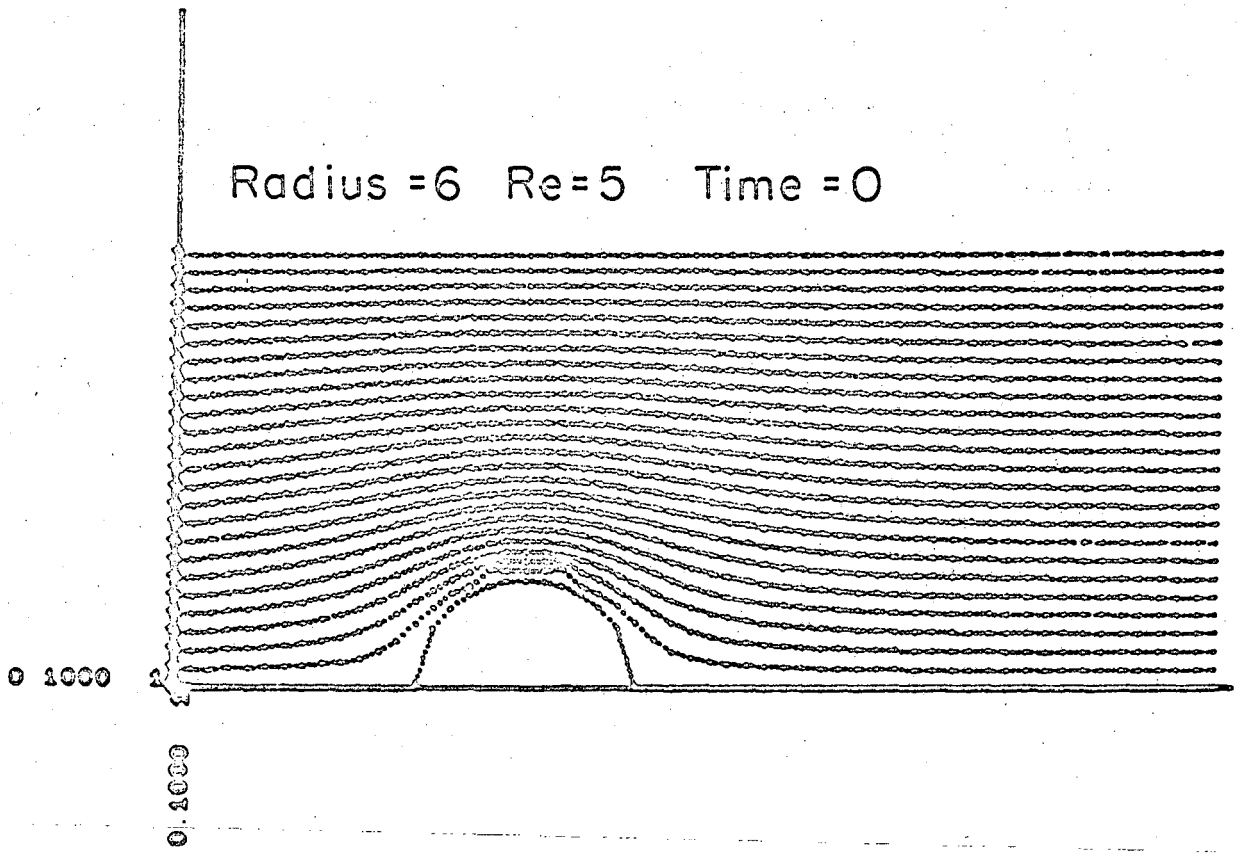

MUB-9387

Fig. 8

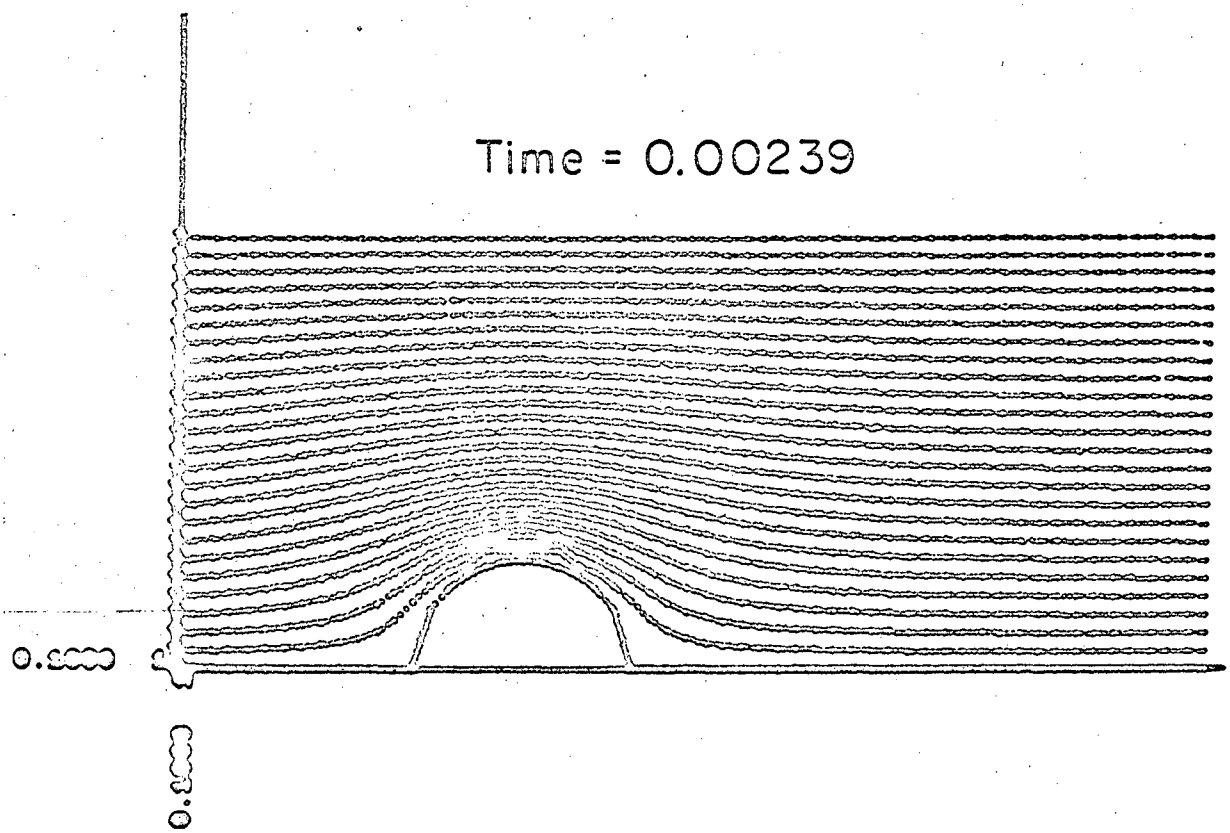

MUB-9386

Fig. 9

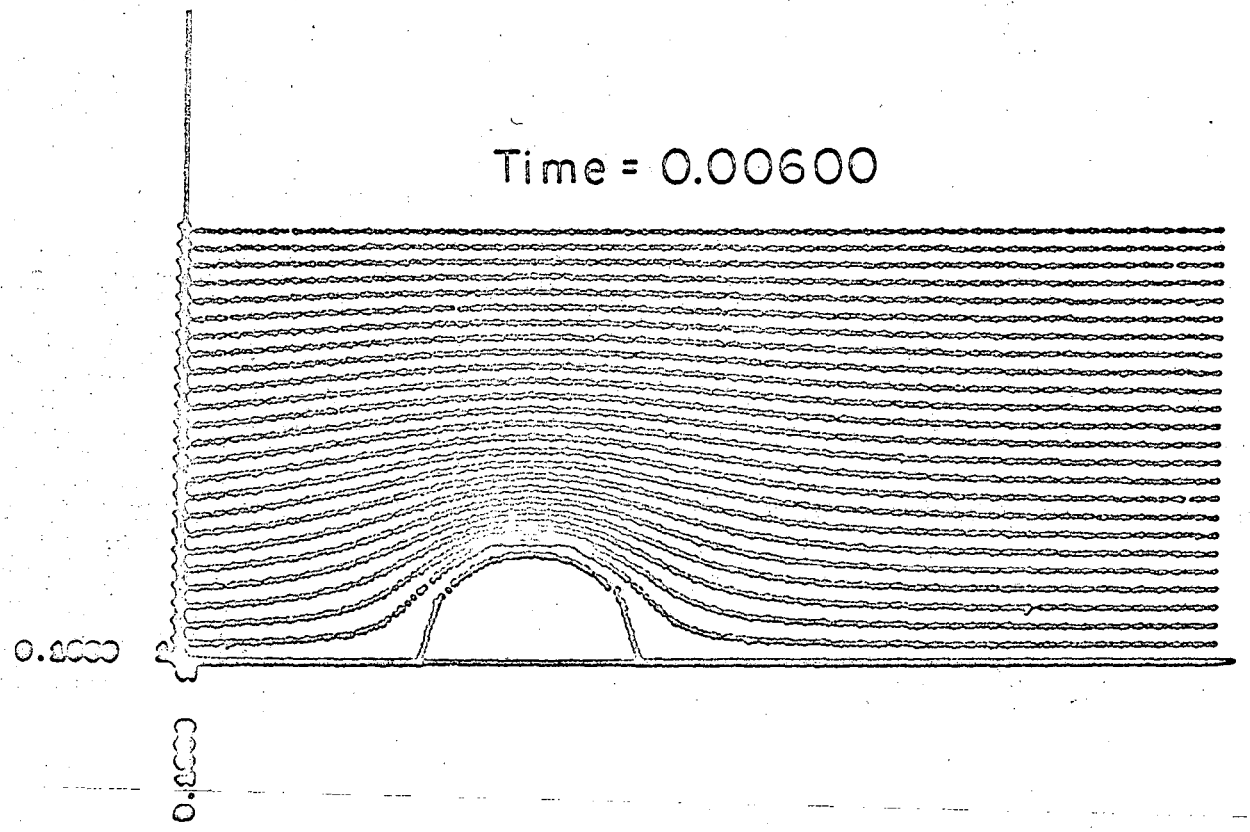

MUB-9385

Fig. 10

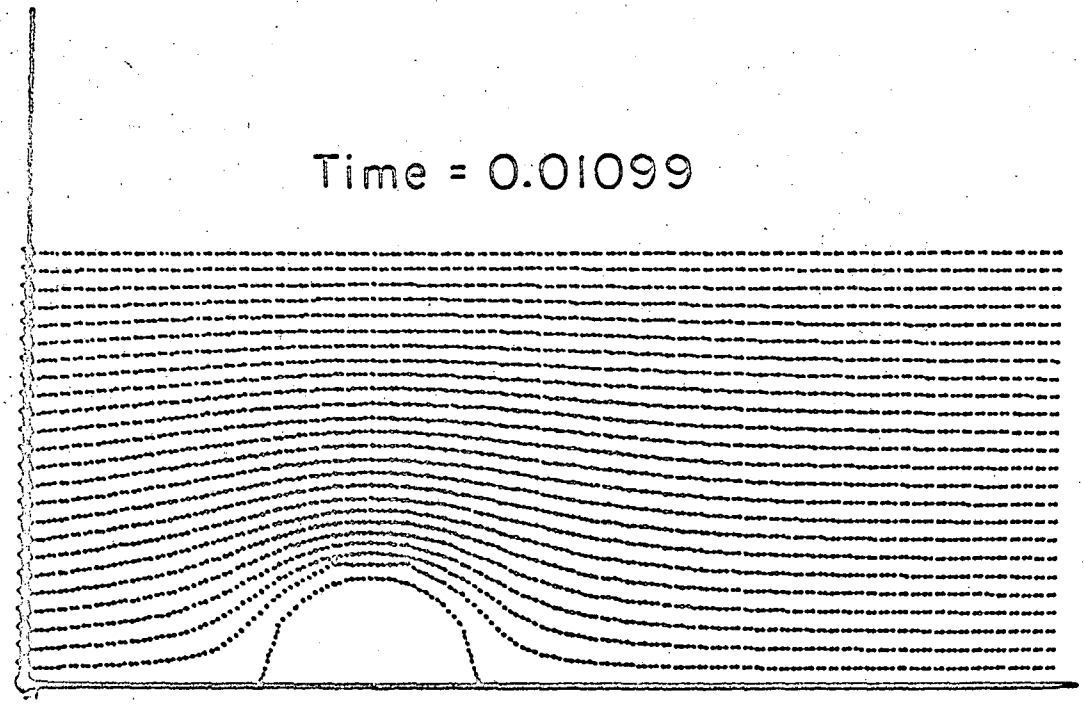

MUB-9384

Fig. 11

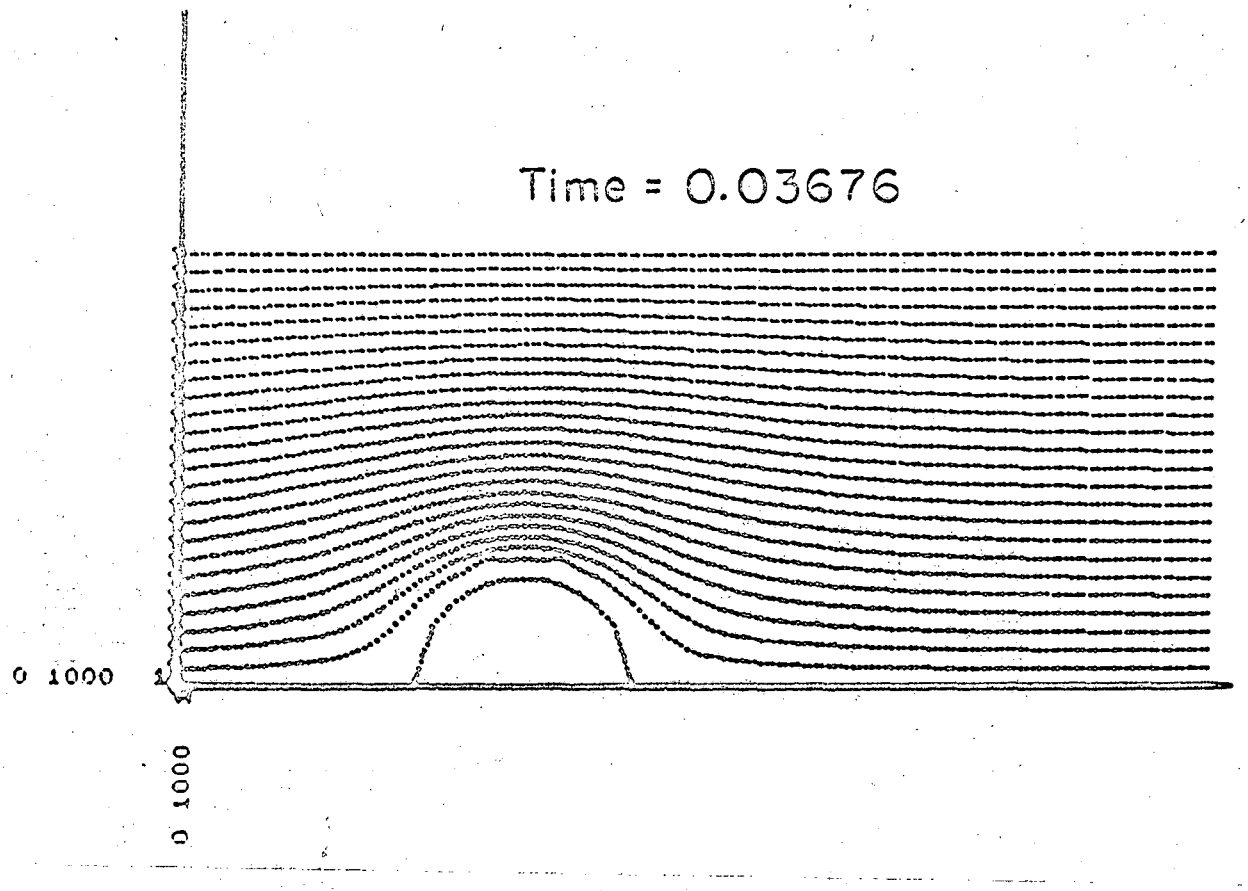

MUB-9380

Fig. 12

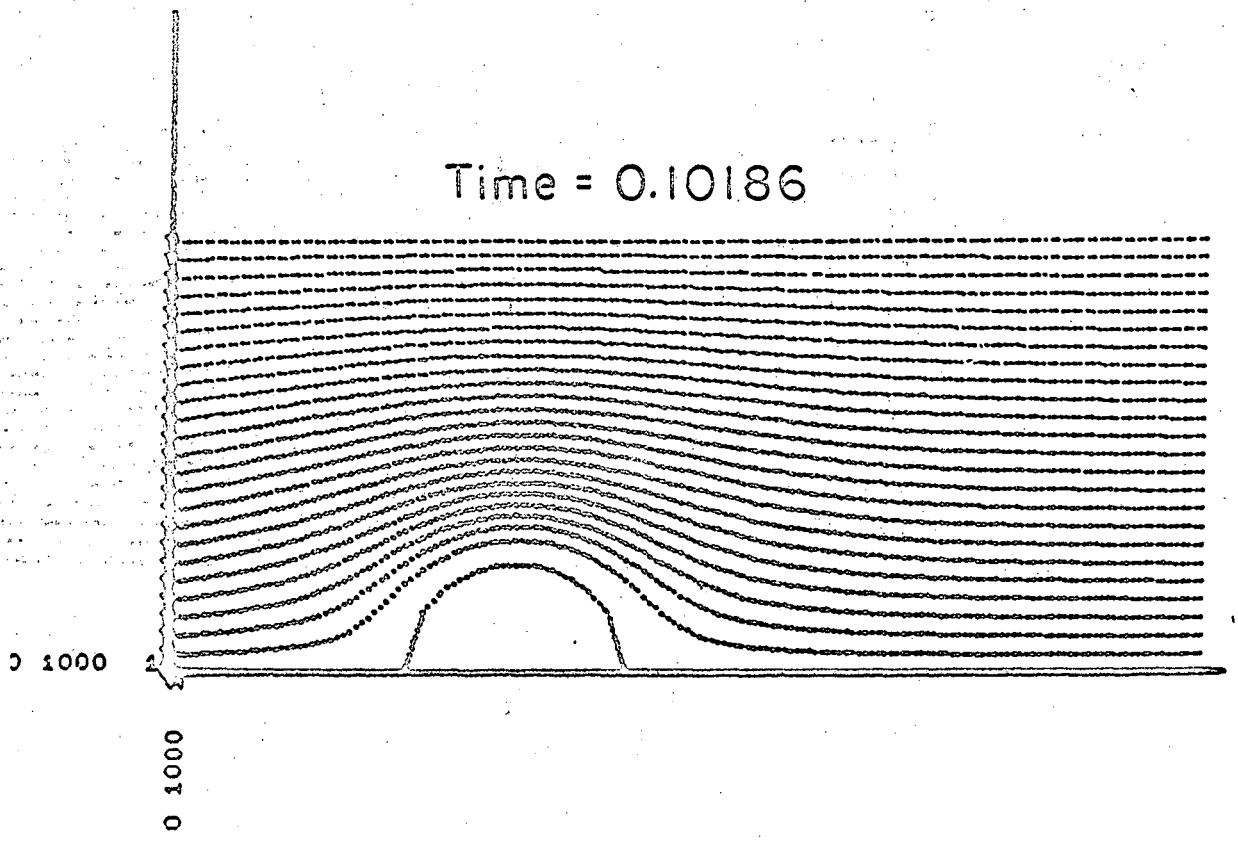

MUB-9383

Fig. 13

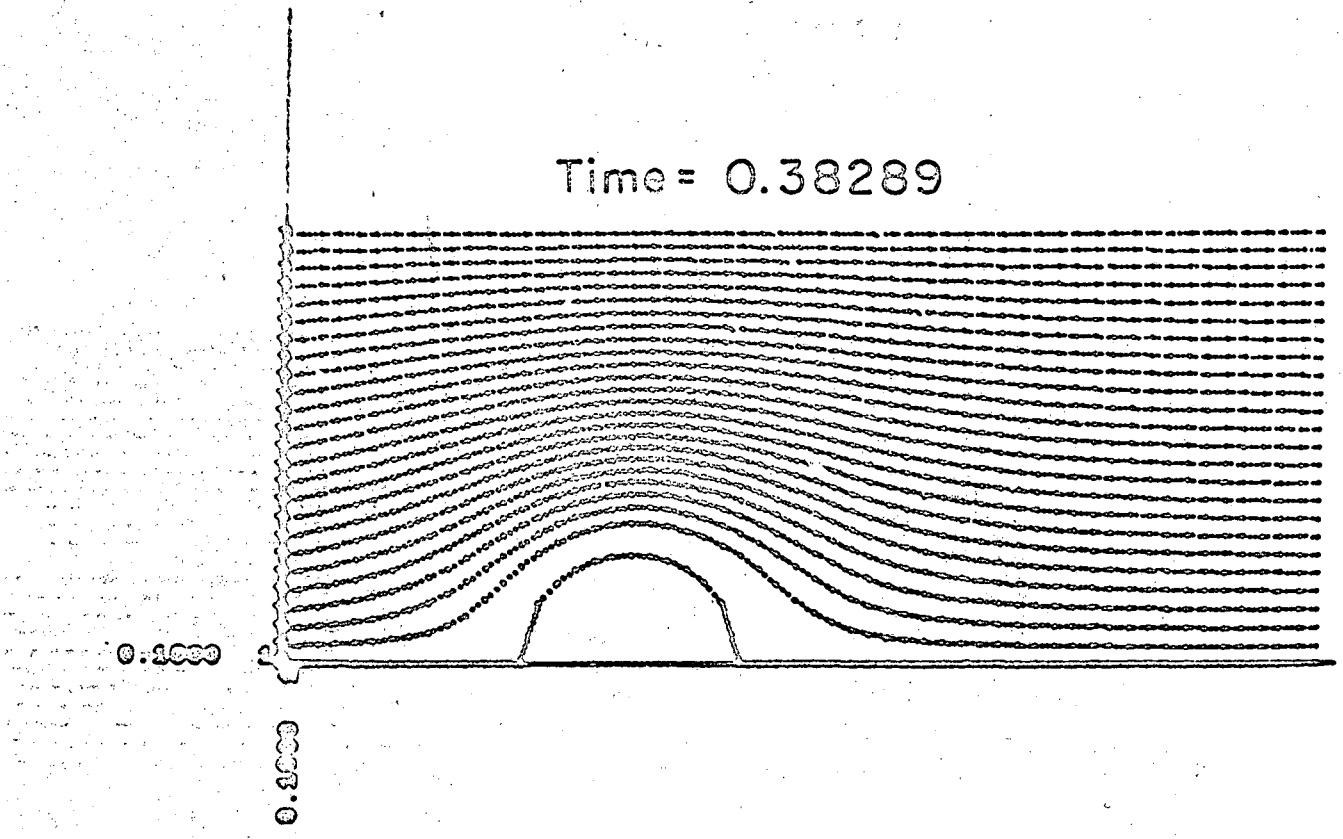

MUB-9382

Fig. 14

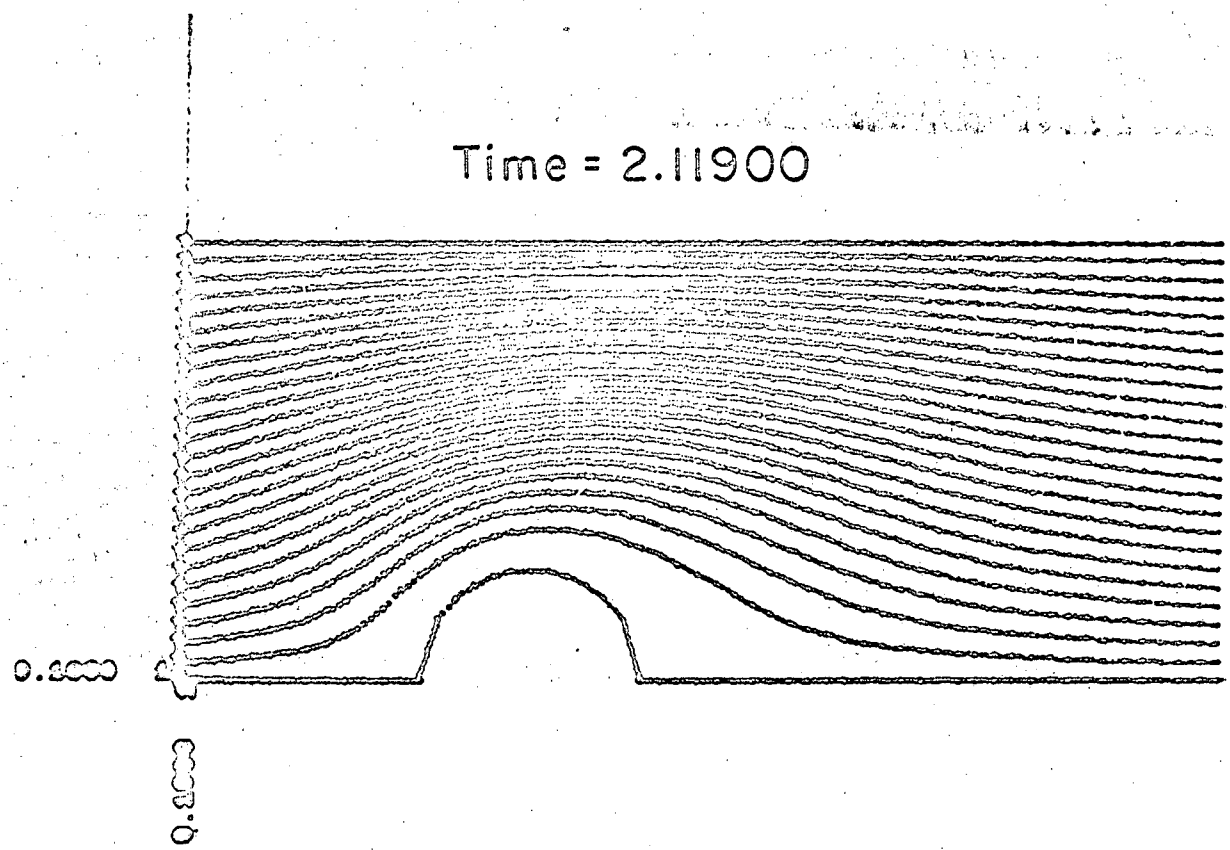

MUB-9379

Fig. 15

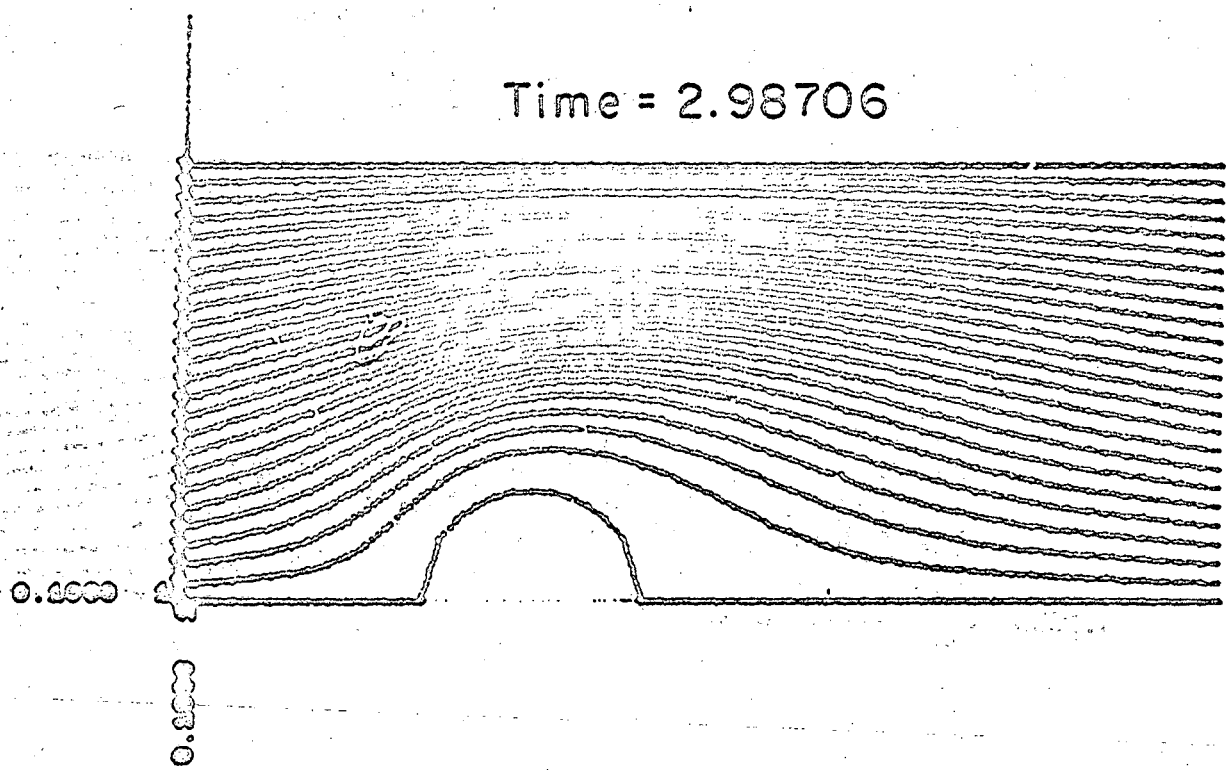

MUB-9381

Fig. 16

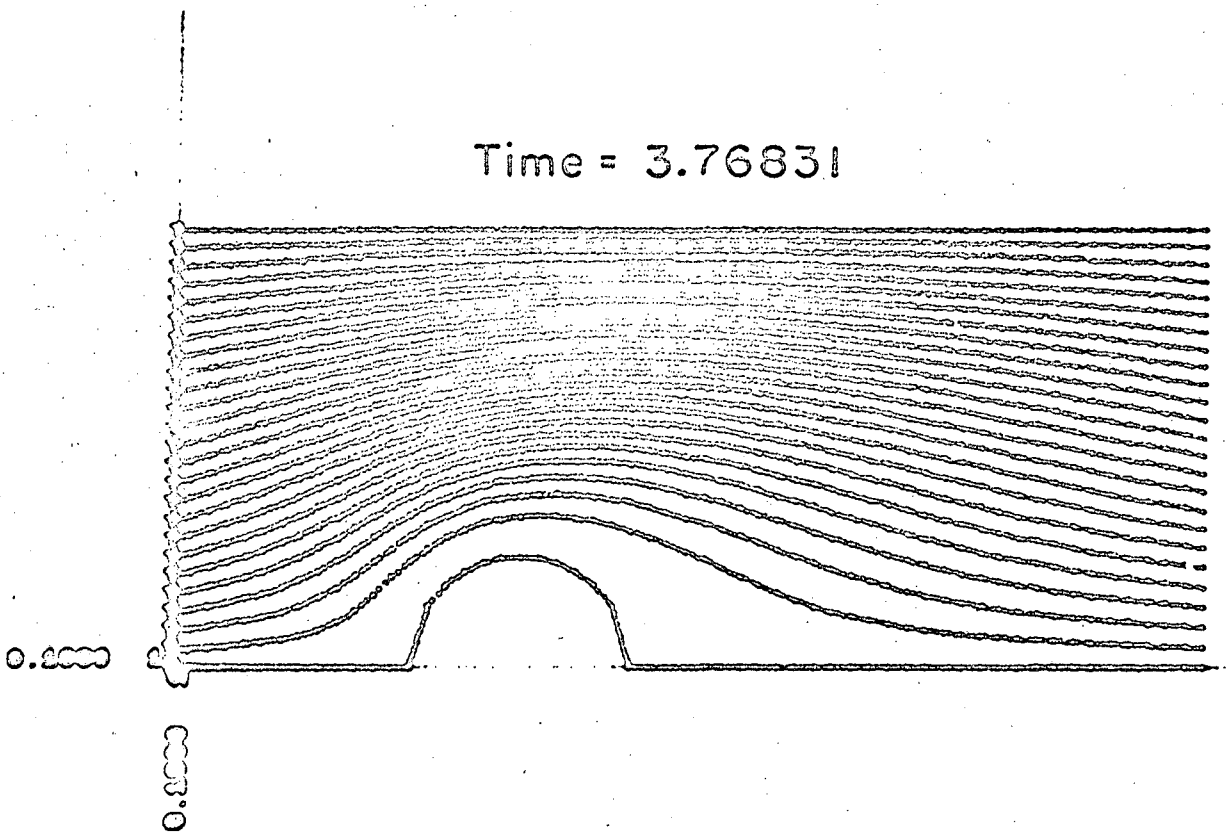

MUB-9378

Fig. 17

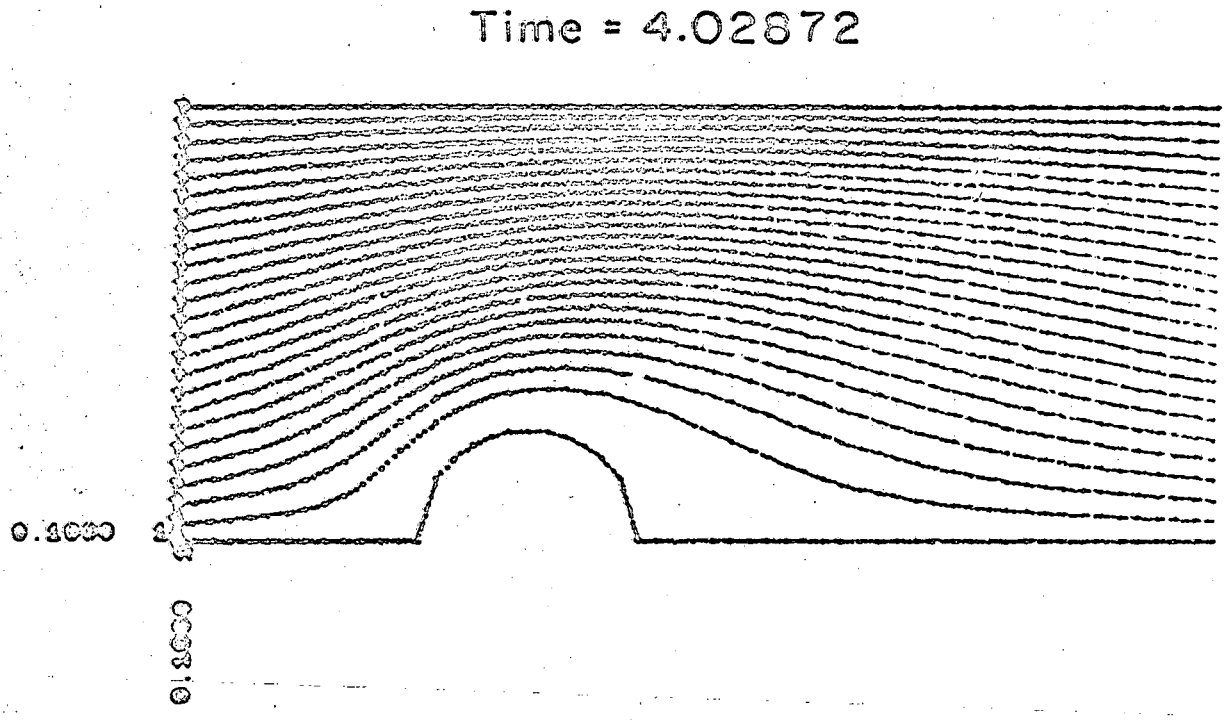

MUB-9377

Fig. 18

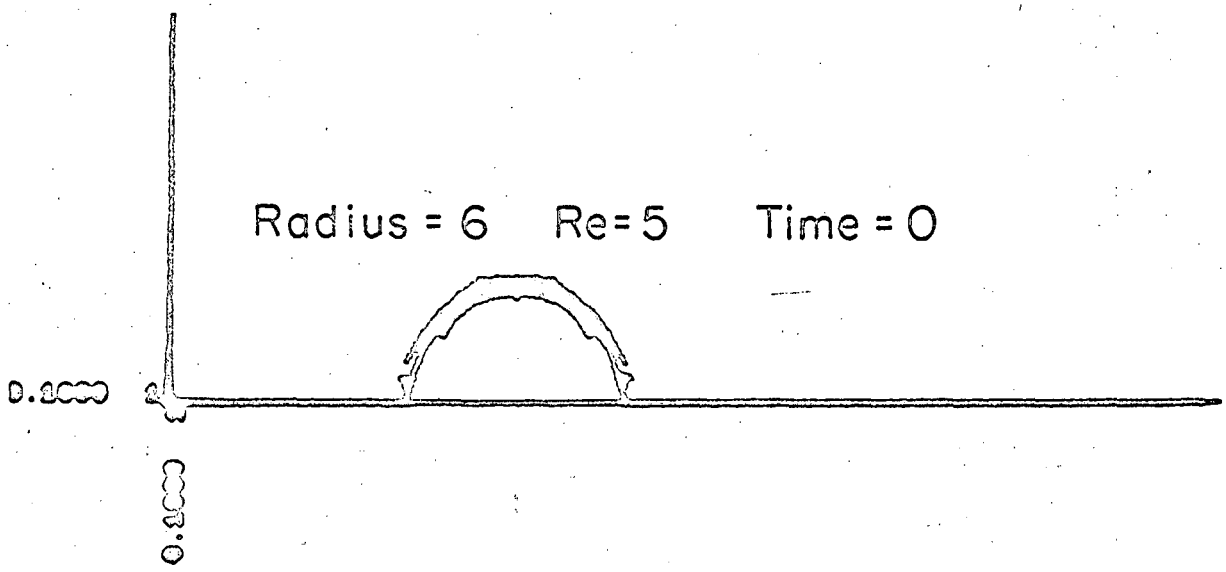

MUB-9388

Fig. 19

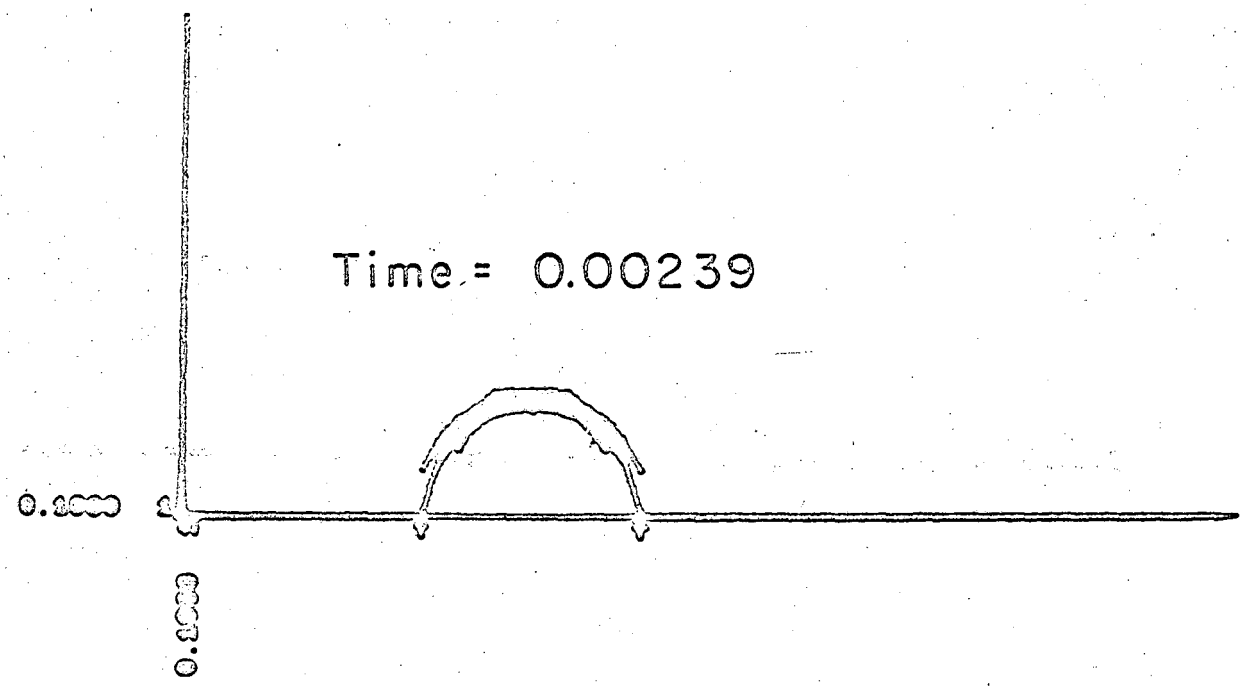

MUB-9376

Fig. 20

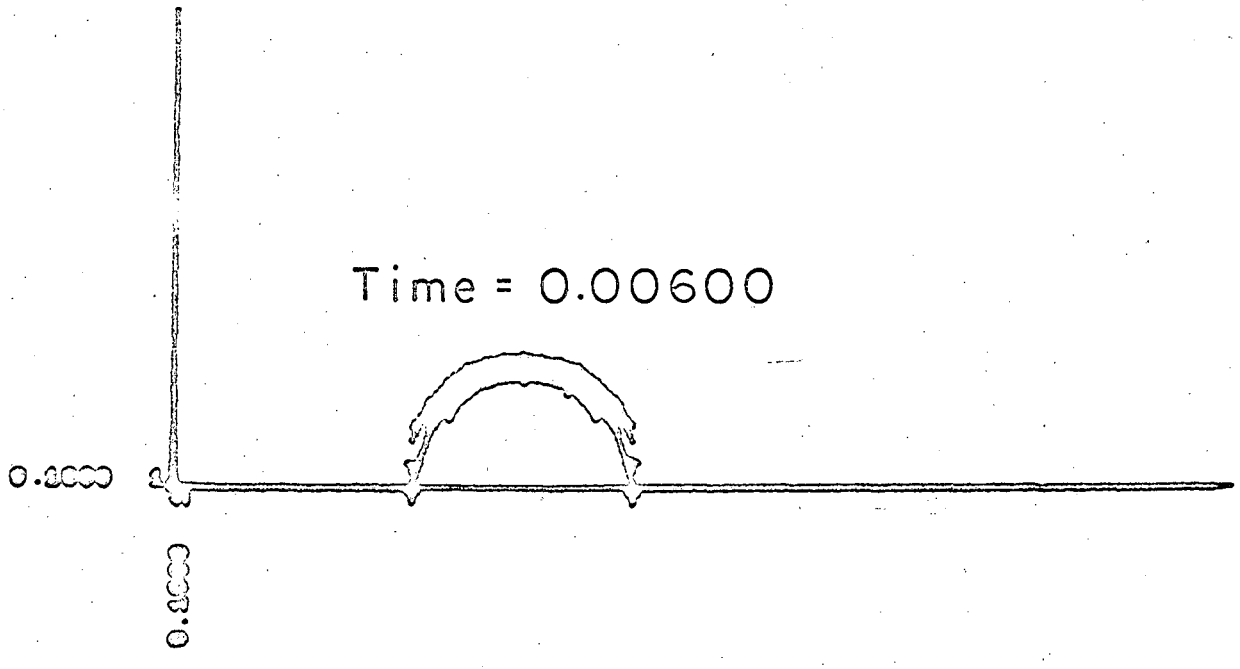

MUB-9375

Fig. 21

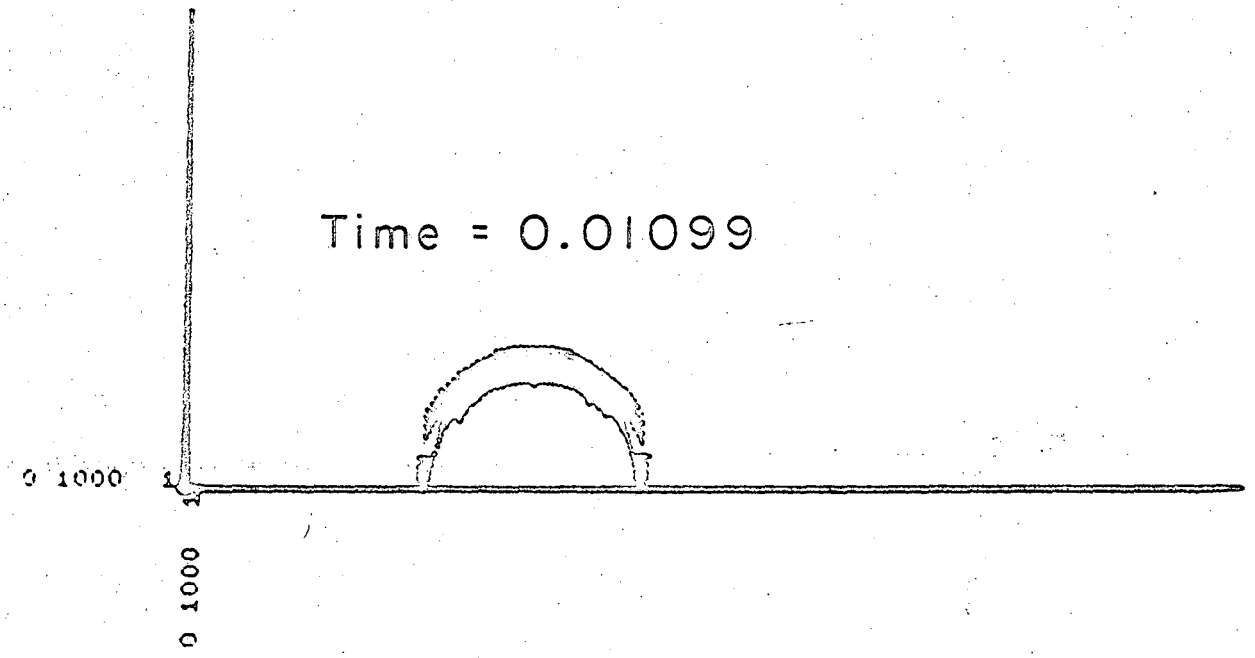

MUB-9374

Fig. 22

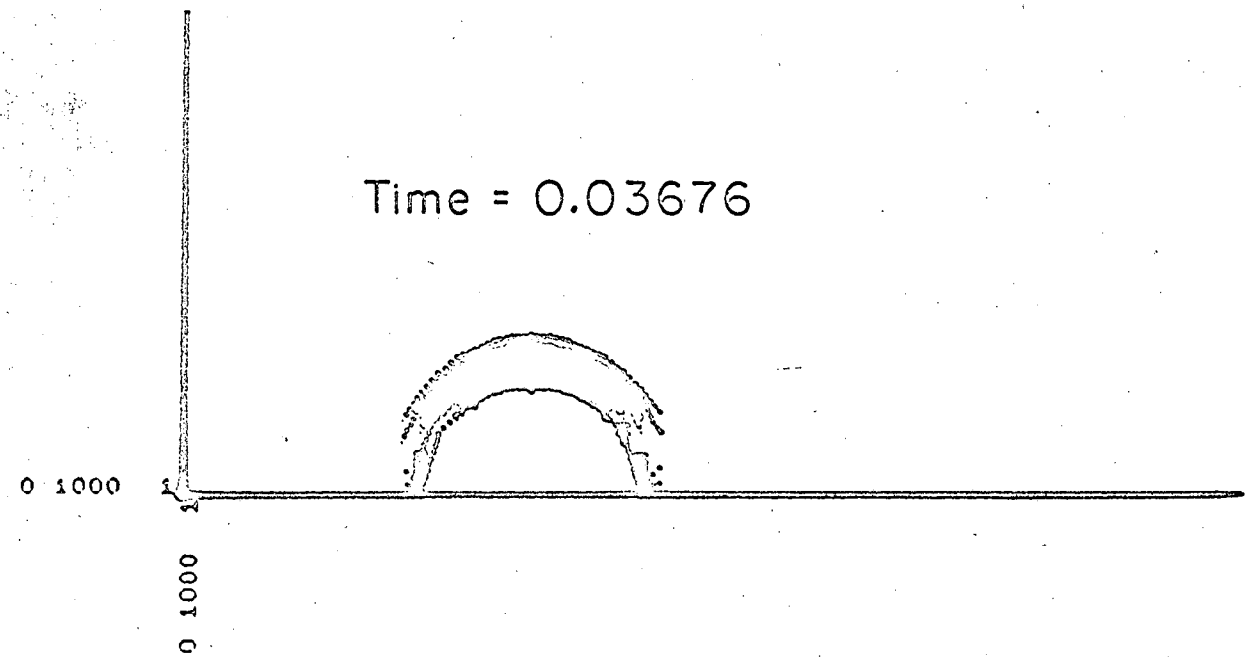

MUB-9373

Fig. 23

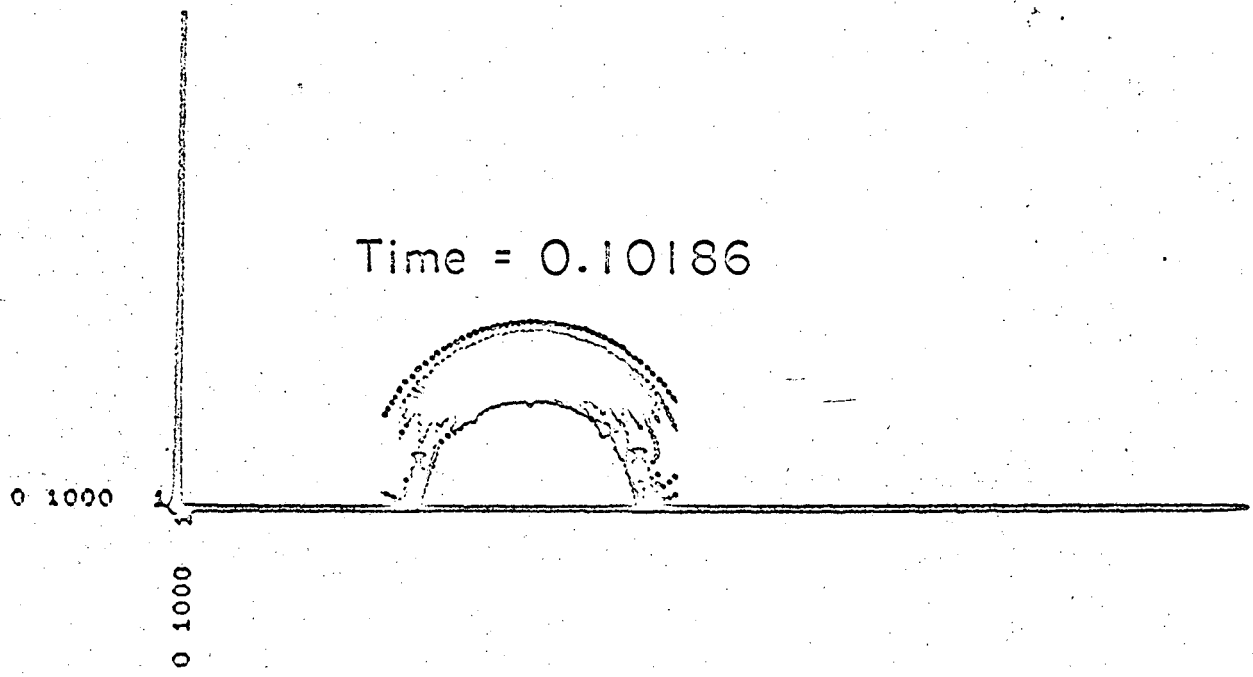

MUB-9372

Fig. 24

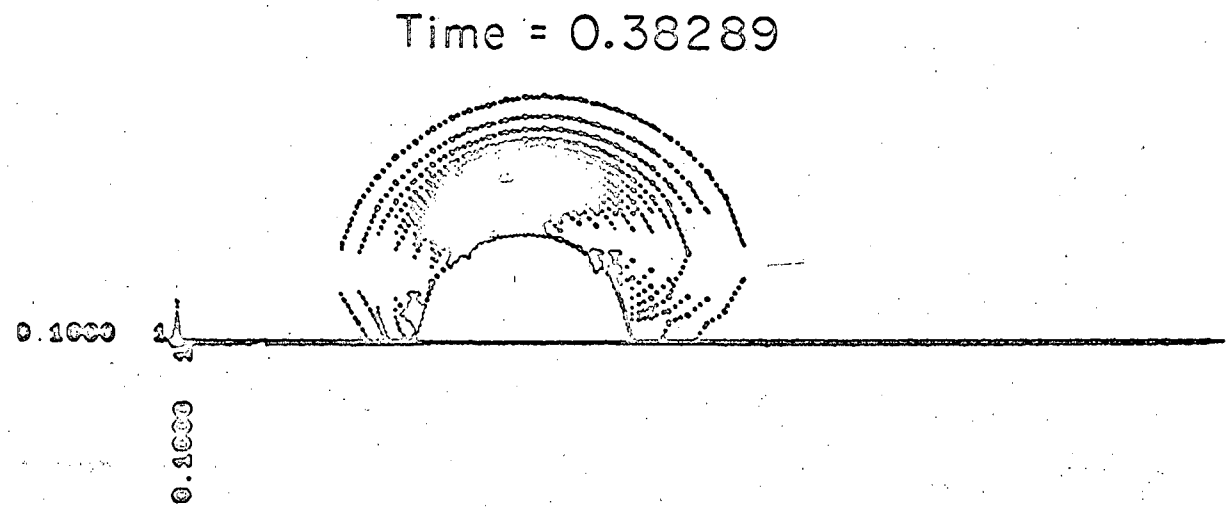

MUB-9371

Fig. 25

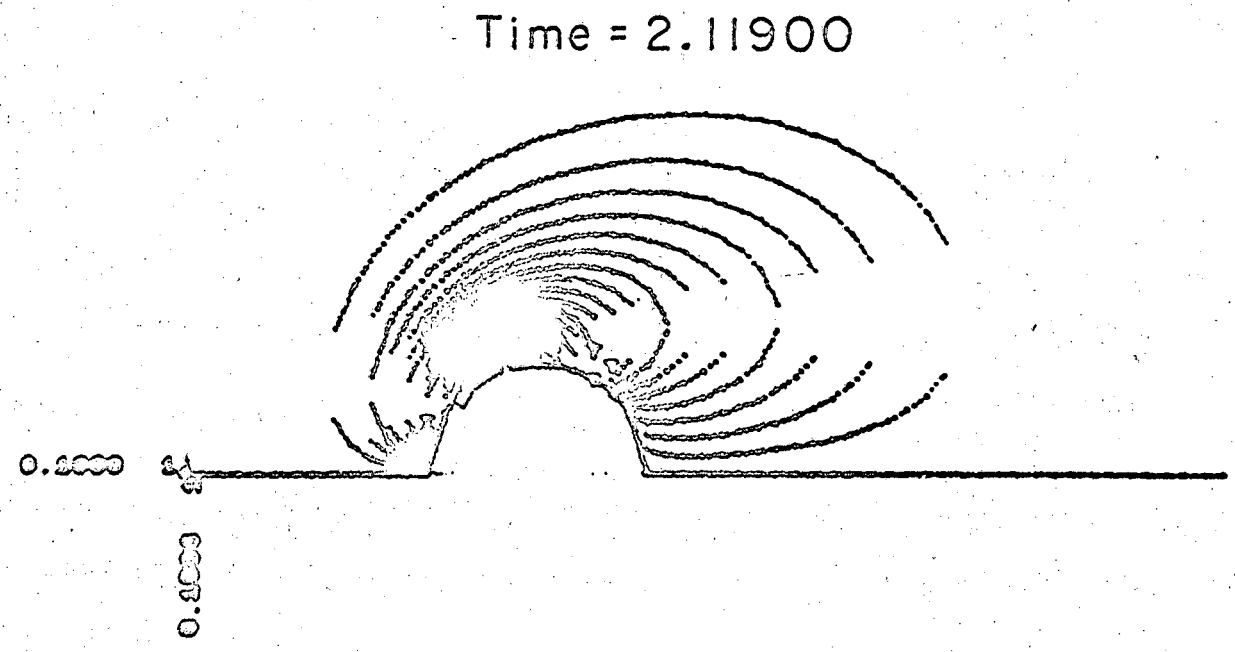

MUB-9370

Fig. 26

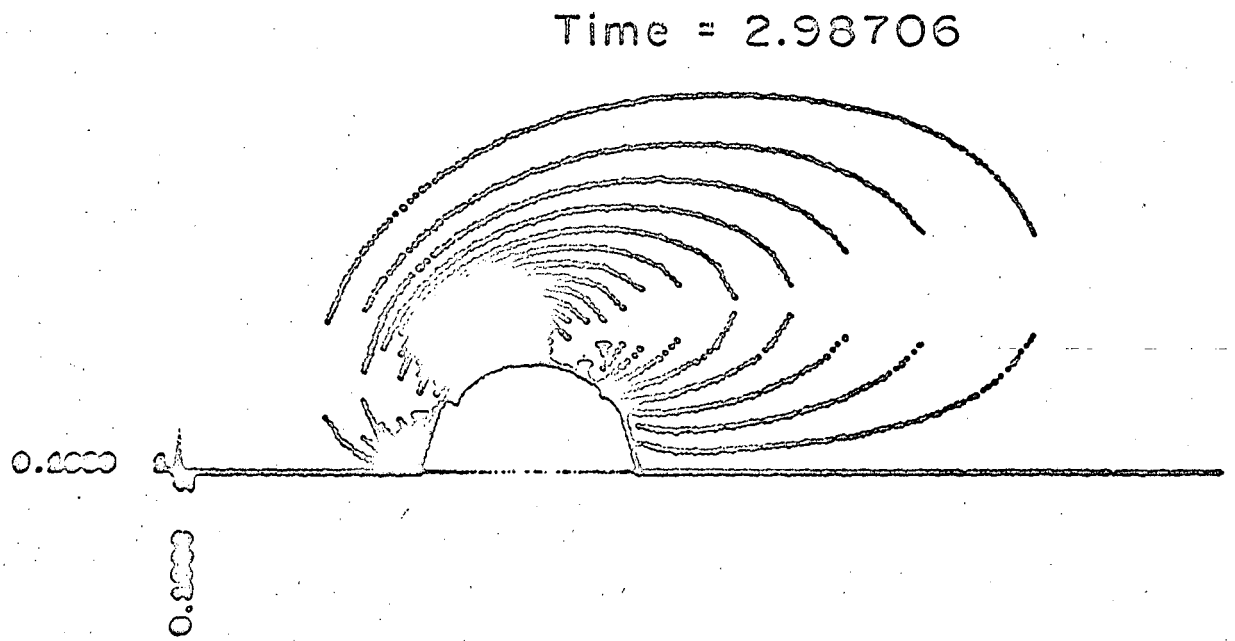

MUB-9369

Fig. 27

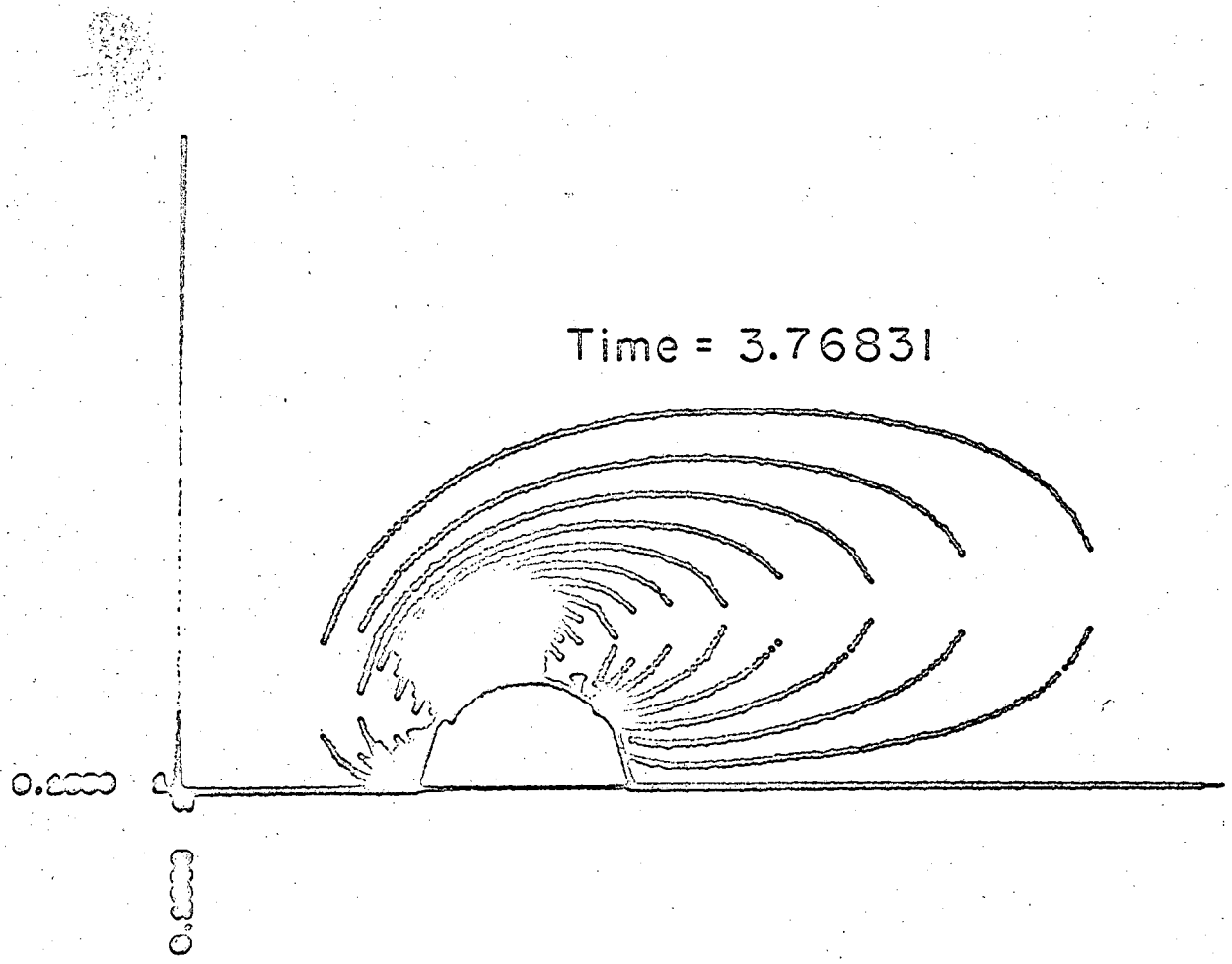

MUB-9368

Fig. 28

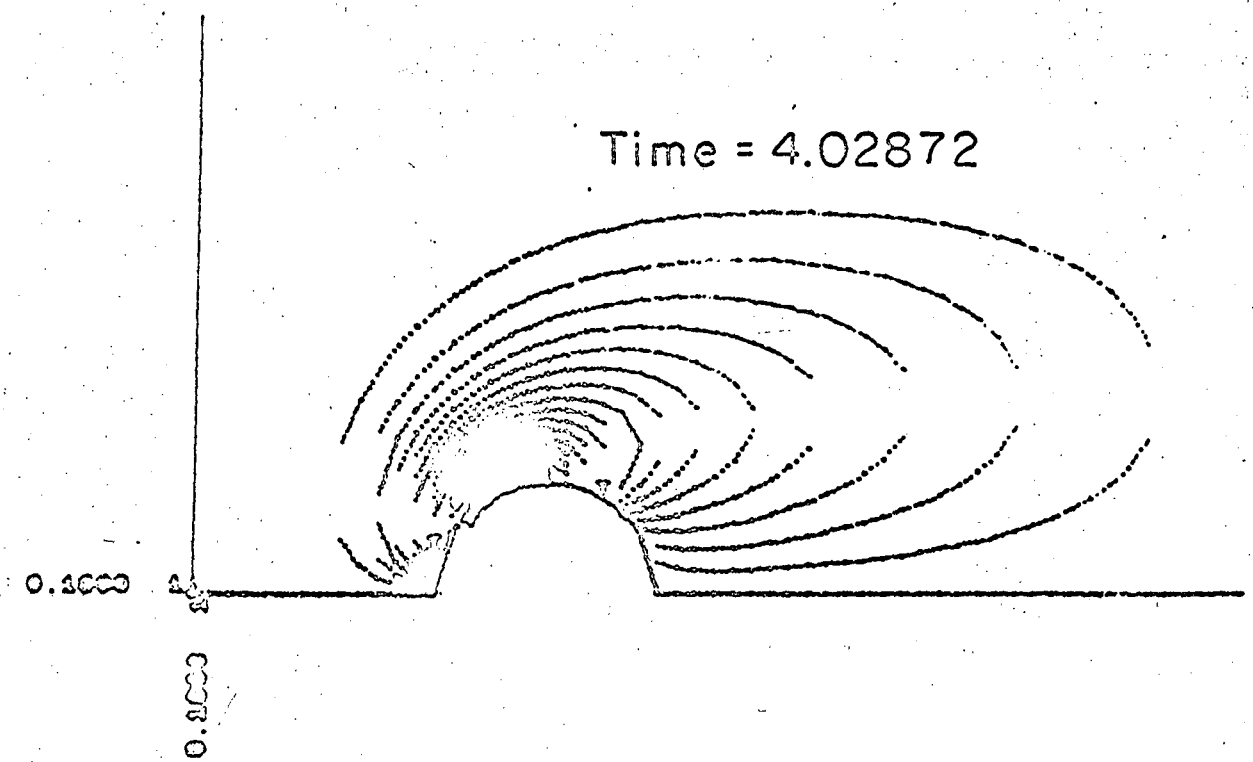

MUB-9367

Fig. 29

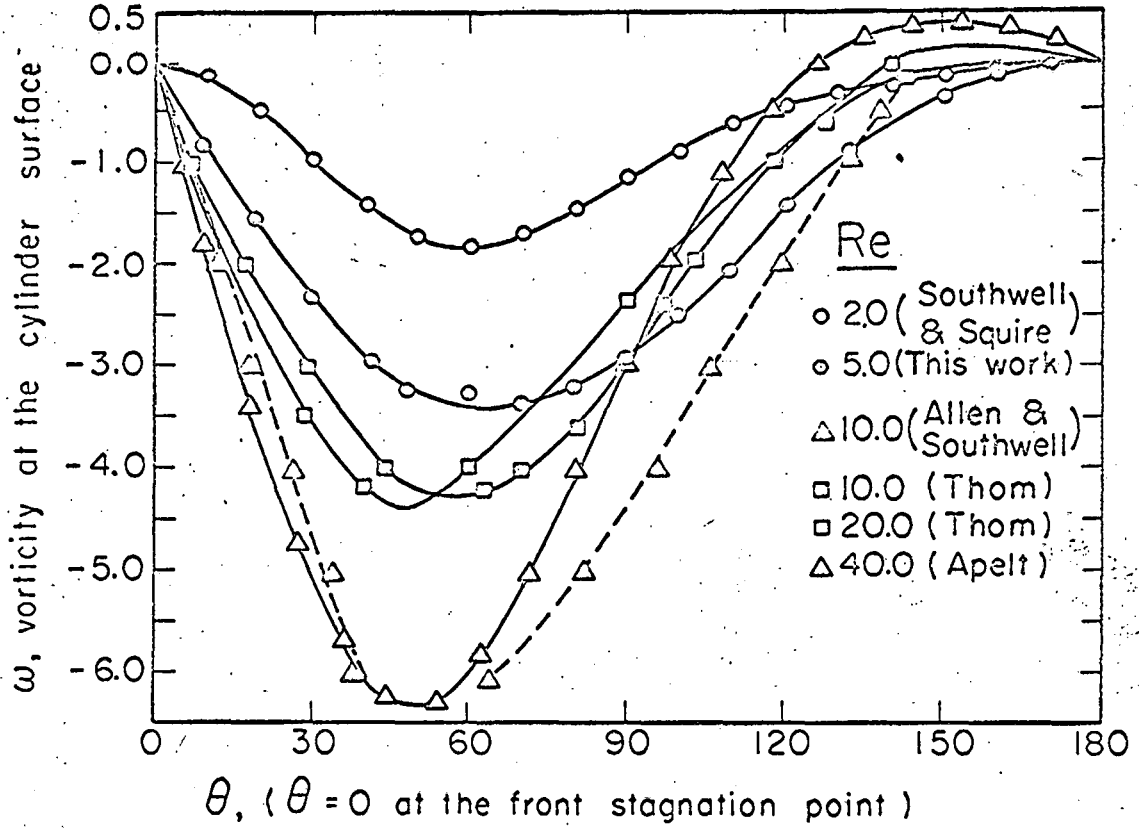

Fig. 30

Steady State Surface Vorticity

REFERENCES

1. G. Allen and R. Southwell, "Relaxation Methods Applied to Determine the Motion, in Two Dimensions, of a Viscous Fluid Past a Fixed Cylinder", Quar. J. Mech and Applied Math, 8, 129 (1955).

2. C. J. Apelt, "Some Studies of Fluid Flow at Low Reynolds Numbers". Dissertation, University of Oxford, June 1957.

3. J. E. Fromm, "A Method for Computing Nonsteady Incompressible, Viscous Fluid Flows", Los Alamos Scientific Report LA-2910, (1963).

4. A. S. Grove, "An Investigation into the Nature of Steady Separated Flows at Large Reynolds Numbers", Dissertation, University of California, 1963.

5. S. Kaplun and P. Lagerstrom, "Low Reynolds Number Flow Past a Circular Cylinder", J. Math. Mech., 6, 585 (1957).

6. L. Lapidus, Digital Computation for Chemical Engineers, (McGraw-Hill Book Company, Inc., 1962.)

7. D. W. Peaceman and H. H. Rachford, Jr., "The Numerical Solution of Parabolic and Elliptic Differential Equations", J. Soc. Indus. Appl. Math, 3, 28 (1955).

8. I. Proudman and J. R. A. Pearson, "Expansions at Small Reynolds Numbers for the Flow Past a Sphere and a Circular Cylinder", J. Fluid Mech., 2, 237 (1957).

9. R. Southwell and H. Squire, "A Modification of Oseen's Approximate Equation for the Motion in Two Dimensions of a Viscous Incompressible Fluid", Phil. Trans. Roy. Soc. London, A232, 27-64 (1933).

10. A. Thom, "The Flow Past Circular Cylinder at Low Speeds", Proc. Roy. Soc. (London), 141A, 651 (1933).

11. A. Thom, "An Investigation of Fluid Flow in Two Dimensions", Aero. Res. Cttee., R and M, No. 1194 (1929).

APPENDIX I

DERIVATION OF FINITE DIFFERENCE EQUATIONS

A set of mesh points is constructed in the channel and to each point the values of the dependent variables ψ, u, v, and ω are considered. The numerical values representing the derivatives in the differential equations are computed from these discrete values.

Let us refer to Fig. 2 where there is a central point E and four adjacent points 1, 2, 3 and 4 around it. These four points are each at P_1h, P_2h, P_3h, and P_4h distance away from point E. h is some arbitrarily chosen unit distance between two adjacent mesh points. P_1, P_2, P_3 and P_4 are some scaling factors. By Taylor's expansion we obtain the following relationships:

$$\psi(1) = \psi(E)-P_1h\psi_x(E)+\frac{P_1^2h^2}{2}\psi_{xx}(E)-\frac{P_1^3h^3}{3!}\psi_{xxx}(E)+O(h^4) \qquad (A\text{-}1)$$

$$\psi(3) = \psi(E)+P_3h\psi_x(E)+\frac{P_3^2h^2}{2}\psi_{xx}(E)+\frac{P_3^3h^3}{3!}\psi_{xxx}(E)+O(h^4) \qquad (A\text{-}2)$$

$$\psi(2) = \psi(E)-P_2h\psi_y(E)+\frac{P_2^2h^2}{2}\psi_{yy}(E)-\frac{P_2^3h^3}{3!}\psi_{yyy}(E)+O(h^4) \qquad (A\text{-}3)$$

$$\psi(4) = \psi(E)+P_4h\psi_y(E)+\frac{P_4^2h^2}{2}\psi_{yy}(E)+\frac{P_4^3h^3}{3!}\psi_{yyy}(E)+O(h^4) \qquad (A\text{-}4)$$

where $\psi(i)$, (i = 1, 2, 3, 4 and E) are the indices on the mesh points. The subscripts on ψ indicates the partial derivatives. $O(h^4)$ indicates that the term neglected is of the order of magnitude h^4.

Equations (A-1) to (A-4) are the four fundamental equations from which the difference equations are derived.

A. Stream Functions

1. Difference Equations for Bulk Flow (Or Interior Mesh Points)

In the bulk we are only concerned with the square mesh points; that is, $P_1 = P_2 = P_3 = P_4 = 1.0$. Hence, Eqs. (A-1) to (A-4) can be written as

$$\psi(1) = \psi(E) - h\psi_x(E) + \frac{h^2}{2!}\psi_{xx}(E) - \frac{h^3}{3!}\psi_{xxx}(E) + O(h^4) \qquad (A-5)$$

$$\psi(3) = \psi(E) + h\psi_x(E) + \frac{h^2}{2!}\psi_{xx}(E) + \frac{h^3}{3!}\psi_{xxx}(E) + O(h^4) \qquad (A-6)$$

$$\psi(2) = \psi(E) - h\psi_y(E) + \frac{h^2}{2!}\psi_{yy}(E) - \frac{h^3}{3!}\psi_{yyy}(E) + O(h^4) \qquad (A-7)$$

$$\psi(4) = \psi(E) + h\psi_y(E) + \frac{h^2}{2!}\psi_{yy}(E) + \frac{h^3}{3!}\psi_{yyy}(E) + O(h^4) \qquad (A-8)$$

Suppose ω is known for all the mesh points and we want to use Eq. (2-10) to compute the stream function, obviously, we need the expression for $\psi_{xx}(E)$ and $\psi_{yy}(E)$ in terms of $\psi(1)$, $\psi(2)$, $\psi(3)$, $\psi(4)$ and $\psi(E)$. Let us add Eq. (A-6) to Eq. (A-5) , then we have

$$\psi(1) + \psi(3) = 2\psi(E) + h^2\psi_{xx}(E) + O(h^4)$$

or

$$\psi_{xx}(E) = \frac{1}{h^2}\left(\psi(1) + \psi(3) - 2\psi(E)\right) + O(h^2) \qquad (A-9) \text{ or } (3-2)$$

Similarly, from Eq. (A-7) and Eq. (A-8) we can obtain

$$\psi_{yy}(E) = \frac{1}{h^2}\left(\psi(2) + \psi(4) - 2\psi(E)\right) + O(h^2) \qquad (A-10) \text{ or } (3-2)$$

Thus, to the accuracy $O(h^2)$, Eq. (2-10) can be expressed by

$$\frac{1}{h^2}\left[\psi(1) + \psi(2) + \psi(3) + \psi(4) - 4\psi(E)\right] = \omega(E) + O(h^2)$$

or

$$\psi^{(r+1)}(E) = (\psi^{(r)}(1) + \psi^{(r)}(2) + \psi^{(r)}(3) + \psi^{(r)}(4) - \psi(E) \cdot h^2)/4.0 + O(h^2) \qquad \text{(A-11)}$$

Equation (A-11) can be used for iteration with known values on the right-hand side. The superscripts (r) indicate the iteration step.

An alternative way to write Eq. (A-11) is

$$\psi^{(r+1)}(E) = \psi^{(r)}(E) + \frac{1}{4.0}(\psi^{(r)}(1) + \psi^{(r)}(2) + \psi^{(r)}(3) + \psi^{(r)}(4) - 4\psi^{(r)}(E) + \omega(E)h^2) + O(h^2) \qquad \text{(A-12)}$$

The second term of the equation may be considered as the correction term and $\psi^{(r)}(E) \Longrightarrow \psi^{(r+1)}(E)$ as this term vanishes.

As discussed in Chapter 3, Sec.(B-3), for better efficiency the most "up-to-date" ψ values should be used during each iteration process. Thus, the more efficient form of Eq. (A-12) is

$$\psi^{(r+1)}(E) = \psi^{(r)}(E) + \frac{\Omega}{4}(\psi^{(r+1)}(1) + \psi^{(r+1)}(2) + \psi^{(r)}(3) + \psi^{(r)}(4) - 4\psi^{(r)}(E) + \omega(E)h^2) + O(h^2) \qquad \text{(A-13)}$$

where Ω is the "overrelaxation" factor, and its purpose and limits are discussed in Chapter 3, Sec. (B-3).

However, for the mesh points near the curved boundaries the second order partials cannot be expressed by the simple relation shown in Eq.(A-9) and Eq. (A-10). A more general representation which involves the P values has to be used.

Let us denote the finite difference formulas for $h^2\psi_{xx}(E)$ and $h^2\psi_{yy}(E)$ to the accuracy $O(h^4)$ by $L_{xx}(E)$ and $L_{yy}(E)$, respectively. Then, L_{ii} is an linear finite difference operator. Its form depends upon the geometry and the order of accuracy of the finite difference formula. By this notation, the stream function iteration equation can be written, in a more general form, as

$$\psi^{(r+1)}(E) = \psi^{(r)}(E) + \frac{\Omega}{C_E}\left(L_{xx}(E) + L_{yy}(E) + \omega(E)h^2\right) + O(h^2) \qquad \text{(A-14)}$$

where C_E is the sum of the coefficients in front of $\psi(E)$ from the difference formula $L_{xx}(E)$ and $L_{yy}(E)$. In the next few sections, the finite difference forms of $\psi_{xx}(E)$ and $\psi_{yy}(E)$ for various geometris are discussed so that appropriate substitution for $L_{xx}(E)$ and $L_{yy}(E)$ can be made.

2. Difference Equations for Mesh Points Adjacent to the Curved Boundary

The curved boundary present in this work is the solid curved boundary where ψ is set to zero. Let us refer to Fig. 3 where we show a boundary point B and three interior points E, 3 and I. The direction of the grid-line may be x or y and can either be positive or negative, but the equation is derived by assuming it is in the positive direction. By expanding ψ about point E we can express $\psi(B)$, $\psi(3)$ and $\psi(I)$ as follows

$$0 = \psi(B) = \psi(E) - Ph\psi'(E) + \frac{1}{2}P^2h^2\psi''(E) - \frac{1}{6}P^3h^3\psi'''(E) + O(h^4) \qquad \text{(A-15)}$$

$$\psi(3) = \psi(E) + h\psi'(E) + \frac{1}{2}h^2\psi''(E) + \frac{1}{6}h^3\psi'''(E) + O(h^4) \qquad \text{(A-16)}$$

$$\psi(I) = \psi(E) + 2h\psi'(E) + 2h^2\psi''(E) + \frac{4}{3}h^3\psi'''(E) + O(h^4) \qquad \text{(A-17)}$$

where the prime indicates the order of the derivatives.

After eliminating $\psi'(E)$ and $\psi'''(E)$, we have

$$h^2\psi''(E) = 2\,\frac{2-P}{1+P}\,\psi(3) + \frac{P-1}{P-2}\,\psi(I) - \frac{3-P}{P}\,\psi(E) + O(h^4) \qquad \text{(A-18)}$$

Equation (A-18) can be substituted into Eq. (A-14) when the curved boundary configuration is met.

3. Difference Equation for the Outlet

As discussed in the boundary condition section, at the inlet ψ is set

to equal to y (numerically) and at the frictionless walls ψ is constant. So for these boundaries no computation on ψ is needed. However, at the outlet the boundary condition prescribed is $\frac{\partial^2\psi}{\partial x^2} = 0$; hence, ψ at the outlet has to be calculated.

If point E of Fig. 2 is at the outlet then point 3 is undefined and Eq. (A-13) cannot be used directly. To remedy the situation let us apply the boundary condition $\frac{\partial^2\psi}{\partial x^2} = 0$. The finite difference equation for $\frac{\partial^2\psi}{\partial x^2} = 0$ is Eq. (A-9).

$$\psi_{xx}(E) = \frac{1}{h^2}\left(\psi(1) + \psi(3) - 2\psi(E) + O(h^2)\right)$$

So, at the outlet

$$\psi(1) + \psi(3) - 2\psi(E) = 0$$

or

$$\psi(3) = 2\psi(E) - \psi(1)$$

By substituting $\psi(3)$ into Eq. (A-13) we obtain the difference equation for the outlet ψ calculation.

$$\overset{(r+1)}{\psi(E)} = \overset{(r)}{\psi(E)} + \frac{\Omega}{4.0}\left(\overset{(r+1)}{\psi(2)} + \overset{(r)}{\psi(4)} - 2\overset{(r)}{\psi(E)} + \omega(E)h^2\right) \qquad \text{(A-19)}$$

B. Velocity

1. Difference Equations for Interior Points

By definition the velocity is

$$u = \frac{\partial \psi}{\partial y} \quad \text{and} \quad v = - \frac{\partial \psi}{\partial x} \tag{2-9}$$

Since square meshes are used at the bulk, P values are unity, Eqs. (A-5) to (A-8) are applicable.

Subtraction of Eq. (A-5) from Eq. (A-6) yields

$$\psi(3) - \psi(1) = 2h\, \psi_x(E) + \frac{2h^3}{3!} \psi_{xxx}(E) + O(h^4)$$

The desired accuracy in this work is $O(h^2)$, so the $O(h^3)$ term may be neglected.

$$\psi(3) - \psi(1) = 2h\, \psi_x(E) + O(h^3)$$

After rearrangement we obtain

$$v(E) = - \psi_x(E) = \frac{-1}{2h} \Big(\psi(3) - \psi(1) \Big) \tag{A-20}$$

Similarly, we can obtain from Eq. (A-7) and (A-8)

$$u(E) = \psi_y(E) = \frac{1}{2h} \Big(\psi(4) - \psi(2) \Big) \tag{A-21}$$

2. Difference Equations for the Boundary Points

a. Inlet and Outlet. From the boundary condition section, at the inlet and outlet $\frac{\partial^2 \psi}{\partial x^2} = 0$ which implies that $\psi(1) + \psi(3) - 2\psi(E) = 0$ (point E is on the boundary). At the inlet $\psi(1)$ is undefined, hence Eq. (A-20) cannot be used directly. But from the above statement we see that

$$\psi(1) = 2\psi(E) - \psi(3)$$

So, Eq. (A-20) can be written as

$$v(E) = -\psi_x(E) = -\frac{1}{h}\left(\psi(3) - \psi(E)\right) \qquad \text{(A-22)}$$

where $\psi(3)$ and $\psi(E)$ are defined points. Similarly at the oulet, where $\psi(3)$ is undefined we can show that

$$v(E) = \frac{1}{h}\left(\psi(1) - \psi(E)\right) \qquad \text{(A-23)}$$

b. Frictionless Walls. The frictionless walls present in this work are parallel to the x-axis. Since the fluid is not supposed to penetrate through the walls, it becomes necessary that v, the y-component of velocity, equals zero. This implies that ψ on the walls must be constant. But for u(E) Eq. (A-21) cannot be used directly, since either $\psi(4)$ or $\psi(2)$ may be undefined. From the definition of frictionless walls, Chapter II, Sec. C, we see that

$$\frac{\partial^2\psi}{\partial y^2} = 0 \quad \text{at these walls.}$$

This boundary condition, in analog to the inlet and outlet condition, provides a way to eliminate the undefined stream functions.

c. Solid Boundary or Frictional Walls. By no slip condition u = v = 0, so no computation is needed.

d. Points Adjacent to the Curved Boundary. All the previous equations are based on Eqs. (A-5) to (A-8) where $P_i = 1$, but for those points adjacent to the curved boundary this is no longer correct.

Let us refer to Fig. 3 again. The point PB is a regular mesh point except that it is interior to the solid, hence no values are defined there. However, if mathematically we can estimate the ψ value at this point then

Eq. (A-20) or (A-21) remain applicable for computing v(E) or u(E).

Let us make Taylor's expansion in the x-direction of Fig. 3 from point PB to the adjacent points.

$$\psi(E) = \psi(PB) + \psi_x(PB)h + \frac{h^2}{2!}\psi_{xx}(PB) + O(h^3) \tag{A-24}$$

$$\psi(B) = 0 = \psi(PB) + \psi_x(PB)(1-P)h + \frac{(1-P)^2h^2}{2}\psi_{xx}(PB)+O(h^3) \tag{A-25}$$

$$\psi_x(B) = 0 = \psi_x(PB) + \psi_{xx}(PB)\, h(1-P) - O(h^2) \tag{A-26}$$

Rearranging these three equations we get

$$\psi(PB) = \frac{(1-P)^2}{P^2}\ \psi(E) + O(h^3) \tag{A-27}$$

Eatuions (A-27) can be substituted into either Eq. (A-20) or Eq. (A-21) depending on which velocity component is to be calculated. For example, according to Fig. 3, let us compute v(E)

$$v(E) = -\frac{1}{2h}\left(\psi(3) - \psi(PB)\right)$$

$$= -\frac{1}{2h}\left(\psi(3) - \frac{(1-P)^2}{P^2}\ \psi(E)\right) \tag{A-28}$$

C. Vorticity

The vorticity transport equation (2-8) may be transformed into various difference equations depending on the type of approximation used.

1. Difference Equations by the Method of Peaceman and Rachford.

Eq. (2-8):

$$\frac{\partial \omega}{\partial t} + u \frac{\partial \omega}{\partial x} + v \frac{\partial \omega}{\partial y} = \delta \left(\frac{\partial^2 \omega}{\partial x^2} + \frac{\partial^2 \omega}{\partial y^2} \right)$$

Let us consider only the square mesh points. In analog to Eq. (A-5) the vorticity at points 1,2,3,4, and E can be related by

$$\omega(1) = \omega(E) - h\omega_x(E) + \frac{h^2}{2!} \omega_{xx}(E) - \frac{h^3}{3!} \omega_{xxx}(E) + O(h^4) \qquad \text{(A-29)}$$

$$\omega(3) = \omega(E) + h\omega_x(E) + \frac{h^2}{2!} \omega_{xx}(E) + \frac{h^3}{3!} \omega_{xxx}(E) + O(h^4) \qquad \text{(A-30)}$$

$$\omega(2) = \omega(E) - h\omega_y(E) + \frac{h^2}{2!} \omega_{yy}(E) - \frac{h^3}{3!} \omega_{yyy}(E) + O(h^4) \qquad \text{(A-31)}$$

$$\omega(4) = \omega(E) + h\omega_y(E) + \frac{h^2}{2!} \omega_{yy}(E) + \frac{h^3}{3!} \omega_{yyy}(E) + O(h^4) \qquad \text{(A-32)}$$

By proper elimination the following finite difference formula for the derivatives in Eq. (2-8) can be obtained.

$$\omega_x(E) = \frac{\partial \omega(E)}{\partial x} = \frac{\omega(3) - \omega(1)}{2h} + O(h^2) \qquad \text{(A-33)}$$

$$\omega_y(E) = \frac{\partial \omega(E)}{\partial y} = \frac{\omega(4) - \omega(2)}{2h} + O(h^2) \qquad \text{(A-34)}$$

$$\omega_{xx}(E) = \frac{\partial^2 \omega(E)}{\partial x^2} = \frac{\omega(1) + \omega(3) - 2\omega(E)}{h^2} + O(h^2) \qquad \text{(A-35)}$$

$$\omega_{yy}(E) = \frac{\partial^2 \omega(E)}{\partial y^2} = \frac{\omega(2) + \omega(4) - 2\omega(E)}{h^2} + O(h^2) \qquad \text{(A-36)}$$

According to Peaceman and Rachford the time derivative may be written as

$$\omega_t(E) = \frac{\partial \omega(E)}{\partial t} = \frac{\overset{n+\frac{1}{2}}{\omega(E)} - \omega^n(E)}{\Delta t} \qquad \text{(A-37)}$$

where the superscript n indicates the time step.

The method for computing the velocity component u and v is given in the preceding section.

By substituting Eq. (A-33) to Eq. (A-37) into Eq. (2-8) we obtain

$$\frac{\overset{n+\frac{1}{2}}{\omega(E)} - \overset{n}{\omega(E)}}{\Delta t} = \delta \left(\frac{\omega(1) + \omega(3) - 2\omega(E)}{h^2} + \frac{\omega(2) + \omega(4) - 2\omega(E)}{h^2} \right)$$

$$- u(E) \left(\frac{\omega(3) - \omega(1)}{2h} \right) - v(E) \left(\frac{\omega(4) - \omega(2)}{2h} \right) \qquad \text{(A-38)}$$

One can see at this point that there are many possible arrangements for the righthand side. The particular choice Peaceman and Rachford made is the following:

During the first half time step, we will hold the derivatives with respect to y at n and advance the x derivatives to $n+\frac{1}{2}$, so Eq. (A-38) becomes

$$\frac{\overset{n+\frac{1}{2}}{\omega(E)} - \overset{n}{\omega(E)}}{\Delta t} = \delta \left(\frac{\overset{n+\frac{1}{2}}{\omega(1)} + \overset{n+\frac{1}{2}}{\omega(3)} - 2\overset{n+\frac{1}{2}}{\omega(E)}}{h^2} + \frac{\overset{n}{\omega(2)} + \overset{n}{\omega(4)} - 2\overset{n}{\omega(E)}}{h^2} \right)$$

$$- \overset{n}{u(E)} \left(\frac{\overset{n+\frac{1}{2}}{\omega(3)} - \overset{n+\frac{1}{2}}{\omega(1)}}{2h} \right) - \overset{n}{v(E)} \left(\frac{\overset{n}{\omega(4)} - \overset{n}{\omega(1)}}{2h} \right)$$

After further rearrangement we obtain the implicit formula for the x-direction iteration

$$(1+\alpha \overset{n}{u(E)}) \overset{n+\frac{1}{2}}{\omega(1)} - (2 + \frac{1}{\beta}) \overset{n+\frac{1}{2}}{\omega(E)} + (1-\alpha \overset{n}{u(E)}) \overset{n+\frac{1}{2}}{\omega(3)}$$

$$= -\left(1 + \alpha v^n(E)\right)\omega^n(2) + \left(2 - \frac{1}{\beta}\right)\omega^n(E) - \left(1 - \alpha v^n(E)\right)\omega^n(4) \qquad \text{(A-39)}$$

where

$$\alpha = \frac{h}{2\delta} \qquad \text{(A-40)}$$

$$\beta = \frac{\delta \Delta t}{h^2} \qquad \text{(A-41)}$$

During the second half time step, the "direction" is changed. The x-derivatives are held at time step $n+\frac{1}{2}$ while the y-derivatives are advanced to n+1. So Eq. (A-38) becomes

$$\frac{\omega(E)^{n+1} - \omega(E)^{n+\frac{1}{2}}}{\Delta t} = \delta\left(\frac{\omega(1)^{n+\frac{1}{2}} + \omega(3)^{n+\frac{1}{2}} - 2\omega(E)^{n+\frac{1}{2}}}{h^2} + \frac{\omega(2)^{n+1} + \omega(4)^{n+1} - 2\omega(E)^{n+1}}{h^2}\right)$$

$$- u^n(E)\left(\frac{\omega(3)^{n+\frac{1}{2}} - \omega(1)^{n+\frac{1}{2}}}{2h}\right) - v^n(E)\left(\frac{\omega(4)^{n+1} - \omega(2)^{n+1}}{2h}\right)$$

or

$$\left(1 + \alpha v^n(E)\right)\omega(2)^{n+1} - \left(2 + \frac{1}{\beta}\right)\omega(E)^{n+1} + \left(1 - \alpha v^n(E)\right)\omega(4)^{n+1}$$

$$= -\left(1 + \alpha u^n(E)\right)\omega(2)^{n+\frac{1}{2}} + \left(2 - \frac{1}{\beta}\right)\omega(E)^{n+\frac{1}{2}} - \left(1 - \alpha u^n(E)\right)\omega(4)^{n+\frac{1}{2}} \qquad \text{(A-42)}$$

By the stability analysis, in the case where no convective terms are present, Peaceman and Rachford are able to show that when Δt in the two half time steps is the same, and Eq. (A-39) and Ea. (A-42) are applied alternately, the method is always stable; that is, the vorticity field will not diverge. However, with convective terms present this may not be true.

At the outlet, as indicated in the boundary condition section, $\frac{\partial^2 \omega}{\partial x^2} = 0$. By Eq. (A-35) we have

$$\omega(1) + \omega(3) - 2\omega(E) = 0 \qquad \text{(A-43)}$$

If point E is at the boundary, then point 3 is undefined in Eqs. (A-39) and (A-42). By means of Eq. (A-43), $\omega(3)$ can be replaced by $2\omega(E) - \omega(1)$ so we get for the x-direction iteration

$$2\alpha u^{n+\frac{1}{2}}(E)\omega(1) - \left(2\alpha u^{n+\frac{1}{2}}(E) + \frac{1}{\beta}\right) \omega^{n+\frac{1}{2}}(E)$$

$$= -\left(1 - \alpha v^{n}(E)\right) \omega^{n}(2) + \left(2 - \frac{1}{\beta}\right) \omega^{n}(E) - \left(1 + \alpha v^{n}(E)\right) \omega^{n}(4) \qquad \text{(A-44)}$$

and for the y-direction iteration

$$\left(1 + \alpha v^{n}(E)\right) \omega^{n+1}(2) - \left(2 + \frac{1}{\beta}\right) \omega^{n+1}(E) + \left(1 - \alpha v^{n}(E)\right) \omega^{n+1}(4)$$

$$= \left(2\alpha u^{n}(E) - \frac{1}{\beta}\right) \omega^{n+\frac{1}{2}}(E) - 2\alpha u^{n}(E)\, \omega^{n+\frac{1}{2}}(1) \qquad \text{(A-45)}$$

2. Difference Equations by the Method of Fromm

The difference equations (A-33) to (A-36) are still applicable. But in place of Eq. (A-39), Fromm used the central difference formula for $\frac{\partial \omega}{\partial t}$; i.e.,

$$\frac{\partial \omega(E)}{\partial t} = \frac{\omega^{n+1}(E) - \omega^{n-1}(E)}{2\Delta t}$$

So. Eq. (2-8) becomes

$$\frac{\omega^{n+1}(E) - \omega^{n-1}(E)}{2\Delta t} = \delta \left(\frac{\omega(1) + \omega(3) - 2\omega(E)}{h^2} + \frac{\omega(2) + \omega(4) - 2\omega(E)}{h^2} \right)$$

$$- u(E)\left(\frac{\omega(3) - \omega(1)}{2h}\right) - v(E)\left(\frac{\omega(4) - \omega(2)}{2h}\right) \qquad \text{(A-46)}$$

The vorticity on the righthand side can all be at time step n, but Fromm

indicated that the $-4\omega(E)$ should be replaced by

$$- 2\omega_{i,j}^{n+1} - 2\omega_{i,j}^{n-1}$$

in order to achieve stability. So. Eq. (A-46) becomes

$$\frac{\omega^{n+1}(E) - \omega^{n-1}(E)}{2\Delta t} = \delta\left(\frac{1}{h^2}\left(\omega^{n}(1)+ \omega^{n}(2) + \omega^{n}(3)+ \omega^{n}(4)- 2\omega^{n-1}(E) - 2\omega^{n+1}(E)\right)\right)$$

$$- u^n(E)\left(\frac{\omega^{n}(3) - \omega^{n}(1)}{2h}\right) - v^n(E)\left(\frac{\omega^{n}(4) - \omega^{n}(2)}{2h}\right)$$

After further rearrangement we obtain

$$\omega^{n+1}(E)\left(1 + \frac{4\delta\Delta t}{h^2}\right) = \omega^{n-1}(E) + \frac{2\delta\Delta t}{h^2}\left(\omega^{n}(1)+ \omega^{n}(2)+ \omega^{n}(3)+ \omega^{n}(4)- 2\omega_{i,j}^{n-1}\right)$$

$$- \frac{\Delta t}{h}\left[u^n(E)\left(\omega^{n}(3)- \omega^{n}(1)\right) + v^n(E)\left(\omega^{n}(4) - \omega^{n}(2)\right)\right] \qquad \text{(A-47)}$$

According to Fromm for stability

$$\frac{\delta\Delta t}{h^2} \leq \frac{1}{4} \quad \text{and} \quad \frac{|u| + |v|}{h}\Delta t < 1.$$

At the outlet Eq. (A-43) is again used to eliminate the undefined $\omega(3)$, except that we write

$$\omega^{n}(3)+ \omega^{n}(1)- \omega^{n+1}(E) - \omega^{n-1}(E) = 0$$

for stability reason. So. Eq. (A-47) becomes

$$\omega^{n+1}(E)\left(1 + \frac{2\delta\Delta t}{h^2} + \frac{\Delta t}{h}u^n(E)\right) = \omega^{n-1}(E) + \frac{2\delta\Delta t}{h^2}\left(\omega^{n}(4) + \omega^{n}(2) - \omega^{n-1}(E)\right)$$

$$- \frac{\Delta t}{h}\left[u^n(E)\left(\omega^{n-1}(E) - 2\omega^{n}(1)\right) + v^n(E)\left(\omega^{n}(4) - \omega^{n}(2)\right)\right] \qquad \text{(A-48)}$$

3. Difference Equations for Computation of Vorticity at a Curved, Solid Boundary

For the case where the solid boundary coincides with the meshes as shown in Fig. 4a, the vorticity at the boundary can be calculated by Eq. (3-34) and Eq. (3-25) as discussed in Chapter III, Sec.(D-3).

For the curved boundary we decided not to change the difference equations for Eq. (2-8). Instead, we introduced the so-called pseudo-boundary points (PB points in Fig. 4b) which are regular mesh points, methematically, but physically they may be interior to the solid object and bear no physical meaning.

In Fig. 4b, we can see that there are two types of PB points:

1) Type 1. adjacent to two actual boundary points.

2) Type 2. adjacent to one actual boundary point only.

For type 1, let us refer to Fig. 3 which indicates a PB point with the boundary point B and two interior points E and 3. According to the figure the grid-line is in the x-direction, but this is immaterial since it can just as well be in the y-direction. Consequently, we shall use primes to indicate the order of the derivatives. By Taylor's expansion around point PB, we have

$$\psi(B) = 0 = \psi(PB) + (1-P)\, h\psi'(PB) + \frac{1}{2}(1-P)^2 h^2 \psi''(PB) + \frac{1}{6}(1-P)^3 h^3 \psi'''(PB) + O(h^4)$$

$$\psi'(B) = 0 = \psi'(PB) + (1-P)h\psi''(PB) + \frac{1}{2}(1-P)^2 h^2 \psi'''(PB) + O(h^3)$$

$$\psi(E) = \psi(PB) + h\psi'(PB) + \frac{h^2}{2!}\psi''(PB) + \frac{1}{6}h^3\psi'''(PB) + O(h^4)$$

$$\psi(3) = \psi(PB) + 2h\psi'(PB) + \frac{4}{2}h^2\psi''(PB) + \frac{8}{6}h^3\psi'''(PB) + O(h^4)$$

By proper elimination we can obtain

$$\psi''(PB) = \frac{4\psi(E)\,(2-P)}{P^2h^2} - \frac{2\psi(3)\,(3-2P)}{h^2(1+P)^2} + O(h^2) \qquad \text{(A-49)}$$

Equation (A-49) can be used to compute $\omega(PB)$ form Eq. (2-10) when the curved boundary of such configuration is encountered.

For type 2, let us define a new coordinate system x', y', where x' is tangential to the boundary and y' is normal to the boundary, and α denotes the angle between y and y' (see Fig. 5). Now, let us expand the stream function about the boundary point.

$$\psi = \psi(B) + x'\psi_{x'}(B) + \frac{1}{2}x'^2\psi_{x'x'}(B) + \frac{1}{6}x'^3\psi_{x'x'x'}(B)$$

$$+ y'\psi_{y'}(B) + y'x'\psi_{y'x'}(B) + \frac{1}{2}y'x'^2\psi_{y'x'x'}(B)$$

$$+ \frac{1}{2}y'^2\psi_{y'y'}(B) + \frac{1}{2}y'^2x'\psi_{y'y'x'}(B) + \frac{1}{6}y'^3\psi_{y'y'y'}(B) + O(h^4) \qquad \text{(A-50)}$$

From boundary conditions:

$\psi(B) \equiv 0$

velocity $= 0 \Longrightarrow \psi_{x'}(B) = \psi_{y'}(B) = 0$

$\psi_{x'}(B)$ is a constant along x' $\Longrightarrow \psi_{x'x'}(B) = 0$

$\psi_{y'}(B)$ is a constant along x' $\Longrightarrow \psi_{x'y'}(B) = 0$

Consequently,

$$\psi_{x'x'x'}(B) = \psi_{x'y'x'}(B) = 0$$

So Equation (A-50) can be simplified to

$$\psi = \frac{1}{2}y'^2\psi_{y'y'}(B) + \frac{1}{2}y'^2x'\psi_{y'y'x'}(B) + \frac{1}{6}y'^3\psi_{y'y'y'}(B) + O(h^4) \qquad \text{(A-51)}$$

There are three unknowns involved. We choose three points. E, 1, and 4 as shown in the figure to evaluate $\psi_{y'y'}(B)$, $\psi_{y'y'x'}(B)$ and $\psi_{y'y'y'}(B)$.

From Fig. 5 we can obtain the following relationships:

$$\left.\begin{aligned} y'_E &= Ph\cos\alpha & x'_E &= Ph\sin\alpha \\ y'_4 &= (1+P)h\cos\alpha & x'_4 &= (1+P)h\sin\alpha \\ y'_1 &= (P+\tan\alpha)h\cos\alpha & x'_1 &= -(h-Ph\tan\alpha)\cos\alpha \\ y'_{PB} &= -(1-P)h\cos\alpha & x'_{PB} &= -(1-P)h\sin\alpha \end{aligned}\right\} \quad (A\text{-}52)$$

By substituting Eq. (A-52) into Eq. (A-51) for the corresponding distance we can write

$$\frac{\psi(4)}{y'^2_4} = \frac{1}{2}\psi_{y'y'}(B) + \frac{1}{2}(1+P)h\sin\alpha\,\psi_{y'y'x'}(B) + \frac{1}{6}(1+P)h\cos\alpha\,\psi_{y'y'y'}(B) + O(h^4)$$

$$\frac{\psi(E)}{y'^2_E} = \frac{1}{2}\psi_{y'y'}(B) + \frac{1}{2}Ph\sin\alpha\,\psi_{y'y'x'}(B) + \frac{1}{6}Ph\cos\alpha\,\psi_{y'y'y'}(B) + O(h^4) \quad (A\text{-}53)$$

$$\frac{\psi(1)}{y'^2_1} = \frac{1}{2}\psi_{y'y'}(B) + \frac{1}{2}h(-P+\tan\alpha)\sin\alpha\,\psi_{y'y'x'}(B) + \frac{1}{6}(P+\tan\alpha)h\cos\alpha\,\psi_{y'y'y'}(B) + O(h^4)$$

After eliminating $\psi_{y'y'x'}(B)$ and $\psi_{y'y'y'}(B)$ we have

$$\psi_{y'y'}(B) = \frac{2(1+P)\psi(E)}{y'^2_E} - \frac{2\psi(4)P}{y'^2_4} + O(h^2) \quad (A\text{-}54)$$

Equation (A-54) is used to compute the vorticity at the boundary points because

$\psi_{x'x'}(B) = 0$ yields,

$$-\omega(B) = \psi_{y'y'}(B). \quad (A\text{-}55)$$

Again by Taylor's expansion we can express

$$\psi_{y'y'}(PB) = \psi_{y'y'}(B) + x'_{PB}\,\psi_{y'y'x'}(B) + y'_{PB}\,\psi_{y'y'y'}(B) + O(h^2)$$

$$\psi_{x'x'}(PB) = \psi_{x'x'}(B) + y'_{PB}\,\psi_{x'x'y'}(B) + x'_{PB}\,\psi_{x'x'x'}(B) + O(h^2) \qquad \text{(A-56)}$$

From the boundary conditions

$$\psi_{x'x'}(PB) = 0$$

Therefore,

$$-\omega(PB) = -\psi_{y'y'}(PB) \qquad \text{(A-57)}$$

From Eq. (A-57) we can obtain

$$\frac{h}{6}\psi_{y'y'y'}(B) = \cos\alpha\left(\frac{\psi(4)}{y'^2_4} - \frac{\psi(E)}{y'^2_E}\right) + \sin\alpha\left(\frac{\psi(1)}{y'^2_1} - \frac{\psi(E)}{y'^2_E}\right)$$

$$\frac{h}{2}\psi_{y'y'x'}(B) = \sin\alpha\left(\frac{\psi(4)}{y'^2_4} - \frac{\psi(E)}{y'^2_E}\right) - \cos\alpha\left(\frac{\psi(1)}{y'^2_1} - \frac{\psi(E)}{y'^2_E}\right) \qquad \text{(A-58)}$$

So Eq. (A-56) may be written as

$$\psi_{y'y'}(PB) = \frac{4\psi(E)}{P^2h^2}\left[\frac{1}{\cos^2\alpha} + (1-P)\left(1 + \frac{\sin\alpha}{\cos\alpha}\right)\right]$$

$$- \frac{2\psi(4)}{(1+P)^2h^2}\left[\frac{1}{\cos^2\alpha} + 2 - 2P\right]$$

$$- \frac{4(1-P)\cos\alpha\,\sin\alpha}{h^2(P\cos\alpha+\sin\alpha)^2}\,\psi(1) + O(h^2) \qquad \text{(A-59)}$$

Summary:

Type 1, PB points accessible in two directions

$$-\omega(PB) = \psi''(PB) = \frac{4\psi(E)\ (2-P)}{P^2h^2} - \frac{2\psi(3)\ (3-2P)}{h^2\ (1+P)^2} + O(h^2) \quad \text{(A-49)}$$

Type 2, PB points accessible in one direction

$$-\omega(PB) = \psi_{y'y'}(PB) = \frac{4\psi(E)}{P^2h^2}\left[\frac{1}{\cos^2\alpha} + (1-P)\left(1 + \frac{\sin\alpha}{\cos\alpha}\right)\right]$$

$$- \frac{2\psi(4)}{(1+P)^2h^2}\left[\frac{1}{\cos^2\alpha} + 2-2P\right]$$

$$- \frac{4(1-P)\cos\alpha\sin\alpha}{h^2(P\cos\alpha + \sin\alpha)^2}\ \psi(1) + O(h^2) \quad \text{(A-60)}$$

Vorticity at the actual boundary points

$$\psi_{y'y'}(B) = \frac{2(1+P)\psi(E)}{y'^2_E} - \frac{2\psi(4)P}{y'^2_4} + O(h^2) \quad \text{(A-54)}$$

APPENDIX II

Computer Program

THE PEACEMAN AND RACHFORD METHOD

```
$IBFTC MAIN    DECK
C      MAIN PROGRAM
       COMMON S,W,JC,VX,VY,B,Y,H,H2,OMEGA,TSTEP,ALPHA,TPRINT,ILO,ICENTR,
      1BETA,DELTA,IR,SM,SERR,TIME,RE,VSOL,P,ANGLE,MAXITR,KEY
      2,KEE,VSMO,DAMP,COS2
       DIMENSION  S(57,25),W(57,25),JC(57,25),VX(57,25),VY(57,25),B(57),
      1Y(57,25),VSOL(100),P(100,4),ANGLE(100)
      2,DAMP(100),VSMO(100)
       DIMENSION COS2(100)
       COMMON SIN,COS,IMAGE,WSOL,XDAMP,JREAD,     NWS,ITIME
       DIMENSION SIN(100),COS(100),WSOL(100)
       DIMENSION VSO(100)
     1 FORMAT(4F8.3,6I3,F4.2,I3,F8.6)
     2 FORMAT (6E12.5)
       READ (2,1) BETA,BETMIN,WLIM1,WLIM2,NMAX,MPRINT,JWRITE
      1,MAXITR,KEY,MAXWIT,XDAMP,JREAD,SERR
       WRITE (3,101)BETA,BETMIN,WLIM1,WLIM2,SERR,XDAMP
   101 FORMAT(7H1BETA..,F8.3,2X,8HBETMIN..,F8.3,2X,7HWLIM1..,F8.3,2X,
      17HWLIM2..,F8.3,2X,6HSERR..,F8.6,2X,7HXDAMP..,F4.2)
C      NMAX=MAX. NUMBER OF TIME STEPS
C      MAXITR=MAX. NUMBER OF ITERATIONS IN STRFUN
       ITIME=0
       NSTEP= 0
       NPRINT= MPRINT
       KEE=0
       CALL SETUP
       IF(JREAD) 9,8,9
     8 DO 154 J=1,100
   154 DAMP(J)=XDAMP
C      ADVANCE VORTICITY
     9 JP=1
       K=0
    10 DO 11 I=1,57
       DO\11 J=1,25
    11 Y(I,J)= W(I,J)
       DO 12 J=1,100
    12 VSO(J)= VSOL(J)
    13 DO 14 J=1,100
    14 VSOL(J)=VSO(J)
    15 CALL VORINT(JP)
       KEE=KEE+1
       CALL STRFUN
       CALL VORSOL
       IF(JWRITE) 156,155,156
   155 WRITE (3,2) (DAMP(J),J=1,100)
       WRITE (3,2) (VSOL(J),J=1,100)
   156 K=K+1
   151 GO TO (16,18),JP
    16 DO 17 J=1,100
       IF(ABS(VSO(J)-VSOL(J))-WLIM1) 17,17,21
    17 CONTINUE
    18 DO 19 J=1,100
       IF(ABS(VSOL(J)-VSMO(J))/DAMP(J)-WLIM2) 19,19,15
```

```
   19 CONTINUE
      GO TO (20,27),JP
   20 JP=2
      GO TO 10
   21 BETA= 2.0*BETA
      DO 22 I=1,57
      DO 22 J=1,25
   22 W(I,J)= Y(I,J)
      GO TO 13
   27 NSTEP= NSTEP + 1
      CALL VELOCI
C     TIME INCREMENT
      DT= H2/(BETA*DELTA)
      TIME =TIME+2.0*DT
      IF(K-MAXWIT) 271,272,272
  272 BETA=BETA*2.0
      GO TO 273
  271 BETA=BETA/2.0
  273 IF (BETA - BETMIN)  28,29,29
   28 BETA= BETMIN
   29 IF(NSTEP-NPRINT) 31,30,31
   30 CALL OUTPUT
      NPRINT= NPRINT + MPRINT
   31 IF (NSTEP - NMAX)  9,32,32
   32 STOP
      END
                    *** 'END-OF-FILE' CARD ***
```

```
$IBFTC OUTPUT  DECK
      SUBROUTINE OUTPUT
      COMMON S,W,JC,VX,VY,B,Y,H,H2,OMEGA,TSTEP,ALPHA,TPRINT,ILO,ICENTR,
     1BETA,DELTA,IR,SM,SERR,TIME,RE,VSOL,P,ANGLE,MAXITR,KEY
     2,KEE,VSMO,DAMP,COS2
      DIMENSION  S(57,25),W(57,25),JC(57,25),VX(57,25),VY(57,25),B(57),
     1Y(57,25),VSOL(100),P(100,4),ANGLE(100)
     2,DAMP(100),VSMO(100)
      DIMENSION COS2(100)
      COMMON SIN,COS,IMAGE,WSOL,XDAMP,JREAD,      NWS,ITIME
      DIMENSION SIN(100),COS(100),WSOL(100)
      COMMON POSTY
      DIMENSION POSTY(57,25)
      ITIME=ITIME+1
      WRITE (35) ITIME,TIME,(S(I,1),I=1,5)
      WRITE (3,120) ITIME,TIME,BETA
  120 FORMAT(8H ITIME..,I3,6HTIME..,F14.8,6HBETA..,F14.3)
      DO 100 I=1,57
      WRITE (35) (S(I,J),J=1,25)
  100 CONTINUE
      DO 110 I=1,57
      WRITE (35) (W(I,J),J=1,25)
  110 CONTINUE
      WRITE (35) (VSOL(I),I=1,NWS)
      WRITE (35) (WSOL(I),I=1,NWS)
      WRITE (35) (DAMP(I),I=1,100)
      RETURN
      END
                    *** 'END-OF-FILE' CARD ***
```

```
$IBFTC SETUP   DECK
      SUBROUTINE SETUP
      COMMON S,W,JC,VX,VY,B,Y,H,H2,OMEGA,TSTEP,ALPHA,TPRINT,ILO,ICENTR,
     1BETA,DELTA,IR,SM,SERR,TIME,RE,VSOL,P,ANGLE,MAXITR,KEY
     2,KEE,VSMO,DAMP,COS2
      DIMENSION  S(57,25),W(57,25),JC(57,25),VX(57,25),VY(57,25),B(57),
     1Y(57,25),VSOL(100),P(100,4),ANGLE(100)
     2,DAMP(100),VSMO(100)
      DIMENSION COS2(100)
      COMMON SIN,COS,IMAGE,WSOL,XDAMP,JREAD,     NWS,ITIME
      DIMENSION SIN(100),COS(100),WSOL(100)
  101 FORMAT(2I2,2F10.4)
  102 FORMAT(6E12.5)
      IF(JREAD) 210,200,210
  200 READ (2,101) IR,ICENTR,RE,TIME
      GO TO 220
  210 READ (35) IR,ICENTR,RE
C     IR=RADIUS OF CIRCULAR CYLINDER
C     ICENTR=CENTER OF CYLINDER
C     RE=REYNOLDS NUMBER
C     SERR=TOLERABLE ERROR IN STREAM FUNCTION
  220 DELTA=2.0/RE
      YMAX=24.0/FLOAT(IR)
      SM=SQRT (1425.0)
      H=YMAX/24.0
      H2=H*H
      OMEGA=1.0+0.8*(2.0/(1.0+3.0/SM)-1.0)
      ALPHA=H/(2.0*DELTA)
      ILO=ICENTR-IR
      WRITE (3,221) IR,ICENTR,RE
  221 FORMAT (5H IR=,I3,9H ICENTR=,I3,5H RE=,F14.3)
      IF(JREAD) 1001,1002,1001
 1001 CALL SETUP1
      GO TO 1003
 1002 IF(YMAX-1.0) 999,999,1
    1 IF(28-IABS (28-ICENTR)-IR) 999,999,2
  999 STOP
    2 DO 3 I=1,57
      DO 3 J=1,25
      W(I,J)=0.0
      S(I,J)=0.0
    3 JC(I,J)=0.0
      DO 4 I=1,57
    4 S(I,25)=YMAX
      DO 5 J=1,100
      DO 5 K=1,4
    5 P(J,K)=1.0
      K=0
      DO 500 J=1,100
  500 COS2(J)=1.0
      DO 590 I=ILO,ICENTR
      DO 580 J=2,24
      IF((J-1)**2+(I-ICENTR)**2-IR**2) 510,510,590
  510 IF(JC(I-1,J))520,530,580
  520 JC(I,J)=-2
      GO TO 580
```

```
      COS(K1)=COS(K)
      SIN(K1)=SIN(K)
      N1=3*(1/IQ)+(IQ/2)*(2/IQ)+(IQ/3)*2
      N2=2*(1/IQ)+2*(IQ/2)*(2/IQ)+(IQ/3)
      P(K1,N1)=P(K,2)
      P(K1,N2)=P(K,3)
  700 CONTINUE
  710 CONTINUE
  720 CONTINUE
      DO 750 I=ILO,ICENTR
      IF=2*ICENTR-I
      DO 740 J=2,24
      IF(JC(I,J)+1) 730,750,730
  730 JC(I,J)=-2
      JC(IF,J)=-2
  740 CONTINUE
  750 CONTINUE
   95 PING=PONG
      DO 15 J=2,24
      S(1,J)=YMAX*FLOAT(J-1)/24.0
      DO 15 I=2,56
      IF(JC(I,J)) 15,14,14
   14 R2=H2*FLOAT((J-1)**2+(I-ICENTR)**2)
      S(I,J)=H*FLOAT(J-1)*(1.0-1.0/R2)
   15 CONTINUE
C     STREAM FUNCTION
C     VORTICITY ON SOLID BOUNDARIES
   17 CALL STRFUN
      CALL VORSOL
C     VELOCITIES
      CALL VELOCI
C      PRINT INITIAL SOLUTION
      WRITE (35) IR,ICENTR,RE
      DO 1004 J=1,25
      WRITE (35) (JC(I,J),I=1,57)
 1004 CONTINUE
      DO 1005 J=1,4
      WRITE (35) (P(I,J),I=1,100)
 1005 CONTINUE
      K=JC(ICENTR,IR+2)
      ANGLE(K)=90.0
      IF=ICENTR+IR+1
      NWS=JC(IF,2)
      WRITE (35) NWS,(ANGLE(I),I=1,NWS),IMAGE
      WRITE (35) (COS(I),I=1,100)
      WRITE (35) (SIN(I),I=1,100)
      WRITE (35) (COS2(I),I=1,100)
      CALL OUTPUT
 1003 RETURN
                        *** 'END-OF-FILE' CARD ***
```

```
$IBFTC SETUP1  DECK
      SUBROUTINE SETUP1
      COMMON S,W,JC,VX,VY,B,Y,H,H2,OMEGA,TSTEP,ALPHA,TPRINT,ILO,ICENTR,
     1BETA,DELTA,IR,SM,SERR,TIME,RE,VSOL,P,ANGLE,MAXITR,KEY
     2,KEE,VSMO,DAMP,COS2
      DIMENSION  S(57,25),W(57,25),JC(57,25),VX(57,25),VY(57,25),B(57),
     1Y(57,25),VSOL(100),P(100,4),ANGLE(100)
     2,DAMP(100),VSMO(100)
      DIMENSION COS2(100)
      COMMON SIN,COS,IMAGE,WSOL,XDAMP,JREAD,      NWS,ITIME
      DIMENSION SIN(100),COS(100),WSOL(100)
      READ(2,101) ISTEP
  101 FORMAT (I3)
      DO 211 J=1,25
      READ (35) (JC(I,J),I=1,57)
  211 CONTINUE
      DO 212 J=1,4
      READ (35) (P(I,J),I=1,100)
  212 CONTINUE
      READ (35) NWS,(ANGLE(I),I=1,NWS),IMAGE
      READ (35) (COS(I),I=1,100)
      READ (35) (SIN(I),I=1,100)
      READ (35) (COS2(I),I=1,100)
 2130 READ (35) ITIME,TIME,(S(L,1),L=1,5)
      IF(ISTEP-ITIME) 213,215,213
  213 DO 214 I=1,57
      DO 214 J=1,2
      READ (35) (S(L,1),L=1,5)
  214 CONTINUE
      READ (35) (S(L,1),L=1,5)
      READ (35) (S(L,1),L=1,5)
      READ (35) (S(L,1),L=1,5)
      GO TO 2130
  215 DO 216 I=1,57
      READ (35) (S(I,J),J=1,25)
  216 CONTINUE
      DO 217 I=1,57
      READ (35) (W(I,J),J=1,25)
  217 CONTINUE
      READ (35) (VSOL(I),I=1,NWS)
      READ (35) (WSOL(I),I=1,NWS)
      READ (35) (DAMP(I),I=1,100)
      CALL VELOCI
      RETURN
      END
      END
                    *** 'END-OF-FILE' CARD ***
```

```
$IBFTC STRFUN  DECK
      SUBROUTINE STRFUN
      COMMON S,W,JC,VX,VY,B,Y,H,H2,OMEGA,TSTEP,ALPHA,TPRINT,ILO,ICENTR,
     1BETA,DELTA,IR,SM,SERR,TIME,RE,VSOL,P,ANGLE,MAXITR,KEY
     2,KEE,VSMO,DAMP,COS2
      DIMENSION  S(57,25),W(57,25),JC(57,25),VX(57,25),VY(57,25),B(57),
     1Y(57,25),VSOL(100),P(100,4),ANGLE(100)
     2,DAMP(100),VSMO(100)
      DIMENSION COS2(100)
      COMMON SIN,COS,IMAGE,WSOL
      DIMENSION SIN(100),COS(100),WSOL(100)
      ITER=0
   31 NERRS=0
      IF(KEY) 231,131,231
  231 CALL OUTPUT
  131 DO 35 I=2,56
      DO 35 J=2,24
      IF(JC(I,J)) 35,51,50
   50 K=JC(I,J)
      IF(JC(I,J-1)) 501,502,502
  501 PP=P(K,2)
      SPP=2.0*S(I,J+1)*(2.0-PP)/(1.0+PP)
     1+S(I,J+2)*(PP-1.0)/(PP+2.0)
      CS=3.0/PP-1.0
      GO TO 505
  502 IF(JC(I,J+1)) 503,504,504
  503 PP=P(K,4)
      SPP =2.0*S(I,J-1)*(2.0-PP)/(1.0+PP)+S(I,J-2)*(PP-1.0)/(PP+2.0)
      CS=3.0/PP-1.0
      GO TO 505
  504 SPP=S(I,J+1)+S(I,J-1)
      CS=2.0
  505 IF(JC(I-1,J)) 506,507,507
  506 PP=P(K,1)
      SPP=SPP+2.0*S(I+1,J)*(2.0-PP)/(1.0+PP)+S(I+2,J)*(PP-1.0)/(PP+2.0)
      CS=CS+3.0/PP-1.0
      GO TO 510
  507 IF(JC(I+1,J))508,509,509
  508 PP=P(K,3)
      SPP=2.0*S(I-1,J)*(2.0-PP)/(1.0+PP)+S(I-2,J)*(PP-1.0)/(PP+2.0)+SPP
      CS=CS+3.0/PP-1.0
      GO TO 510
  509 SPP=SPP+S(I+1,J)+S(I-1,J)
      CS=CS+2.0
  510 SNU=S(I,J)+OMEGA*(SPP+H2*W(I,J)-CS*S(I,J))/CS
      GO TO 52
   51 SNU=S(I,J)+OMEGA*(S(I-1,J)+S(I+1,J)+S(I,J-1)+S(I,J+1)+H2*W(I,J)
     1-4.*S(I,J))/4.
   52 IF(ABS (SNU-S(I,J))-SERR) 34,34,33
   33 NERRS=NERRS+1
   34 S(I,J)=SNU
   35 CONTINUE
      DO 37 J=2,24
      SNU=S(57,J)+(-(S(57,J-1)+S(57,J+1))-H2*W(57,J)+2.0*S(57,J))*
     1OMEGA/(-2.0)
      IF(ABS (SNU-S(57,J))-SERR) 37,37,36
```

```
 36 NERRS=NERRS+1
 37 S(57,J)=SNU
    IF(NERRS) 999,41,38
 38 ITER=ITER+1
    IF(ITER-MAXITR) 31,990,990
990 WRITE (3,991) MAXITR
991 FORMAT(51H1 STREAM FUNCTION DOES NOT CONVERGE AFTER ITERATING, I3,
   17H TIMES.)
    CALL OUTPUT
999 STOP
 41 RETURN
    END
```

*** 'END-OF-FILE' CARD ***

```
$IBFTC VELOCI  DECK
      SUBROUTINE VELOCI
      COMMON S,W,JC,VX,VY,B,Y,H,H2,OMEGA,TSTEP,ALPHA,TPRINT,ILO,ICENTR,
     1BETA,DELTA,IR,SM,SERR,TIME,RE,VSOL,P,ANGLE,MAXITR,KEY
     2,KEE,VSMO,DAMP,COS2
      DIMENSION  S(57,25),W(57,25),JC(57,25),VX(57,25),VY(57,25),B(57),
     1Y(57,25),VSOL(100),P(100,4),ANGLE(100)
     2,DAMP(100),VSMO(100)
      DIMENSION COS2(100)
      COMMON SIN,COS,IMAGE,WSOL
      DIMENSION SIN(100),COS(100),WSOL(100)
C     COMPUTE VELOCITY COMPONENTS FOR EACH MESH POINT
   21 DO 23 I=2,56
      DO 23 J=2,24
      IF(JC(I,J)) 23,22,26
   26 K=JC(I,J)
      VX(I,J)=0.5/H*(S(I,J+1)-S(I,J-1)+S(I,J)*((1.0-1.0/P(K,4))**2
     1-(1.0-1.0/P(K,2))**2))
      VY(I,J)=0.5/H*(S(I-1,J)-S(I+1,J)+S(I,J)*((1.0-1.0/P(K,1))**2
     1-(1.0-1.0/P(K,3))**2))
      GO TO 23
   22 VX(I,J)=0.5*(S(I,J+1)-S(I,J-1))/H
      VY(I,J)=0.5*(S(I-1,J)-S(I+1,J))/H
   23 CONTINUE
      DO 24 I=1,57
      VX(I,1)=S(I,2)/H
      VY(I,1)=0.0
      VY(I,25)=0.0
   24 VX(I,25)=(S(I,25)-S(I,24))/H
      DO 25 J=2,24
      VX(1,J)=1.0
      VY(1,J)=(S(1,J)-S(2,J))/H
      VX(57,J)=0.5*(S(57,J+1)-S(57,J-1))/H
   25 VY(57,J)=(S(56,J)-S(57,J))/H
      RETURN
      END
                    *** 'END-OF-FILE' CARD ***
```

```
530 K=K+1
    COS2(K)=1.0-(FLOAT(J-1)/FLOAT(IR))**2
    COS(K)=SQRT(COS2(K))
    SIN(K)=SQRT(1.0-COS2(K))
    ANGLE(K)=ATAN(SIN(K)/COS(K))*57.29578
    IF(COS2(K)-0.5   ) 540,540,550
550 P(K,3)=IR**2-(J-1)**2
    P(K,3)=1.0+FLOAT(ICENTR-I)-SQRT(P(K,3))
    IF(P(K,3)-0.5) 570,560,560
560 JC(I,J)=-1
    JC(I-1,J)=K
    GO TO 580
570 JC(I,J)=-2
    JC(I-1,J)=-1
    JC(I-2,J)=K
    P(K,3)=P(K,3)+1.0
580 CONTINUE
590 CONTINUE
540 KMAGE=K-1
    COS2(K)=0.0
    IMAGE=I-1
600 DO 630 I=ILO,IMAGE
    DO 620 J=2,24
    IF(JC(I,J)) 620,630,610
610 K=JC(I,J)
    JJ=J
    P(K,2)=IR**2-(ICENTR-I)**2
    P(K,2)=FLOAT(JJ)-1.0 -SQRT(P(K,2))
    GO TO 630
620 CONTINUE
630 CONTINUE
    JC(ICENTR,IR+1)=-1
    JC(ICENTR,IR+2)=2*KMAGE+1
    DO 720 I=ILO,IMAGE
    DO 710 J=2,24
    IF(JC(I,J)+1) 710,640,720
640 K=JC(I-1,J)
    DO 700 IQ=1,3
    GO TO (650,670,680),IQ
650 K1=2*KMAGE-K+1
    ANGLE(K1)=90.0-ANGLE(K)
    I1=ICENTR-J+1
     J1=ICENTR-I+2
660 JC(I1,J1-1)=-1
    GO TO 690
670 K1=2*KMAGE+K+1
    ANGLE(K1)=90.0+ANGLE(K)
    I1=2*ICENTR-I1
    GO TO 660
680 K1=4*KMAGE-K+2
    ANGLE(K1)=180.0-ANGLE(K)
    I1=2*ICENTR-I+1
    J1=J
    JC(I1-1,J1)=-1
690 JC(I1,J1)=K1
    COS2(K1)=COS2(K)
```

```
      SUBROUTINE VORINT(JP)
      GO TO (1,2),JP
C     FIRST SOLVE VORTICITY IN X-DIRECTION
    1 DO 680 J=2,24
      B(1   )=0.0
      DO 640 I=2,56
      IF(JC(I,J)) 610,630,630
  610 B(I   )=0.0
      GO TO 640
  630 C=1.0+ALPHA*VX(I,J)
      A=-(2.0+BETA)
      B(I)=1.0-ALPHA*VX(I,J)
      W(I,J)=-(1.0-ALPHA*VY(I,J))*Y(I,J+1)+(2.0-BETA)*Y(I,J)
     1-(1.0+ALPHA*VY(I,J))*Y(I,J-1)
      A=A/C-B(I-1   )
      B(I   )=B(I   )/(C*A)
      W(I,J)=(W(I,J)/C-W(I-1,J))/A
  640 CONTINUE
C     END BOUNDARY
      C=2.0*ALPHA*VX(57,J)
      A=-BETA-2.0*ALPHA*VX(57,J)
      B(57  )=0.0
      A=A/C-B(56  )
      W(57,J)=((-(1.0-ALPHA*VY(57,J))*Y(57,J+1)+(2.0-BETA)*Y(57,J)
     1-(1.0+ALPHA*VY(57,J))*Y(57,J-1))/C-W(56,J))/A
  690 DO 680 I=2,56
      II=58-I
  680 W(II,J)=W(II,J)-B(II  )*W(II+1,J)
    3 RETURN
C     SOLVE VORTICITY IN Y-DIRECTION
    2 DO 760 I=2,57
      B(  1)=0.0
      B(  25)=0.0
      DO 730 J=2,24
      IF(JC(I,J)) 700,720,720
  700 B(  J)=0.0
      GO TO 730
  720 C=1.0+ALPHA*VY(I,J)
      A=-(2.0+BETA)
      B(J)=1.0-ALPHA*VY(I,J)
      IF(I-56) 722,722,721
  721 W(57,J)=(2.0*ALPHA*VX(57,J)-BETA)*Y(57,J)-2.0*ALPHA*Y(56,J)
     1*VX(57,J)
      GO TO 723
  722 W(I,J)=-(1.0-ALPHA*VX(I,J))*Y(I+1,J)+(2.0-BETA)*Y(I,J)
     1-(1.0+ALPHA*VX(I,J))*Y(I-1,J)
  723 A=A/C-B(  J-1)
      B(  J)=B(  J)/(C*A)
      W(I,J)=(W(I,J)/C-W(I,J-1))/A
  730 CONTINUE
      DO 760 J=2,24
      JJ=26-J
  760 W(I,JJ)=W(I,JJ)-B(  JJ)*W(I,JJ+1)
    4 RETURN
      END
                    *** 'END-OF-FILE' CARD ***
```

```
$IBFTC VORSOL  DECK
      SUBROUTINE VORSOL
      COMMON S,W,JC,VX,VY,B,Y,H,H2,OMEGA,TSTEP,ALPHA,TPRINT,ILO,ICENTR,
     1BETA,DELTA,IR,SM,SERR,TIME,RE,VSOL,P,ANGLE,MAXITR,KEY
     2,KEE,VSMO,DAMP,COS2
      DIMENSION  S(57,25),W(57,25),JC(57,25),VX(57,25),VY(57,25),B(57),
     1Y(57,25),VSOL(100),P(100,4),ANGLE(100)
     2,DAMP(100),VSMO(100)
      DIMENSION COS2(100)
      COMMON SIN,COS,IMAGE,WSOL
      DIMENSION SIN(100),COS(100),WSOL(100)
C     CALCULATE VORTICITY ON SOLID BOUNDARIES.
C     VORTICITY ON CYLINDER
      SECOND (SE,SI,Q)=4.0*SE*(2.0-Q)/Q**2-2.0*SI*(3.0-2.0*Q)/(1.+Q)**2
      THIRD (SE,SI,S4,Q,COSS,SINS,COSSQ)
     1=4.0*SE*(1.0/COSSQ+(1.0-Q)*(1.0+SINS/COSS))/Q**2-2.0*S4*(1.0/COSSQ
     2+2.0-2.0*Q)/(Q+1.0)**2-4.0*(1.0-Q)*COSS*SINS*SI/(Q*COSS+SINS)**2
      SOLIDW (SE,SI,Q)=2.0*(1.0+Q)*SE/Q**2-2.0*SI*Q/(1.0+Q)**2
      IF=2  *ICENTR-IMAGE
      JS=0
      DO 400 I=2,56
      DO 400 J=2,24
      IF(JC(I,J)+1) 400,10,400
   10 JS=JS+1
      IF (JC(I,J+1))  30,400,20
   20 K=JC(I,J+1)
      SE=S(I,J+1)
      SI=S(I,J+2)
      Q=P(K,2)
      W(I,J)=-SECOND (SE,SI,Q)/H2
      IF(I-IF) 21,21,220
   21 WSOL(K)=-SOLIDW (SE,SI,Q)/H2/COS2(K)
      GO TO 220
   30 IF (JC(I-1 ,J))  50,400,40
   40 K= JC(I-1,J)
      W(I,J)=THIRD (S(I-1,J),S(I-1,J+1),S(I-2,J),P(K,3),COS(K),SIN(K),COS2(
     1S2(K))/(-H2)
      WSOL(K)=-SOLIDW (S(I-1,J),S(I-2,J),P(K,3))/H2/COS2(K)
      GO TO 390
   50 K= JC(I+1,J)
      W(I,J)=THIRD (S(I+1,J),S(I+1,J+1),S(I+2,J),P(K,1),COS(K),SIN(K),
     1COS2(K))/(-H2)
      WSOL(K)=-SOLIDW (S(I+1,J),S(I+2,J),P(K,1))/H2/COS2(K)
      GO TO 390
  220 IF(JC(I-1,J)) 240,400,230
  230 K=JC(I-1,J)
      SE=S(I-1,J)
      SI=S(I-2,J)
      Q=P(K,3)
      W(I,J)=W(I,J)-SECOND (SE,SI,Q)/H2
      IF(I-IMAGE) 231,231,390
  231 WSOL(K)=-SOLIDW (SE,SI,Q)/H2/COS2(K)
      GO TO 390
  240 IF(JC(I+1,J)) 300,400,310
  310 K=JC(I+1,J)
      SE=S(I+1,J)
```

```
      SI=S(I+2,J)
      Q=P(K,1)
      W(I,J)=W(I,J)-SECOND (SE,SI,Q)/H2
      IF(I-IF) 390,311,311
  311 WSOL(K)=-SOLIDW (SE,SI,Q)/H2/COS2(K)
      GO TO 390
  300 K=JC(I,J+1)
      IF(I-ICENTR) 320,320,330
  320 W(I,J)=THIRD (S(I,J+1),S(I-1,J+1),S(I,J+2),P(K,2),COS(K),SIN(K),
     1COS2(K))/(-H2)
      GO TO 390
  330 W(I,J)=THIRD (S(I,J+1),S(I+1,J+1),S(I,J+2),P(K,2),COS(K),SIN(K),
     1COS2(K))/(-H2)
  390 IF(KEE-1) 393,393,395
  395 IF((W(I,J)-VSOL(JS))*(VSOL(JS)-VSMO(JS))) 391,392,392
  391 DAMP(JS)=0.9*DAMP(JS)
      GO TO 394
  392 DAMP(JS)=DAMP(JS)/0.9
      IF(DAMP(JS)-1.0) 394,394,393
  393 DAMP(JS)=1.0
  394 VSMO(JS)=VSOL(JS)
      VSOL(JS)=VSOL(JS)+DAMP(JS)*(W(I,J)-VSOL(JS))
      W(I,J)=VSOL(JS)
  400 CONTINUE
  500 PING =PONT
      RETURN
      END
                        *** 'END-OF-FILE' CARD ***
```

METHOD BY FROMM

```
$IBFTC MAIN    DECK
C       MAIN PROGRAM
        COMMON S,W,JC,VX,VY,B,Y,H,H2,OMEGA,TSTEP,ALPHA,TPRINT,ILO,ICENTR,
       1BETA,DELTA,IR,SM,SERR,TIME,RE,VSOL,P,ANGLE,MAXITR,KEY
       2,KEE,VSMO,DAMP,COS2
        DIMENSION  S(57,25),W(57,25),JC(57,25),VX(57,25),VY(57,25),B(57),
       1Y(57,25),VSOL(100),P(100,4),ANGLE(100)
       2,DAMP(100),VSMO(100)
        DIMENSION COS2(100)
        COMMON SIN,COS,IMAGE,WSOL,XDAMP,JREAD,     NWS,ITIME
        DIMENSION SIN(100),COS(100),WSOL(100)
        COMMON POSTY
        DIMENSION POSTY(57,25)
        DIMENSION VSO(100)
    1   FORMAT(2F8.0,2F8.3,6I3,F4.2,I3,F8.6)
    2   FORMAT (6E12.5)
        READ (2,1) BETA,BETMIN,WLIM1,WLIM2,NMAX,MPRINT,JWRITE
       1,MAXITR,KEY,MAXWIT,XDAMP,JREAD,SERR
        WRITE (3,101)BETA,BETMIN,WLIM1,WLIM2,SERR,XDAMP
  101   FORMAT(7H1BETA..,F8.0,2X,8HBETMIN..,F8.0,2X,7HWLIM1..,F8.3,2X,
       17HWLIM2..,F8.3,2X,6HSERR..,F8.6,2X,7HXDAMP..,F4.2)
  102   FORMAT(7HOBETA..,F8.0)
C       NMAX=MAX. NUMBER OF TIME STEPS
C       MAXITR=MAX. NUMBER OF ITERATIONS IN STRFUN
        ITIME=0
        NSTEP= 0
        NPRINT= MPRINT
        KEE=0
        CALL SETUP
        IF (JREAD) 81,8,81
    8   DO 154 J=1,100
  154   DAMP(J)=XDAMP
   81   ALPHA=H/(BETA*DELTA)
C       ADVANCE VORTICITY
    9   K=0
   10   DO 11 I=1,57
        DO 11 J=1,25
        POSTY(I,J)=Y(I,J)
   11   Y(I,J)= W(I,J)
        DO 12 J=1,100
   12   VSO(J)= VSOL(J)
   13   DO 14 J=1,100
   14   VSOL(J)=VSO(J)
   15   CALL VORINT
        KEE=KEE+1
        CALL STRFUN
        CALL VORSOL
        IF (JWRITE) 152,151,152
  151   WRITE (3,102) BETA
         WRITE (3,2) (VSOL(J),J=1,100)
  152   K=K+1
   16   DO 17 J=1,100
        IF(ABS(VSO(J)-VSOL(J))-WLIM1) 17,17,21
```

```
   17 CONTINUE
   18 DO 19 J=1,100
      IF(ABS(VSOL(J)-VSMO(J))/DAMP(J)-WLIM2) 19,19,15
   19 CONTINUE
      GO TO 27
   21 BETA= 2.0*BETA
      ALPHA=ALPHA/2.0
      DO 22 I=1,57
      DO 22 J=1,25
      POSTY(I,J)=Y(I,J)+0.5*(POSTY(I,J)-Y(I,J))
   22 W(I,J)= Y(I,J)
      GO TO 13
   27 NSTEP= NSTEP + 1
      BETOLD=BETA
      CALL VELOCI
C     TIME INCREMENT
      DT= H2/(BETA*DELTA)
      TIME=TIME+ DT
      IF(K-MAXWIT) 271,272,272
  272 BETA=BETA*2.0
      ALPHA=ALPHA/2.0
      GO TO 273
  271 BETA=BETA/2.0
      ALPHA=ALPHA*2.0
  273 IF (BETA - BETMIN)  28,29,29
   28 BETA= BETMIN
      ALPHA=H/(BETA*DELTA)
   29 DO 291I=1,57
      DO 291 J=1,25
  291 Y(I,J)=W(I,J)+BETOLD/BETA*(Y(I,J)-W(I,J))
      IF(NSTEP-NPRINT) 31,30,31
   30 CALL OUTPUT
      NPRINT= NPRINT + MPRINT
   31 IF (NSTEP - NMAX)  9,32,32
   32 STOP
      END
                    *** 'END-OF-FILE' CARD ***
```

```
$IBFTC OUTPUT  DECK
      SUBROUTINE OUTPUT
      COMMON S,W,JC,VX,VY,B,Y,H,H2,OMEGA,TSTEP,ALPHA,TPRINT,ILO,ICENTR,
     1BETA,DELTA,IR,SM,SERR,TIME,RE,VSOL,P,ANGLE,MAXITR,KEY
     2,KEE,VSMO,DAMP,COS2
      DIMENSION  S(57,25),W(57,25),JC(57,25),VX(57,25),VY(57,25),B(57),
     1Y(57,25),VSOL(100),P(100,4),ANGLE(100)
     2,DAMP(100),VSMO(100)
      DIMENSION COS2(100)
      COMMON SIN,COS,IMAGE,WSOL,XDAMP,JREAD,      NWS,ITIME
      DIMENSION SIN(100),COS(100),WSOL(100)
      COMMON POSTY
      DIMENSION POSTY(57,25)
      ITIME=ITIME+1
      WRITE (35) ITIME,TIME,(S(I,1),I=1,5)
      WRITE (3,120) ITIME,TIME,BETA
  120 FORMAT(8H ITIME..,I3,6HTIME..,F14.8,6HBETA..,F14.3)
      DO 100 I=1,57
      WRITE (35) (S(I,J),J=1,25)
  100 CONTINUE
      DO 110 I=1,57
      WRITE (35) (W(I,J),J=1,25)
      WRITE (35) (Y(I,J),J=1,25)
  110 CONTINUE
      WRITE (35) (VSOL(I),I=1,NWS)
      WRITE (35) (WSOL(I),I=1,NWS)
      WRITE (35) (DAMP(I),I=1,100)
      RETURN
      END
                    *** 'END-OF-FILE' CARD ***
```

```
$IBFTC SETUP   DECK
      SUBROUTINE SETUP
      COMMON S,W,JC,VX,VY,B,Y,H,H2,OMEGA,TSTEP,ALPHA,TPRINT,ILO,ICENTR,
     1BETA,DELTA,IR,SM,SERR,TIME,RE,VSOL,P,ANGLE,MAXITR,KEY
     2,KEE,VSMO,DAMP,COS2
      DIMENSION  S(57,25),W(57,25),JC(57,25),VX(57,25),VY(57,25),B(57),
     1Y(57,25),VSOL(100),P(100,4),ANGLE(100)
     2,DAMP(100),VSMO(100)
      DIMENSION COS2(100)
      COMMON SIN,COS,IMAGE,WSOL,XDAMP,JREAD,     NWS,ITIME
      DIMENSION SIN(100),COS(100),WSOL(100)
      COMMON POSTY
      DIMENSION POSTY(57,25)
  101 FORMAT(2I2,2F10.4)
  102 FORMAT(6E12.5)
      IF(JREAD) 210,200,210
  200 READ (2,101) IR,ICENTR,RE,TIME
      GO TO 220
  210 READ (35) IR,ICENTR,RE
C     IR=RADIUS OF CIRCULAR CYLINDER
C     ICENTR=CENTER OF CYLINDER
C     RE=REYNOLDS NUMBER
C     SERR=TOLERABLE ERROR IN STREAM FUNCTION
  220 DELTA=2.0/RE
      YMAX=24.0/FLOAT(IR)
      SM=SQRT (1425.0)
      H=YMAX/24.0
      H2=H*H
      OMEGA=1.0+0.8*(2.0/(1.0+3.0/SM)-1.0)
      ILO=ICENTR-IR
      WRITE (3,221) IR,ICENTR,RE
  221 FORMAT (5H IR..,I3,9H ICENTR..,I3,5H RE..,F14.3)
      IF(JREAD) 1001,1002,1001
 1001 CALL SETUP1
      GO TO 1003
 1002 IF(YMAX-1.0) 999,999,1
    1 IF(28-IABS (28-ICENTR)-IR) 999,999,2
  999 STOP
    2 DO 3 I=1,57
      DO 3 J=1,25
      W(I,J)=0.0
      POSTY(I,J)=0.0
      S(I,J)=0.0
    3 JC(I,J)=0.0
      DO 4 I=1,57
    4 S(I,25)=YMAX
      DO 5 J=1,100
      DO 5 K=1,4
    5 P(J,K)=1.0
      K=0
      DO 500 J=1,100
  500 COS2(J)=1.0
      DO 590 I=ILO,ICENTR
      DO 580 J=2,24
      IF((J-1)**2+(I-ICENTR)**2-IR**2) 510,510,590
  510 IF(JC(I-1,J))520,530,580
```

```
520 JC(I,J)=-2
    GO TO 580
530 K=K+1
    COS2(K)=1.0-(FLOAT(J-1)/FLOAT(IR))**2
    COS(K)=SQRT(COS2(K))
    SIN(K)=SQRT(1.0-COS2(K))
    ANGLE(K)=ATAN(SIN(K)/COS(K))*57.29578
    IF(COS2(K)-0.5   ) 540,540,550
550 P(K,3)=IR**2-(J-1)**2
    P(K,3)=1.0+FLOAT(ICENTR-I)-SQRT(P(K,3))
    IF(P(K,3)-0.5) 570,560,560
560 JC(I,J)=-1
    JC(I-1,J)=K
    GO TO 580
570 JC(I,J)=-2
    JC(I-1,J)=-1
    JC(I-2,J)=K
    P(K,3)=P(K,3)+1.0
580 CONTINUE
590 CONTINUE
540 KMAGE=K-1
    COS2(K)=0.0
    IMAGE=I-1
600 DO 630 I=ILO,IMAGE
    DO 620 J=2,24
    IF(JC(I,J)) 620,630,610
610 K=JC(I,J)
    JJ=J
    P(K,2)=IR**2-(ICENTR-I)**2
    P(K,2)=FLOAT(JJ)-1.0 -SQRT(P(K,2))
    GO TO 630
620 CONTINUE
630 CONTINUE
    JC(ICENTR,IR+1)=-1
    JC(ICENTR,IR+2)=2*KMAGE+1
    DO 720 I=ILO,IMAGE
    DO 710 J=2,24
    IF(JC(I,J)+1) 710,640,720
640 K=JC(I-1,J)
    DO 700 IQ=1,3
    GO TO (650,670,680),IQ
650 K1=2*KMAGE-K+1
    ANGLE(K1)=90.0-ANGLE(K)
    I1=ICENTR-J+1
     J1=ICENTR-I+2
660 JC(I1,J1-1)=-1
    GO TO 690
670 K1=2*KMAGE+K+1
    ANGLE(K1)=90.0+ANGLE(K)
    I1=2*ICENTR-I1
    GO TO 660
680 K1=4*KMAGE-K+2
    ANGLE(K1)=180.0-ANGLE(K)
    I1=2*ICENTR-I+1
    J1=J
    JC(I1-1,J1)=-1
```

```
  690 JC(I1,J1)=K1
      COS2(K1)=COS2(K)
      COS(K1)=COS(K)
      SIN(K1)=SIN(K)
      N1=3*(1/IQ)+(IQ/2)*(2/IQ)+(IQ/3)*2
      N2=2*(1/IQ)+2*(IQ/2)*(2/IQ)+(IQ/3)
      P(K1,N1)=P(K,2)
      P(K1,N2)=P(K,3)
  700 CONTINUE
  710 CONTINUE
  720 CONTINUE
      DO 750 I=ILO,ICENTR
      IF=2*ICENTR-I
      DO 740 J=2,24
      IF(JC(I,J)+1) 730,750,730
  730 JC(I,J)=-2
      JC(IF,J)=-2
  740 CONTINUE
  750 CONTINUE
   95 PING=PONG
      DO 15 J=2,24
      S(1,J)=YMAX*FLOAT(J-1)/24.0
      DO 15 I=2,56
      IF(JC(I,J)) 15,14,14
   14 R2=H2*FLOAT((J-1)**2+(I-ICENTR)**2)
      S(I,J)=H*FLOAT(J-1)*(1.0-1.0/R2)
   15 CONTINUE
C     STREAM FUNCTION
   17 CALL STRFUN
C     VORTICITY ON SOLID BOUNDARIES
      CALL VORSOL
C     VELOCITIES
      CALL VELOCI
C      PRINT INITIAL SOLUTION
      WRITE (35) IR,ICENTR,RE
      DO 1004 J=1,25
      WRITE (35) (JC(I,J),I=1,57)
 1004 CONTINUE
      DO 1005 J=1,4
      WRITE (35) (P(I,J),I=1,100)
 1005 CONTINUE
      K=JC(ICENTR,IR+2)
      ANGLE(K)=90.0
      IF=ICENTR+IR+1
      NWS=JC(IF,2)
      WRITE (35) NWS,(ANGLE(I),I=1,NWS),IMAGE
      WRITE (35) (COS(I),I=1,100)
      WRITE (35) (SIN(I),I=1,100)
      WRITE (35) (COS2(I),I=1,100)
      CALL OUTPUT
 1003 RETURN
      END
                    *** 'END-OF-FILE' CARD ***
```

```
$IBFTC SETUP1  DECK
      SUBROUTINE SETUP1
      COMMON S,W,JC,VX,VY,B,Y,H,H2,OMEGA,TSTEP,ALPHA,TPRINT,ILO,ICENTR,
     1BETA,DELTA,IR,SM,SERR,TIME,RE,VSOL,P,ANGLE,MAXITR,KEY
     2,KEE,VSMO,DAMP,COS2
      DIMENSION  S(57,25),W(57,25),JC(57,25),VX(57,25),VY(57,25),B(57),
     1Y(57,25),VSOL(100),P(100,4),ANGLE(100)
     2,DAMP(100),VSMO(100)
      DIMENSION COS2(100)
      COMMON SIN,COS,IMAGE,WSOL,XDAMP,JREAD,      NWS,ITIME
      DIMENSION SIN(100),COS(100),WSOL(100)
      READ(2,101) ISTEP
  101 FORMAT (I3)
      DO 211 J=1,25
      READ (35) (JC(I,J),I=1,57)
  211 CONTINUE
      DO 212 J=1,4
      READ (35) (P(I,J),I=1,100)
  212 CONTINUE
      READ (35) NWS,(ANGLE(I),I=1,NWS),IMAGE
      READ (35) (COS(I),I=1,100)
      READ (35) (SIN(I),I=1,100)
      READ (35) (COS2(I),I=1,100)
 2130 READ (35) ITIME,TIME,(S(L,1),L=1,5)
      IF(ISTEP-ITIME) 213,215,213
  213 DO 214 I=1,57
      DO 214 J=1,3
      READ (35) (S(L,1),L=1,5)
  214 CONTINUE
      READ (35) (S(L,1),L=1,5)
      READ (35) (S(L,1),L=1,5)
      READ (35) (S(L,1),L=1,5)
      GO TO 2130
  215 DO 216 I=1,57
      READ (35) (S(I,J),J=1,25)
  216 CONTINUE
      DO 217 I=1,57
      READ (35) (Y(I,J),J=1,25)
      READ (35) (W(I,J),J=1,25)
  217 CONTINUE
      READ (35) (VSOL(I),I=1,NWS)
      READ (35) (WSOL(I),I=1,NWS)
      READ (35) (DAMP(I),I=1,100)
      CALL VELOCI
      RETURN
      END
      END
```

```
$IBFTC SETUP1  DECK
      SUBROUTINE SETUP1
      COMMON S,W,JC,VX,VY,B,Y,H,H2,OMEGA,TSTEP,ALPHA,TPRINT,ILO,ICENTR,
     1BETA,DELTA,IR,SM,SERR,TIME,RE,VSOL,P,ANGLE,MAXITR,KEY
     2,KEE,VSMO,DAMP,COS2
      DIMENSION  S(57,25),W(57,25),JC(57,25),VX(57,25),VY(57,25),B(57),
     1Y(57,25),VSOL(100),P(100,4),ANGLE(100)
     2,DAMP(100),VSMO(100)
      DIMENSION COS2(100)
      COMMON SIN,COS,IMAGE,WSOL,XDAMP,JREAD,      NWS,ITIME
      DIMENSION SIN(100),COS(100),WSOL(100)
      READ(2,101) ISTEP
  101 FORMAT (I3)
      DO 211 J=1,25
      READ (35) (JC(I,J),I=1,57)
  211 CONTINUE
      DO 212 J=1,4
      READ (35) (P(I,J),I=1,100)
  212 CONTINUE
      READ (35) NWS,(ANGLE(I),I=1,NWS),IMAGE
      READ (35) (COS(I),I=1,100)
      READ (35) (SIN(I),I=1,100)
      READ (35) (COS2(I),I=1,100)
 2130 READ (35) ITIME,TIME,(S(L,1),L=1,5)
      IF(ISTEP-ITIME) 213,215,213
  213 DO 214 I=1,57
      DO 214 J=1,3
      READ (35) (S(L,1),L=1,5)
  214 CONTINUE
      READ (35) (S(L,1),L=1,5)
      READ (35) (S(L,1),L=1,5)
      READ (35) (S(L,1),L=1,5)
      GO TO 2130
  215 DO 216 I=1,57
      READ (35) (S(I,J),J=1,25)
  216 CONTINUE
      DO 217 I=1,57
      READ (35) (Y(I,J),J=1,25)
      READ (35) (W(I,J),J=1,25)
  217 CONTINUE
      READ (35) (VSOL(I),I=1,NWS)
      READ (35) (WSOL(I),I=1,NWS)
      READ (35) (DAMP(I),I=1,100)
      CALL VELOCI
      RETURN
      END
      END
```

```
$IBFTC VORINT  DECK
      SUBROUTINE VORINT
      COMMON S,W,JC,VX,VY,B,Y,H,H2,OMEGA,TSTEP,ALPHA,TPRINT,ILO,ICENTR,
     1BETA,DELTA,IR,SM,SERR,TIME,RE,VSOL,P,ANGLE,MAXITR,KEY
     2,KEE,VSMO,DAMP,COS2
      DIMENSION  S(57,25),W(57,25),JC(57,25),VX(57,25),VY(57,25),B(57),
     1Y(57,25),VSOL(100),P(100,4),ANGLE(100)
     2,DAMP(100),VSMO(100)
      DIMENSION COS2(100)
      COMMON SIN,COS,IMAGE,WSOL,XDAMP,JREAD,      NWS,ITIME
      DIMENSION SIN(100),COS(100),WSOL(100)
      COMMON POSTY
      DIMENSION POSTY(57,25)
      DO 80 J=2,24
      DO 60 I=2,56
      IF (JC(I,J)) 60,50,50
   50 W(I,J) =(POSTY(I,J)+2.0*(Y(I+1,J)+Y(I-1,J)+Y(I,J+1)+Y(I,J-1)-2.0
     1*POSTY(I,J))/BETA-ALPHA*(VX(I,J)*(Y(I+1,J)-Y(I-1,J))+VY(I,J)*(Y(I,J+1)-Y(I
     2J+1)-Y(I,J-1))))/(1.0+4.0/BETA)
   60 CONTINUE
      W(57,J)=(POSTY(57,J)+2.0*(Y(57,J+1)+Y(57,J-1)-POSTY(57,J))/BETA
     1-ALPHA*(VX(57,J)*(POSTY(57,J)-2.0*Y(56,J))+VY(57,J)*(Y(57,J+1)
     2-Y(57,J-1))))/(1.0+2.0/BETA+ALPHA*VX(57,J))
   80 CONTINUE
      RETURN
      END
                    *** 'END-OF-FILE' CARD ***
```

STRFUN, VELOCI, AND VORSOL ARE THE SAME AS THE PEACEMAN AND RACHFORD METHOD.

*** 'END-OF-FILE' CARD ***

PLOT AND PRINT RESULTS

THE PEACEMAN AND RACHFORD METHOD

```
$IBFTC MAIN    DECK
       DIMENSION JC(57,25),P(100,4),DUMMY(5),D(57,25),Y(57,25,2),WS(100),
      1ANGLE(100),Z(16),CYLDR(57),X(100),YY(100)
       COMMON IDF,IEF,IR,ICENTR,RE,JC,P,TIME,DUMMY,D,Y,WS,ANGLE,NWS,Z,
      1CYLDR,X,YY,ITIME
       KCHECK=1
C      IDF = PLOT EVERY DF TH. TIME STEP
C      IEF = PLOT EXACTLY THE EF TH. TIME STEP
    1  FORMAT(3I3)
       READ (35) IR,ICENTR,RE
       DO 65 J=1,25
       READ(35) (JC(I,J),I=1,57)
   65  CONTINUE
       DO 67 J=1,4
       READ (35) (P(I,J),I=1,100)
   67  CONTINUE
       READ (35) NWS,(ANGLE(I),I=1,NWS),IMAGE
       CALL PREID(2HPS,2)
       DO 68 I=1,3
       READ (35) (DUMMY(L),L=1,5)
   68  CONTINUE
   10  READ (2,1) IDF,IEF,KEY
       IF(IDF)50,50,100
   50  IF(IEF) 999,999,60
   60  READ (35) ITIME,TIME,(DUMMY(L),L=1,5)
       IF(ITIME-IEF)70,90,70
   70  DO 80 I=1,57
       DO 80 J=1,2
       READ(35) (DUMMY(L),L=1,5)
   80  CONTINUE
       READ (35) (DUMMY(L),L=1,5)
       READ (35) (DUMMY(L),L=1,5)
       READ (35) (DUMMY(L),L=1,5)
       GO TO 60
   90  IF(KEY-KCHECK) 92,91,92
   91  CALL OUTPUT
       GO TO 10
   92  CALL PLOTER
       GO TO 10
  100  IF(KEY-KCHECK) 102,101,102
  101  CALL OUTPUT
       GO TO 103
  102  CALL PLOTER
  103  DO 120 I=1,IDF
       READ (35) (DUMMY(L),L=1,5)
       DO 110 II=1,57
       DO 110 J=1,3
       READ (35) (DUMMY(L),L=1,5)
  110  CONTINUE
       READ (35) (DUMMY(L),L=1,5)
```

```
      READ (35) (DUMMY(L),L=1,5)
      READ (35) (DUMMY(L),L=1,5)
  120 CONTINUE
      GO TO 100
  999 CALL POSTID(2HPS,2)
      STOP
      END
```

*** 'END-OF-FILE' CARD ***

```
$IBFTC OUTPUT  DECK
      SUBROUTINE OUTPUT
      DIMENSION JC(57,25),P(100,4),DUMMY(5),D(57,25),Y(57,25,2),WS(100),
     1ANGLE(100),Z(16),CYLDR(57),X(100),YY(100)
      COMMON IDF,IEF,IR,ICENTR,RE,JC,P,TIME,DUMMY,D,Y,WS,ANGLE,NWS,Z,
     1CYLDR,X,YY,ITIME
  100 FORMAT(9H1RADIUS..,I2, 9H CENTER..,I2, 5H RE..,F10.4,7H TIME..,E12
     1.5,14HOUTPUT COUNT..,I4//18H STREAM FUNCTION../)
  101 FORMAT(1H0,I2,13F8.4/3X,12F8.4)
  102 FORMAT(//12H VORTICITY../)
  103 FORMAT(//27H SOLID BOUNDARY VORTICITY..)
  104 FORMAT(1H0,12F8.4)
      WRITE (3,100) IR,ICENTR,RE,TIME,ITIME
      DO 10 I=1,57
      READ (35) (D(I,J),J=1,25)
   10 CONTINUE
      WRITE(3,101) (I,(D(I,J),J=1,25),I=1,57)
      WRITE (3,102)
      DO 20 I=1,57
      READ (35) (D(I,J),J=1,25)
   20 CONTINUE
      WRITE (3,101) (I,(D(I,J),J=1,25),I=1,57)
      WRITE (3,103)
      READ (35) (DUMMY(L),L=1,5)
      READ (35) (WS(I),I=1,NWS)
      READ (35) (DUMMY(L),L=1,5)
      WRITE (3,104) (ANGLE(I),WS(I),I=1,NWS)
      RETURN
      END
                    *** 'END-OF-FILE' CARD ***
```

```
$IBFTC PLOTER  DECK
      SUBROUTINE PLOTER
      DIMENSION JC(57,25),P(100,4),DUMMY(5),D(57,25),Y(57,25,2),WS(100),
     1ANGLE(100),Z(16),CYLDR(57),X(100),YY(100)
      COMMON IDF,IEF,IR,ICENTR,RE,JC,P,TIME,DUMMY,D,Y,WS,ANGLE,NWS,Z,
     1CYLDR,X,YY,ITIME
      YAXIS (DP1,DP2,DP3,Q)=((DP1-DP2)/(DP3-DP2))*Q
      KEE=0
    5 DO 10 I=1,57
      DO 10 J=1,25
      DO 10 K=1,2
   10 Y(I,J,K)=0.0
      DO 20 I=1,57
   20 READ (35) (D(I,J),J=1,25)
      IF(KEE) 30,80,30
   30 WMAX=0.0
      WMIN=0.0
      DO 60 I=1,57
      DO 60 J=1,25
      IF(ABS(D(I,J))-WMAX) 50,50,40
   40 WMAX=ABS(D(I,J))
      GO TO 60
   50 IF(ABS(D(I,J))-WMIN) 55,60,60
   55 WMIN=ABS(D(I,J))
   60 CONTINUE
      WSCALE=(WMAX-WMIN)/24.0
      DO 70 J=1,25
   70 D(1,J)=WSCALE*FLOAT(J-1)
      GO TO 100
   80 DO 90 K=1,2
      DO 90 J=1,25
   90 Y(1,J,K)=J
  100 L=1
      DO 240 I=2,57
      DO 230 JJ=2,25
      DO 220 J=1,24
      IF(JC(I,J)+1) 220,110,110
  110 IF(D(1,JJ)-ABS(D(I,J))) 120,215,200
  120 IF(D(1,JJ)-ABS(D(I,J+1))) 220,130,130
  130 L=1
  140 IF(KEE)150,145,150
  145 K=JC(I,J+1)
      IF(K) 160,150,160
  150 Q=1.0
      GO TO 170
  160 Q=P(K,2)
  170 IF(D(I,J)) 190,175,180
  175 IF(D(I,J+1)) 190,180,180
  180 Y(I,JJ,L)=FLOAT(J)+YAXIS(D(1,JJ),D(I,J),D(I,J+1),Q)
      GO TO 220
  190 Y(I,JJ,L)=FLOAT(J)+YAXIS(-D(1,JJ),D(I,J),D(I,J+1),Q)
      GO TO 220
  200 IF(D(1,JJ)-ABS(D(I,J+1))) 210,210,220
  210 L=2
      GO TO 140
  215 Y(I,JJ,L)=FLOAT(J)
```

```
  220 CONTINUE
  230 CONTINUE
  240 CONTINUE
      CALL FRAME
      CALL TITLE
      CALL PLOT
      IF (KEE) 260,250,260
  250 KEE=KEE+1
      WRITE (3,500) IR,ICENTR,RE,TIME,ITIME
  500 FORMAT(9H1RADIUS..,I2, 9H CENTER..,I2, 5H RE..,F10.4,7H TIME..,E12
     1.5,14HOUTPUT COUNT..,I4//18H STREAM FUNCTION../)
      WRITE (3,501) (I,(D(I,J),J=1,25),I=1,57)
  501 FORMAT(1HO,I2,13F8.4/3X,12F8.4)
      GO TO 5
C     PLOT VORTICITY ON SOLID
  260 READ (35) (DUMMY(L),L=1,5)
      READ (35) (WS(I),I=1,NWS)
      READ (35)(DUMMY(L),L=1,5)
      WRITE (3,502)
  502 FORMAT(//12H VORTICITY../)
      WRITE (3,501) (I,(D(I,J),J=1,25),I=1,57)
      WRITE (3,503)
  503 FORMAT(//27H SOLID BOUNDARY VORTICITY..)
      WRITE (3,504) (ANGLE(I),WS(I),I=1,NWS)
  504 FORMAT(1HO,12F8.4)
      CALL PLOTA(1)
      CALL TITLE
      CALL FRAMES
      RETURN
      END
                    *** 'END-OF-FILE' CARD ***
```

```
$IBFTC FRAME   LIST,REF,DECK
       SUBROUTINE FRAME
       DIMENSION JC(57,25),P(100,4),DUMMY(5),D(57,25),Y(57,25,2),WS(100),
      1ANGLE(100),Z(16),CYLDR(57),X(100),YY(100)
       COMMON IDF,IEF,IR,ICENTR,RE,JC,P,TIME,DUMMY,D,Y,WS,ANGLE,NWS,Z,
      1CYLDR,X,YY,ITIME
       DO 10 I=1,16
    10 Z(I)=0.0
       Z(1)=57
       Z(2)=1.0
       Z(3)=0.0
       Z(4)=1.0
       Z(5)=1.0
       Z(8)=0.0
       Z(11)=1.0
       Z(12)=57.
       Z(13)=1.0
       Z(14)=57.0
       Z(15)=1.0
       Z(16)=8.
C      PLOT THE HALF CYLINDER
       ILO = ICENTR-IR
       DO 20 I=1,ILO
    20 CYLDR(I)=1.0
       IHI=ICENTR+IR
       DO 30 I=IHI,57
    30 CYLDR(I)=1.0
       ILO=ICENTR-IR
       DO 50 I=ILO,ICENTR
       IF=2*ICENTR-I
       CYLDR(I)=1.0+SQRT(FLOAT(IR)**2-FLOAT(ICENTR-I)**2)
       CYLDR(IF)=CYLDR(I)
    50 CONTINUE
       DO 60 I=1,57
    60 X(I)=I
       CALL GRAPH(X,CYLDR,Z,0,0,0)
       RETURN
       END
                        *** 'END-OF-FILE' CARD ***
```

```
$IBFTC FRAMES  DECK
      SUBROUTINE FRAMES
      DIMENSION JC(57,25),P(100,4),DUMMY(5),D(57,25),Y(57,25,2),WS(100),
     1ANGLE(100),Z(16),CYLDR(57),X(100),YY(100)
      COMMON IDF,IEF,IR,ICENTR,RE,JC,P,TIME,DUMMY,D,Y,WS,ANGLE,NWS,Z,
     1CYLDR,X,YY,ITIME
      DO 10 I=1,16
   10 Z(I)=0.0
      Z(1)=NWS+2
      Z(3)=0
      Z(4)=1.0
      Z(5)=1.0
      Z(8)=3.0
      Z(9)=5.0
      WMAX=0.0
      WMIN=0.0
      DO 80 I=1,NWS
      IF(WMAX-WS(I)) 50,80,60
   50 WMAX=WS(I)
      GO TO 80
   60 IF(WS(I)-WMIN) 70,80,80
   70 WMIN=WS(I)
   80 CONTINUE
      Z(10)=(WMAX-WMIN)/10.0
      Z(11)=1.0
      Z(12)=180.0
      Z(13)=0.0
      Z(14)=WMAX
      Z(15)=WMIN
      Z(16)=8.0
      X(1)=0.0
      X(NWS+2)=180
      YY(1)=0.0
      YY(NWS+2)=0.0
      DO 90 I=1,NWS
      X(I+1)=ANGLE(I)
   90 YY(I+1)=WS(I)
      CALL GRAPH(X,YY,Z,7H VORSOL,17H ANGLE IN DEGREES,19H VORTICITY ON
     1SOLID)
      RETURN
      END
                    *** 'END-OF-FILE' CARD ***
```

```
$IBFTC PLOT    DECK
       SUBROUTINE PLOT
       DIMENSION JC(57,25),P(100,4),DUMMY(5),D(57,25),Y(57,25,2),WS(100),
      1ANGLE(100),Z(16),CYLDR(57),X(100),YY(100)
       COMMON IDF,IEF,IR,ICENTR,RE,JC,P,TIME,DUMMY,D,Y,WS,ANGLE,NWS,Z,
      1CYLDR,X,YY,ITIME
       DO 10 I=1,16
    10 Z(I)=0.0
       Z(1)=57.
       Z(4)=1.0
       Z(11)=1.0
       Z(12)=57.
       Z(13)=1.0
       Z(14)=57.0
       Z(15)=1.0
       Z(16)=8.
       DO 50 I=1,57
    50 X(I)=I
       DO 160 K=1,2
       DO 150 J=1,25
       DO 60 I=1,57
    60 YY(I)=Y(I,J,K)
       IEND=0
    65 KEE=0
       IEND=IEND+1
       DO 110 I=IEND,57
       IF (KEE) 140,70,90
    70 IF(YY(I)) 110,110,80
    80 ISTART=I
       KEE=1
       GO TO 110
    90 IF(YY(I)) 110,100,110
   100 IEND=I-1
       KEE=-1
   110 CONTINUE
   120 IF(KEE) 140,150,130
   130 IEND=57
   140 Z(1)=IEND-ISTART+1
       CALL GRAPH(X(ISTART),YY(ISTART),Z,0,0,0)
       IF(IEND-56)65,150,150
   150 CONTINUE
   160 CONTINUE
       RETURN
       END
                        *** 'END-OF-FILE' CARD ***
```

```
$IBFTC TITLE   LIST,REF,DECK
       SUBROUTINE TITLE
       DIMENSION JC(57,25),P(100,4),DUMMY(5),D(57,25),Y(57,25,2),WS(100),
      1ANGLE(100),Z(16),CYLDR(57),X(100),YY(100)
       COMMON IDF,IEF,IR,ICENTR,RE,JC,P,TIME,DUMMY,D,Y,WS,ANGLE,NWS,Z,
      1CYLDR,X,YY,ITIME
       Y1=0.96
       SCALE=(6.0/1023.0)*2.0
       X1=0.04+12.0*SCALE
       CALL CHPLOT(X1,Y1,8,2,8HRADIUS..)
       X1=X1+SCALE*10.0
       CALL NPLOT(X1,Y1,8,2,3,IR)
       X1=X1+SCALE*6.0
       CALL CHPLOT(X1,Y1,8,2,4HRE..)
       X1=X1+SCALE*6.0
       CALL NPLOT(X1,Y1,8,2,4.4,RE)
       X1=X1+SCALE*15.0
        CALL CHPLOT(X1,Y1,8,2,6HTIME..)
       X1=X1+SCALE*7.0
       CALL NPLOT(X1,Y1,8,2,2.7,TIME)
       RETURN
       END
                    *** 'END-OF-FILE' CARD ***
```

METHOD BY FROMM

```
$IBFTC MAIN    DECK
      DIMENSION JC(57,25),P(100,4),DUMMY(5),D(57,25),Y(57,25,2),WS(100),
     1ANGLE(100),Z(16),CYLDR(57),X(100),YY(100)
      COMMON IDF,IEF,IR,ICENTR,RE,JC,P,TIME,DUMMY,D,Y,WS,ANGLE,NWS,Z,
     1CYLDR,X,YY,ITIME
      KCHECK=1
C     IDF = PLOT EVERY DF TH. TIME STEP
C     IEF = PLOT EXACTLY THE EF TH. TIME STEP
    1 FORMAT(3I3)
      READ (35) IR,ICENTR,RE
      DO 65 J=1,25
      READ(35) (JC(I,J),I=1,57)
   65 CONTINUE
      DO 67 J=1,4
      READ (35) (P(I,J),I=1,100)
   67 CONTINUE
      READ (35) NWS,(ANGLE(I),I=1,NWS),IMAGE
      CALL PREID(2HPS,2)
      DO 68 I=1,3
      READ (35) (DUMMY(L),L=1,5)
   68 CONTINUE
   10 READ (2,1) IDF,IEF,KEY
      IF(IDF)50,50,100
   50 IF(IEF) 999,999,60
   60 READ (35) ITIME,TIME,(DUMMY(L),L=1,5)
      IF(ITIME-IEF)70,90,70
   70 DO 80 I=1,57
      DO 80 J=1,3
      READ(35) (DUMMY(L),L=1,5)
   80 CONTINUE
      READ (35) (DUMMY(L),L=1,5)
      READ (35) (DUMMY(L),L=1,5)
      READ (35) (DUMMY(L),L=1,5)
      GO TO 60
   90 IF(KEY-KCHECK) 92,91,92
   91 CALL OUTPUT
      GO TO 10
   92 CALL PLOTER
      GO TO 10
  100 IF(KEY-KCHECK) 102,101,102
  101 CALL OUTPUT
      GO TO 103
  102 CALL PLOTER
  103 DO 120 I=1,IDF
      READ (35) (DUMMY(L),L=1,5)
      DO 110 II=1,57
      DO 110 J=1,3
      READ (35) (DUMMY(L),L=1,5)
  110 CONTINUE
      READ (35) (DUMMY(L),L=1,5)
      READ (35) (DUMMY(L),L=1,5)
      READ (35) (DUMMY(L),L=1,5)
  120 CONTINUE
```

```
      GO TO 100
  999 CALL POSTID(2HPS,2)
      STOP
      END
```

*** 'END-OF-FILE' CARD ***

```
$IBFTC OUTPUT  DECK
      SUBROUTINE OUTPUT
      DIMENSION JC(57,25),P(100,4),DUMMY(5),D(57,25),Y(57,25,2),WS(100),
     1ANGLE(100),Z(16),CYLDR(57),X(100),YY(100)
      COMMON IDF,IEF,IR,ICENTR,RE,JC,P,TIME,DUMMY,D,Y,WS,ANGLE,NWS,Z,
     1CYLDR,X,YY,ITIME
  100 FORMAT(9H1RADIUS..,I2, 9H CENTER..,I2, 5H RE..,F10.4,7H TIME..,E12
     1.5,14HOUTPUT COUNT..,I4//18H STREAM FUNCTION../)
  101 FORMAT(1H0,I2,13F8.4/3X,12F8.4)
  102 FORMAT(//12H VORTICITY../)
  103 FORMAT(//27H SOLID BOUNDARY VORTICITY..)
  104 FORMAT(1H0,12F8.4)
      WRITE (3,100) IR,ICENTR,RE,TIME,ITIME
      DO 10 I=1,57
      READ (35) (D(I,J),J=1,25)
   10 CONTINUE
      WRITE(3,101) (I,(D(I,J),J=1,25),I=1,57)
      WRITE (3,102)
      DO 20 I=1,57
      READ (35) (D(I,J),J=1,25)
      READ (35) (DUMMY(L),L=1,5)
   20 CONTINUE
      WRITE (3,101) (I,(D(I,J),J=1,25),I=1,57)
      WRITE (3,103)
      READ (35) (DUMMY(L),L=1,5)
      READ (35) (WS(I),I=1,NWS)
      READ (35) (DUMMY(L),L=1,5)
      WRITE (3,104) (ANGLE(I),WS(I),I=1,NWS)
      RETURN
      END
                    *** 'END-OF-FILE' CARD ***
```

```
$IBFTC PLOTER  DECK
      SUBROUTINE PLOTER
      DIMENSION JC(57,25),P(100,4),DUMMY(5),D(57,25),Y(57,25,2),WS(100),
     1ANGLE(100),Z(16),CYLDR(57),X(100),YY(100)
      COMMON IDF,IEF,IR,ICENTR,RE,JC,P,TIME,DUMMY,D,Y,WS,ANGLE,NWS,Z,
     1CYLDR,X,YY,ITIME
      YAXIS (DP1,DP2,DP3,Q)=((DP1-DP2)/(DP3-DP2))*Q
      KEE=0
    5 DO 10 I=1,57
      DO 10 J=1,25
      DO 10 K=1,2
   10 Y(I,J,K)=0.0
      IF (KEE) 12,11,12
   11 DO 20 I=1,57
   20 READ (35) (D(I,J),J=1,25)
      GO TO 80
   12 DO 21 I=1,57
      READ (35) (D(I,J),J=1,25)
   21 READ (35) (DUMMY(L),L=1,5)
   30 WMAX=0.0
      WMIN=0.0
      DO 60 I=1,57
      DO 60 J=1,25
      IF(ABS(D(I,J))-WMAX) 50,50,40
   40 WMAX=ABS(D(I,J))
      GO TO 60
   50 IF(ABS(D(I,J))-WMIN) 55,60,60
   55 WMIN=ABS(D(I,J))
   60 CONTINUE
      WSCALE=(WMAX-WMIN)/24.0
      DO 70 J=1,25
   70 D(1,J)=WSCALE*FLOAT(J-1)
      GO TO 100
   80 DO 90 K=1,2
      DO 90 J=1,25
   90 Y(1,J,K)=J
  100 L=1
      DO 240 I=2,57
      DO 230 JJ=2,25
      DO 220 J=1,24
      IF(JC(I,J)+1) 220,110,110
  110 IF(D(1,JJ)-ABS(D(I,J)))120,215,200
  120 IF(D(1,JJ)-ABS(D(I,J+1))) 220,130,130
  130 L=1
  140 IF(KEE)150,145,150
  145 K=JC(I,J+1)
      IF(K) 160,150,160
  150 Q=1.0
      GO TO 170
  160 Q=P(K,2)
  170 IF(D(I,J)) 190,175,180
  175 IF(D(I,J+1)) 190,180,180
  180 Y(I,JJ,L)=FLOAT(J)+YAXIS(D(1,JJ),D(I,J),D(I,J+1),Q)
      GO TO 220
  190 Y(I,JJ,L)=FLOAT(J)+YAXIS(-D(1,JJ),D(I,J),D(I,J+1),Q)
      GO TO 220
```

```
200 IF(D(I,JJ)-ABS(D(I,J+1))) 210,210,220
210 L=2
    GO TO 140
215 Y(I,JJ,L)=FLOAT(J)
220 CONTINUE
230 CONTINUE
240 CONTINUE
    CALL FRAME
    CALL TITLE
    CALL PLOT
    IF (KEE) 260,250,260
250 KEE=KEE+1
    WRITE (3,500) IR,ICENTR,RE,TIME,ITIME
500 FORMAT(9H1RADIUS..,I2, 9H CENTER..,I2, 5H RE..,F10.4,7H TIME..,E12
   1.5,14HOUTPUT COUNT...I4//18H STREAM FUNCTION../)
    WRITE (3,501) (I,(D(I,J),J=1,25),I=1,57)
501 FORMAT(1HO,I2,13F8.4/3X,12F8.4)
    GO TO 5
C   PLOT VORTICITY ON SOLID
260 READ (35) (DUMMY(L),L=1,5)
    READ (35) (WS(I),I=1,NWS)
    READ (35)(DUMMY(L),L=1,5)
    WRITE (3,502)
502 FORMAT(//12H VORTICITY../)
    WRITE (3,501) (I,(D(I,J),J=1,25),I=1,57)
    WRITE (3,503)
503 FORMAT(//27H SOLID BOUNDARY VORTICITY..)
    WRITE (3,504) (ANGLE(I),WS(I),I=1,NWS)
504 FORMAT(1HO,12F8.4)
    CALL PLOTA(1)
    CALL TITLE
    CALL FRAMES
    RETURN
    END
```

*** 'END-OF-FILE' CARD ***

FRAME,FRAMES,PLOT,TITLE ARE THE SAME AS THE PEACEMAN AND RACHFORD METHOD.